Interference Alignment Techniques for Heterogeneous Wireless Networks

Esra Aycan Beyazit

CONSERVATOIRE NATIONAL DES ARTS ET MÉTIERS | le cnam

École doctorale Informatique, Télécommunication et Électronique de Paris

Laboratoire LAETITIA/CEDRIC

THÈSE DE DOCTORAT

présentée par : **Esra AYCAN BEYAZIT**

soutenue le : **02 Septembre 2016**

pour obtenir le grade de : **Docteur du Conservatoire National des Arts et Métiers**

Discipline / Spécialité : **Télécommunications / Communications sans fil**

INTERFERENCE ALIGNMENT TECHNIQUES FOR HETEROGENEOUS WIRELESS NETWORKS

THÈSE DIRIGÉE PAR

M. LE RUYET Didier	*Professeur, Conservatoire National des Arts et Métiers*
Mme. ÖZBEK Berna	*Asst. Prof. Dr., Izmir Institute of Technology*

RAPPORTEURS

M. CANCES Jean-Pierre	*Professeur, Université de Limoges - XLIM*
M. ÇIRPAN Hakan	*Professeur, Istanbul Technical University*

EXAMINATEURS

M. CHEVALIER Pascal	*Professeur, Conservatoire National des Arts et Métiers*
M. AKAN Aydın	*Professeur, Istanbul University*

CONSERVATOIRE NATIONAL DES ARTS ET MÉTIERS | le cnam

PhD Deparment in Computer Science, Telecommunication and Electronics

LAETITIA/CEDRIC Research Lab

PhD THESIS

presented by : **Esra AYCAN BEYAZIT**

defended on : **02 September 2016**

in partial fulfillement of the requirements for the Degree of : **Doctor of Philosophy from the Conservatoire National des Arts et Métiers**

Discipline / Specialization: **Telecommunications / Wireless Communications**

INTERFERENCE ALIGNMENT TECHNIQUES FOR HETEROGENEOUS WIRELESS NETWORKS

THESIS DIRECTED BY

M. LE RUYET Didier	*Professeur, Conservatoire National des Arts et Métiers*
Mme. ÖZBEK Berna	*Asst. Prof. Dr., Izmir Institute of Technology*

REPORTERS

M. CANCES Jean-Pierre	*Professeur, Université de Limoges - XLIM*
M. ÇIRPAN Hakan	*Professeur, Istanbul Technical University*

EXAMINATORS

M. CHEVALIER Pascal	*Professeur, Conservatoire National des Arts et Métiers*
M. AKAN Aydın	*Professeur, Istanbul University*

"To the memory of my late grandfathers,
Rıza AYCAN and Mehmet ÖZKALKANLI..."
Esra AYCAN BEYAZIT

Acknowledgments

I would like to express my sincere gratitude to my two supervisors, Assist. Prof. Dr. Berna ÖZBEK (Izmir Institute of Technology) and Prof. Dr. Didier Le Ruyet (Conservatoire National des Arts et Métiers) for giving me the opportunity to carry out a jointly-supervised PhD thesis (cotutelle). This thesis would not have been possible without their guidance, invaluable advice, patience and encouragement. It was a great opportunity for me to be guided by them.

I would like to thank my thesis progress committee members, Assoc. Prof. Dr. Oğuz Sunay and Assoc. Prof. Dr. Mustafa A. Altınkaya, for their contributions and guidance throughout my thesis study.

My sincere thanks also goes to my former colleague İlhan Baştürk for many valuable discussions and sharing of his experiences. He has always been a brother to me with his tremendous support. I am also grateful to his beloved wife, Bahar Baştürk, for her motivations throughout my studies.

I thank to Başak Esin Köktürk Güzel, Oktay Karakuş and all my former colleagues in IYTE for being such good friends and sharing all the happiness and sadness during my research studies. During my study in CNAM, I am happy to know many friends in Research lab CEDRIC. Besides, I sincerely thank to my all friends who helped me along the way.

I also owe thanks to my dear husband, Mutlu Beyazıt who always helped me throughout this thesis with code implementations and useful ideas. Beyond his academic support, his endless love kept me always motivated and gave me a great strength during my thesis study. There is no doubt for me that I have not been able to come thus far and achieved this much without him.

Finally, I thank to my whole family for their endless encouragement and loving support during my whole life. I thank to Gözde Aycan Tarıer for being a great sister. Her friendship in my first visit to CNAM gave me invaluable support. I also thank to her beloved husband İlhan Tarıer and Beyazıt family for their encouragements during my studies. I am forever indebted to my parents, Memnune Aycan and Mehmet Ali Aycan for their unconditional love and support. Words are never enough for expressing my gratitude to them.

Résumé

Dans cette thèse, nous étudions les algorithmes d'alignement d'interférence dans les réseaux hétérogènes basés sur la sélection des flux. Tout d'abord, nous considérons différents scénarios de déploiement des pico-cellules dans un contexte de connaissance parfaite des canaux de transmission au niveau des émetteurs. Deux algorithmes sont proposés respectivement pour les réseaux totalement et partiellement connectés. Afin d'assurer une équité entre les liens, les algorithmes garantissent qu'au moins un flux de chaque lien émetteur soit sélectionné. La séquence des flux est choisie parmi un ensemble qui contient les séquences les plus souvent sélectionnées en effectuant une recherche exhaustive. Ces algorithmes sont significativement moins complexes que la recherche exhaustive tout en ayant une performance proche de celle-ci. Après la sélection d'un flux, les interférences entre ce flux et les flux qui n'ont pas encore été sélectionnées sont alignées par projections orthogonales. Dans une deuxième partie de la thèse, l'impact de la connaissance partielle des canaux de transmission sur les algorithmes proposés est analysé. Il est montré que les interférences entre flux causent alors une forte dégradation des performances en raison des erreurs de quantification. Pour réduire cette dégradation, un nouvel algorithme est développé pour ce contexte. Finalement, des schémas d'allocation adaptative des bits pour les voies de retour sont proposés afin d'augmenter les performances des algorithmes précédents. Les performances de ces schémas et de ces algorithmes sont évaluées en considérant différents scénarios. Nous avons montré que les algorithmes proposés pour le cas des transmissions avec voie de retour sont significativement plus robustes et plus performants.

Mots clés : les réseaux de communication hétérogenes; alignement d'interférences; sélection de flux, rétroaction limitée

Abstract

In this thesis, we study the stream selection based interference alignment (IA) algorithms, which can provide large multiplexing gain, to deal with the interference in the heterogeneous networks. Firstly, different deployment scenarios for the pico cells are investigated assuming perfect channel state information (CSI) at the transmitters. Two different stream selection IA algorithms are proposed for fully and partially connected interference networks and selecting at least one stream is guaranteed for each user. A stream sequence is selected among a predetermined set of sequences that mostly contribute to the sum-rate while performing an exhaustive search. In the proposed algorithms, the complexity of the exhaustive search is significantly decreased while keeping the performance relatively close. After selecting a stream, the interference generated between the selected and the unselected streams is aligned by orthogonal projections. Then, the influence of the imperfect CSI on the proposed algorithms is analyzed and it is observed that the intra-stream interference causes a significant degradation in the performance due to the quantization error. Therefore, we propose an algorithm for the limited feedback scheme. Finally, adaptive bit allocation schemes are presented to maximize the overall capacity for all the proposed algorithms. The performance evaluations are carried out considering different scenarios with different number and placements of pico cells. It is shown that the proposed algorithm for the limited feedback is more robust to channel imperfections compared to the existing IA algorithms. The presented bit allocation schemes improve the performances of the algorithms compared to the equal bit allocation.

Keywords : heterogeneous networks, interference alignment, stream selection, feedback schemes

Contents

List of Tables

List of Figures

Part I

part 1

Chapter 1

Résumé en français

1.1 Introduction

Les réseaux hétérogènes sont considérés comme une technique prometteuse pour les réseaux cellulaires puisqu'ils permettent le déploiement d'un grand nombre de petites cellules avec différents niveaux d'émission au sein de la couverture d'une macro cellule classique. Bien que ce réseau cellulaire superposé apporte une extension de couverture et une augmentation de la capacité, la topologie du réseau pose le problème de la gestion des interférences.

L'alignement d'interférence (IA) est l'une des techniques permettant de réduire efficacement les interférences dans des réseaux cellulaires (Jafar [2011]). Le concept clé est d'aligner les signaux d'interférences dans un sous-espace dimensionnel au niveau de chaque récepteur en concevant des vecteurs de pré codage et de post codage de sorte que le signal utile puisse être obtenu dans les sous-espaces sans interférences.

Des solutions au problème d'IA en boucle fermée sont difficiles à obtenir pour des réseaux à grande échelle, c'est pourquoi des approches IA distribuée et itératives ont été intensivement étudiées dans la littérature (Gomadam et al. [2008a]). L'inconvénient des approches itératives est qu'elles nécessitent généralement un trop grand nombre d'itérations. Un autre souci de tels algorithmes itératifs est que la convergence vers une solution optimale n'a pas été démontrée.

Toutes les études précédemment citées reposent sur une transmission avec un nombre

de flux fixe qui dépend des conditions de faisabilité. Les algorithmes de sélection de flux sont capables de choisir un nombre de flux différent pour chaque utilisateur (Amara et al. [2011], Sun and Jorswieck [2016]).

Puisque les approches d'IA fondées sur la sélection de flux ne sont pas itératives et permettent de sélectionner des flux pour chaque utilisateur de manière dynamique, ce sont des techniques prometteuses. C'est pourquoi, dans cette thèse, nous étudions les algorithmes d'IA fondés sur la sélection de flux pour les réseaux hétérogènes. Les algorithmes de sélection proposés reposent sur la construction d'ensembles de séquences de flux à partir des caractéristiques du réseau hétérogène.

L'inconvénient le plus sévère de l'approche IA est la nécessité de connaître les informations d'état de canal (CSI) au niveau des transmetteurs. C'est pourquoi nous proposons dans cette thèse des algorithmes d'IA fondés sur la sélection de flux pour des schémas de retour limités dans des réseaux hétérogènes. Des schémas d'allocation de bit avec retour adaptatif sont présentés afin d'améliorer la performance des algorithmes proposés avec un CSI imparfait.

1.2 Modèle du système pour le cas du CSI parfait

Dans cette section, un canal d'interférence K paires est considéré avec une antenne d'émission N_{T_k} et une antenne de réception N_{R_k} . Dans cette section, on suppose que les CSI parfait est disponible au niveau de tous les émetteurs et de tous les récepteurs.

Le signal de sortie au niveau de l'utilisateur k est défini comme suit.

$$\mathbf{y}_k = \alpha_{kk}\mathbf{H}_{kk}\mathbf{x}_k + \sum_{\substack{j=1,\\ j\neq k}}^{K} \alpha_{kj}\mathbf{H}_{kj}\mathbf{x}_j + \mathbf{n}_k \tag{1.1}$$

où $\alpha_{kj}\mathbf{H}_{kj}$ est la matrice de canal entre l'émetteur j et le récepteur k, de dimension $N_{R_k} \times N_{T_j}$. Chaque élément de $\mathbf{H}_{kj}$ contient l'évanouissement qui est modélisé comme une variable aléatoire gaussienne indépendante et identiquement distribuée avec $\mathcal{CN}(0,1)$. α_{kj} décrit les pertes en espace libre et le shadowing. Pour chaque récepteur k, $\mathbf{n}_k$ est un vecteur $N_{R_k} \times 1$. Chaque élément de $\mathbf{n}_k$ représente un bruit blanc gaussien additif avec une moyenne nulle et une variance de σ^2. $\mathbf{x}_k$ est le signal transmis depuis le $k^{\text{ème}}$ émetteur

avec une dimension $N_{T_k} \times 1$, calculé comme suit.

$$\mathbf{x}_k = \sqrt{P_k}\mathbf{T}_k\mathbf{s}_k \tag{1.2}$$

où P_k est la puissance transmise par la station de base k. $\mathbf{T}_k$ est la matrice de pré codage unitaire de l'émetteur k, de dimension $N_{T_k} \times q_k$, l'émetteur k pouvant émettre q_k flux indépendants avec $q_k \leq d_k$ où $d_k = \min(N_{R_k}, N_{T_k})$. $\mathbf{s}_k$ est le vecteur symbole de dimension $q_k \times 1$ et noté $\mathbf{s}_k = [s_{k,1} ... s_{k,q_k}]^T$ où $\mathbb{E}\left[\|\mathbf{s}_k\|^2\right] = 1$ et on suppose que la puissance transmise est équitablement répartie entre les symboles, $\mathbb{E}\left[|s_{k,n}|^2\right] = 1/q_k$, $n = 1, ..., q_k$. De plus, le nombre total maximum de flux dans le réseau est calculé comme suit $r = \sum_{k=1}^{K} d_k$.

Les signaux utiles s'obtiennent en multipliant $\mathbf{y}_k$ par le vecteur de post codage, $\mathbf{D}_k$ de dimension $N_{R_k} \times q_k$. Les symboles de données décodés ainsi obtenus peuvent s'écrire comme $\hat{\mathbf{y}}_k = \mathbf{D}_k^H \mathbf{y}_k$.

Le débit de données du $i^{\text{ème}}$ flux pour le $k^{\text{ème}}$ utilisateur peut être exprimé comme suit.

$$\mathrm{R}_{ki} = \log_2(1 + \gamma_{ki}) \tag{1.3}$$

où γ_{ki} est le SINR du $i^{\text{ème}}$ flux pour le $k^{\text{ème}}$ utilisateur, calculé comme

$$\gamma_{ki} = \frac{(P_k/q_k)\alpha_{kk}^2 \mathbf{d}_k^{iH}\mathbf{H}_{kk}\mathbf{t}_k^i\mathbf{t}_k^{iH}\mathbf{H}_{kk}^H\mathbf{d}_k^i}{\mathbf{d}_k^{iH}\mathbf{B}_{ki}\mathbf{d}_k^i} \qquad \forall k = 1, ..., K, \quad \forall i = 1, ..., q_k \tag{1.4}$$

où $\mathbf{t}_k^i$ est le $i^{\text{ème}}$ vecteur colonne de la matrice de pré codage N_{T_k} de dimension $N_{T_k} \times 1$ et $\mathbf{d}_k^i$ est le $i^{\text{ème}}$ vecteur colonne de la matrice de post codage $\mathbf{D}_k$ de dimension $N_{R_k} \times 1$. De plus, $\mathbf{B}_{ki}$ est définie comme la matrice de covariance de l'interférence plus bruit pour le $i^{\text{ème}}$ flux du $k^{\text{ème}}$ récepteur est donnée par

$$\mathbf{B}_{ki} = \sum_{\substack{l=1,\\ l\neq i}}^{q_k} \frac{P_k}{q_k}\alpha_{kk}^2\mathbf{H}_{kk}\mathbf{t}_k^l(\mathbf{t}_k^l)^H\mathbf{H}_{kk}^H + \sum_{\substack{j=1\\ j\neq k}}^{K}\sum_{q=1}^{q_j}\frac{P_j}{q_j}\alpha_{kj}^2\mathbf{H}_{kj}\mathbf{t}_j^q(\mathbf{t}_j^q)^H\mathbf{H}_{kj}^H + \sigma^2\mathbf{I}_{N_{R_k}} \qquad \forall k = 1, ..., K, \quad \forall i = 1, ..., q_k \tag{1.5}$$

Par conséquent, le sum rate (SR) est calculé comme suit.

$$\mathrm{SR} = \sum_{k=1}^{K}\sum_{i=1}^{q_k}\log_2(1 + \gamma_{ki}) \tag{1.6}$$

1.3 Algorithmes d'IA itératifs

L'étude de Gomadam et al. [2008b] a présenté la première solution distribuée utilisant la réciprocité du canal pour identifier des pré codeurs et des post codeurs d'IA MIMO. De nombreux algorithmes d'IA dans la littérature reposent sur des approches d'IA itératives. Cependant l'inconvénient des approches itératives est qu'elles nécessitent généralement de nombreuses itérations dans des régimes à fort SNR. De plus, l'hypothèse que le canal de propagation n'évolue pas durant l'échange de données entre les émetteurs et les récepteurs n'est pas réaliste.

L'algorithme de fuite d'interférence minimale réduit l'interférence de manière itérative en concevant les vecteurs de post codage au niveau de chaque récepteur de chaque réseau. Bien que cet algorithme exploite la réciprocité du canal pour réaliser l'opération, il peut également être exécuté dans un nœud centralisé en utilisant une topologie centralisée.

Au lieu de minimiser la puissance d'interférence à chaque itération, le SINR est itérativement maximisé dans un algorithme max-SINR. A chaque itération, l'algorithme met à jour les matrices de post codage du réseau considéré, puis le sens de la communication est inversé. L'algorithme continue jusqu'à convergence.

1.4 Algorithmes de sélection du flux

Dans les algorithmes d'IA basés sur la sélection du flux, chaque flux est sélectionné dans le noyau des flux précédemment sélectionnés à chaque itération où les flux sont calculés à partir de la décomposition en valeurs singulières (SVD) de l'ensemble des canaux $(\alpha_{kk}\mathbf{H}_{kk}) = \mathbf{U}_k\mathbf{S}_k\mathbf{V}_k^H$. De plus le $l^{\text{ème}}$ vecteur colonne de $\mathbf{V}_k$ et $\mathbf{U}_k$ est noté $\mathbf{v}_k^l$ et $\mathbf{u}_k^l$ respectivement. L'interférence est alignée après chaque étape de sélection de flux en utilisant des projections orthogonales.

Il y a deux sortes d'interférences entre les flux. La première est l'interférence du flux sélectionné vers les autres flux et la seconde est l'interférence des autres flux vers le flux sélectionné. C'est pourquoi, deux types de canaux virtuels sont définis : les Canaux Virtuels de Réception (VRC) et les Canaux Virtuels de Transmission (VTC) (Amara et al. [2012b]).

Ils peuvent être exprimés comme suit.

- Canal Virtuel de Réception: le VRC est le canal entre l'émetteur k et le récepteur k^* comprenant le vecteur de post codage du flux sélectionné l^*, $\mathbf{u}_{k^*}^{l^*}$.

$$\mathbf{VRC}_{k^*k}^{l^*} = (\mathbf{u}_{k^*}^{l^*})^H \mathbf{H}_{k^*k} \tag{1.7}$$

- Canal Virtuel de Transmission: le VTC est le canal entre l'émetteur k^* et le récepteur k comprenant le vecteur de pré codage du flux sélectionné l^*, $\mathbf{v}_{k^*}^{l^*}$.

$$\mathbf{VTC}_{kk^*}^{l^*} = \mathbf{H}_{kk^*} \mathbf{v}_{k^*}^{l^*} \tag{1.8}$$

Les matrices de pré codage et de post codage sont construites à partir des vecteurs de pré codage et de post codage correspondant aux flux sélectionnés et elles sont exprimées comme $\mathbf{T}_{k^*} = [\mathbf{v}_{k^*}^1, \mathbf{v}_{k^*}^2, ..., \mathbf{v}_{k^*}^{q_k}]$ and $\mathbf{D}_{k^*} = [\mathbf{u}_{k^*}^1, \mathbf{u}_{k^*}^2, ..., \mathbf{u}_{k^*}^{q_k}]$, respectivement.

Les vecteurs des matrices projetées $\mathbf{H}_{kk}^{\perp}$, initialement $\mathbf{H}_{kk}^{\perp} = \mathbf{H}_{kk}$, $\forall k \neq k^*$, sont dans le noyau des VRC et VTC de tous les flux précédemment sélectionnés. La procédure de projection est implémentée en deux étapes. Dans la première étape, l'interférence en provenance des flux restants vers le flux sélectionné est réduite en projetant les matrices de canal $\mathbf{H}_{kk}^{\perp}$ générées orthogonalement aux $\mathbf{VRC}$, $(\mathbf{u}_{k^*}^{l^*})^H \mathbf{H}_{k^*k}$ et calculée comme

$$\mathbf{H}_{kk}^{\perp} = \mathbf{H}_{kk}^{\perp} \mathbf{P}_{((\mathbf{u}_{k^*}^{l^*})^H \mathbf{H}_{k^*k})}^{\perp} \tag{1.9}$$

où $\mathbf{P}_{(\mathbf{u}_{k^*}^{l^*H} \mathbf{H}_{k^*k})}^{\perp}$ est la matrice de projection orthogonale associée à la matrice $(\mathbf{u}_{k^*}^{l^*})^H \mathbf{H}_{k^*k}$ et peut s'exprimer comme

$$\mathbf{P}_{((\mathbf{u}_{k^*}^{l^*})^H \mathbf{H}_{k^*k})}^{\perp} = \mathbf{I}_{N_{T_k}} - \frac{((\mathbf{u}_{k^*}^{l^*})^H \mathbf{H}_{k^*k})^H ((\mathbf{u}_{k^*}^{l^*})^H \mathbf{H}_{k^*k})}{\left\| ((\mathbf{u}_{k^*}^{l^*})^H \mathbf{H}_{k^*k}) \right\|^2}. \tag{1.10}$$

La seconde étape de la procédure de projection est de réduire l'interférence générée par les flux restants et consiste à projeter les matrices de canal $\mathbf{H}_{kk}^{\perp}$ générées sur les $\mathbf{VTC}$,$\mathbf{H}_{kk^*} \mathbf{v}_{k^*}^{l^*}$. L'objectif principal est de réduire l'interférence tout en identifiant la meilleure séquence de flux. Le schéma de sélection de flux qui maximise le sum rate global donné dans l'équation Eq. (1.6) peut être formulé comme suit.

$$\{(\mathbf{T}_k^*, \mathbf{D}_k^*)\}_{k \in [1,...,K]} = \underset{\mathbf{T}_k, \mathbf{D}_k}{\operatorname{argmax}} \, (\mathrm{SR}) \tag{1.11}$$

La procédure d'alignement d'interférence pour un flux sélectionné l^* de l'utilisateur k^* est résumée dans Alg. 1.

Alg. 1 Algorithme d'Alignement d'Interférences

Entrée: α_{kk}, $\mathbf{H}_{kk}^{\perp}$, $\mathbf{H}_{kk^*}$ and $\mathbf{H}_{k^*k}$ $\forall k$; $\mathbf{v}_{k^*}^{l^*}$, $\mathbf{u}_{k^*}^{l^*}$, $\mathbf{T}_{k^*}$, $\mathbf{D}_{k^*}$
Projeter orthogonalement à **VRC**, $(\mathbf{u}_{k^*}^{l^*})^H \mathbf{H}_{k^*k}$
$\mathbf{H}_{kk}^{\perp} = \mathbf{H}_{kk}^{\perp} \mathbf{P}^{\perp}_{\mathbf{u}_{k^*}^{l^*H} \mathbf{H}_{k^*k}}$ for $k = 1, ..., K$ où $k \neq k^*$
Projeter orthogonalement à **VTC**, $\mathbf{H}_{kk^*} \mathbf{v}_{k^*}^{l^*}$
$\mathbf{H}_{kk}^{\perp} = \mathbf{P}^{\perp}_{\mathbf{H}_{kk^*} \mathbf{v}_{k^*}^{l^*}} \mathbf{H}_{kk}^{\perp}$ pour $k = 1, ..., K$ où $k \neq k^*$
Calculer la SVD des matrices projetées
$(\alpha_{kk} \mathbf{H}_{kk}^{\perp}) = \mathbf{U}_k \mathbf{S}_k \mathbf{V}_k^H$ pour $k = 1, ..., K$
Mettre à jour
$\mathbf{T}_{k^*} = [\mathbf{T}_{k^*} \ \mathbf{v}_{k^*}^{l^*}]$
$\mathbf{D}_{k^*} = [\mathbf{D}_{k^*} \ \mathbf{u}_{k^*}^{l^*}]$
Sortie: $\mathbf{H}_{kk}^{\perp}$, $\mathbf{V}_k$, $\mathbf{U}_k$ et $\mathbf{S}_k$ $\forall k$; $\mathbf{T}_{k^*}$, $\mathbf{D}_{k^*}$

1.4.1 Recherche exhaustive d'une sélection de flux successifs

L'objectif des algorithmes de sélection de flux est de sélectionner des flux successivement tout en maximisant le sum rate. La meilleure séquence de flux parmi toutes les séquences de flux possibles peut être établie par une recherche exhaustive (Amara et al. [2012b]). Les flux, les séquences de flux et les ensembles qui s'y rapportent sont définis comme suit.

Chaque flux i peut être exprimé comme $\pi_i = (k_i, l_i)$ où $k_i \in \{1, \ldots, K\}$, $l_i \in \{1, \ldots, q_{k_i}\}$ et $i \in \{1, \ldots, r\}$. L'ensemble de toutes les séquences de flux possibles peut être défini comme suit,

$$\Phi = \Phi_1 \cup \ldots \cup \Phi_j \cup \ldots \cup \Phi_r \tag{1.12}$$

où Φ_j est l'ensemble de toutes les permutations de longueur $j \in \{1, \ldots, r\}$ donné par

$$\begin{aligned} \Phi_j = \Big\{ & \pi = (\pi_1 \pi_2 \ldots \pi_j) \mid \\ & \forall i, i' \in \{1, \ldots, j\}, \ \pi_i \neq \pi_{i'} \text{ if } i \neq i' \Big\} \end{aligned} \tag{1.13}$$

Alg. 2 détermine les matrices de pré codage et de post codage pour une séquence de flux π donnée. Il calcule également le sum rate obtenu par la sélection de cette séquence.

En utilisant Alg. 2, Alg. 3 réalise une recherche exhaustive qui teste toutes les séquences de flux pertinentes et sélectionne la séquence avec le plus fort sum rate.

Alg. 2 Algorithme de sélection de flux

Entrée: α_{kj}, $\mathbf{H}_{kj}$ $\forall k, j$, π
Initialisation des variables
$\mathbf{T} = \emptyset$; $\mathbf{D} = \emptyset$; $i = 1$; $q_k = 0$ and $\mathbf{H}_{kk}^{\perp} = \mathbf{H}_{kk}$ pour $k = 1, ..., K$
Calculer de la SVD de tous les canaux
$(\alpha_{kk}\mathbf{H}_{kk}^{\perp}) = \mathbf{U}_k\mathbf{S}_k\mathbf{V}_k^H$ pour $k = 1, ..., K$
while $i \leq |\pi|$ **do**
Choisir le $i^{\text{ième}}$ flux dans π
$(k^*, l^*) = \pi_i$
Mettre à jour
$q_{k^*} = q_{k^*} + 1$
Appliquer **Alg. 1**
Incrémenter i
$i = i + 1$
end while
Calculer le sum-rate SR_π donné dans Eq. (1.6)
Initialisation des variables pour le flux sélectionne
$(\mathbf{T}_k)_\pi = \mathbf{T}_k$, $(\mathbf{D}_k)_\pi = \mathbf{D}_k$ pour $k = 1, ..., K$
Sortie: $(\mathbf{T}_k)_\pi$, $(\mathbf{D}_k)_\pi$ $\forall k$

Alg. 3 Recherche exhaustive

Entrée: α_{kj}, $\mathbf{H}_{kj}$ $\forall k, j$
Initialiser l'ensemble Φ
for chaque séquence de flux $\pi \in \Phi$ **do**
Appliquer **Alg. 2**
end for
Sélectionner la meilleur sséquence de flux d'après Eq. (1.11)
$\pi^* = \underset{\pi \in \Pi}{\text{argmax}}\ \text{SR}_\pi$
$\mathbf{T}_k^* = (\mathbf{T}_k)_{\pi^*}$, $\mathbf{D}_k^* = (\mathbf{D}_k)_{\pi^*}$ pour $k = 1, ..., K$
Sortie: $\mathbf{T}_k^*$, $\mathbf{D}_k^*$ $\forall k$

L'inconvénient majeur de la recherche exhaustive est sa complexité, directement liée au nombre de flux.

1.4.2 Sélection successive de flux (SNSSS)

Dans cet algorithme, une seule séquence de flux est construite en sélectionnant successivement les flux avec les valeurs singulières les plus élevées (c.à.d. les flux les plus forts) (Amara et al. [2012b]). Alors que les flux sont sélectionnés, leurs contributions au sum rate sont évaluées, que la capacité du système augmente ou non. Puisque la puissance d'émission est équitablement répartie entre tous les flux, ajouter un flux pour un utilisateur déjà servi n'augmente pas nécessairement le sum rate total. La valeur singulière maximale augmentant le sum rate est choisie à chaque itération dans l'ensemble Ω, où Ω est l'ensemble où sont stockées les valeurs propres des flux disponibles. En outre, la séquence de flux construite à la fin de l'algorithme est notée Ψ.

1.4.3 Sélection successive améliorée de flux (ESNSSS)

Dans l'algorithme SNSSS, seul un chemin spécifique est construit en sélectionnant la plus grande valeur singulière augmentant le sum rate. Cependant cette stratégie peut conduire à une solution sous-optimale. C'est pourquoi construire des initialisations autres que la valeur de flux maximale peut conduire à de plus grandes valeurs de sum rate. Afin de réduire la complexité de la recherche exhaustive et de surmonter le caractère sous-optimal de l'algorithme SNSSS, l'algorithme ESNSSS introduit des points d'initialisation différents dans le processus de recherche de flux. Chaque séquence de flux est initialisée avec tous les flux possibles dont les valeurs singulières sont initialement calculées et stockées dans l'ensemble Ω_0.

1.5 Sélection de flux basée sur l'alignement d'interférences pour les réseaux hétérogènes

Le modèle de système utilisé pour les réseaux hétérogènes est le même que le modèle de système décrit dans les sections précédentes. Par exemple, le signal reçu par l'utilisateur k, le SINR du $i^{\text{ème}}$ flux du $k^{\text{ème}}$ récepteur et le sum rate total (SR) peuvent être calculés

en utilisation Eq. (1.2), Eq. (1.4) et Eq. (1.6), respectivement.

L'objectif principal des algorithmes d'IA basés sur la sélection de flux est donné par Eq. (1.11). Du fait de l'hétérogénéité, une contrainte supplémentaire permettant d'allouer au moins un flux à chaque utilisateur est ajoutée dans l'objectif principal. Le schéma de sélection de flux qui maximise le sum rate total du réseau tout en garantissant la sélection d'au moins un flux pour chaque utilisateur peut être comme suit.

$$\{(\mathbf{T}_k^*, \mathbf{D}_k^*)\}_{k=1,\ldots,K} = \underset{\mathbf{T}_k, \mathbf{D}_k}{\operatorname{argmax}} \, (\mathrm{SR}) \tag{1.14a}$$

$$\text{s.t.} \quad q_k \geq 1, \quad \forall k \tag{1.14b}$$

1.6 Réseaux d'interférences partiellement connectés

Dans cette section, nous proposons l'algorithme ISNSSS pour les réseaux d'interférences partiellement connectés.

Algorithme (ISNSSS) de sélection successive perfectionnée de flux

L'algorithme ISNSSS construit d'abord des séquences de flux en commençant par un pico-flux, puisque le SNR moyen des pico-utilisateurs est plus grand que celui des macro-utilisateurs. Après avoir sélectionné un pico-flux, les flux avec la contribution la plus forte au sum rate sont sélectionnés. A chaque étape de la sélection, nous effectuons des projections orthogonales successives sur le noyau du flux sélectionné. La clé de cette approche réside dans la détermination des séquences de flux qui produisent le plus haut sum rate parmi toutes les combinaisons de flux initialisées par les pico-flux.

L'ensemble d'initialisation qui inclut uniquement les flux des pico-utilisateurs est Ξ. Une fois le premier flux sélectionné parmi les pico-flux, le flux avec la valeur singulière maximale augmentant le sum rate est choisi dans l'ensemble Ω, qui contient tous les flux disponibles. Si un tel flux n'existe pas, le flux qui entraîne la réduction minimale du sum rate est choisi pour un utilisateur sans flux associé. La construction de la séquence de flux se poursuit jusqu'à ce qu'aucun flux ne puisse être sélectionné. La séquence de flux obtenue après convergence de l'algorithme est notée Ψ. L'ensemble de la procédure est décrit dans l'Alg. 4.

Alg. 4 Algorithme de sélection successive perfectionnée de flux(ISNSSS)

Entrée: α_{kj}, $\mathbf{H}_{kj}$ $\forall k, j$

Construction de l'ensemble d'initialisation Ξ

$\Xi = \{(k,l)|\ k \in \Gamma \text{ and } l = 1, ..., d_k\}$

for chaque flux $(k^*, l^*) \in \Xi$ **do**

1. Initialisation des variables

$\Psi = \emptyset$; $\mathbf{T} = \emptyset$; $\mathbf{D} = \emptyset$; $q_k = 0$ et $\mathbf{H}_{kk}^{\perp} = \mathbf{H}_{kk}$ for $k = 1, ..., K$; finish = FALSE

2. Calculer la SVD de tous les canaux

$(\alpha_{kk}\mathbf{H}_{kk}) = \mathbf{U}_k\mathbf{S}_k\mathbf{V}_k^H$ pour $k = 1, ..., K$

3. Initialisation l'ensemble à sélectionner (k^*, l^*)

$\Psi = \Psi \cup (k^*, l^*)$

$q_{k^*} = q_{k^*} + 1$

4. Appliquer **Alg. 1**

6. Construire

$\Omega = \{(\mathbf{S}_k)(l,l)|k = 1, ..., K \text{ and } l = 1, ..., d_k\}$

8. Continuer la sélection de flux (cette étape est décrite à la page suivante)

9. Calculer $(\mathbf{T}_k)_\Psi$, $(\mathbf{D}_k)_\Psi$ et SR_Ψ pour la séquence de flux Ψ

end for

Sélectionner la meilleure séquence de flux d'après Eq. (1.11)

$\Psi^* = \underset{\Psi}{\text{argmax}}\ \mathrm{SR}_\Psi$

$\mathbf{T}_k^* = (\mathbf{T}_k)_{\Psi^*}$, $\mathbf{D}_k^* = (\mathbf{D}_k)_{\Psi^*}$ pour $k = 1, ..., K$

Sortie: $\mathbf{T}_k^*$, $\mathbf{D}_k^*$ $\forall k$

8. Continuer la sélection de flux
while finish = FALSE **do**
8.1. Calculer le SR_{Ψ}
8.2. Sélectionner un flux
Construire l'ensemble des flux qui augmente le sum-rate

$$\Omega' = \left\{ \mathbf{S}_k(l,l) \in \Omega |\ \mathrm{SR}_{\Psi \cup (k,l)} > \mathrm{SR}_{\Psi} \right\}$$

if $\Omega' \neq \emptyset$ **then**

$$(k',l') = \underset{(k,l) \text{ such that } \mathbf{S}_k(l,l) \in \Omega'}{\operatorname{argmax}} \mathbf{S}_k(l,l)$$

else
Construire l'ensemble des flux qui réduit le moins le sum-rate parmi les utilisateurs sans flux associé

$$\Omega_k'' = \begin{cases} \emptyset, & \text{if } q_k \neq 0 \\ \left\{ \mathbf{S}_k(l',l') |\ l' = \underset{l}{\operatorname{argmin}} \left\{ \mathrm{SR}_{\Psi} - \mathrm{SR}_{\Psi \cup (k,l)} \right\} \right\}, & \text{if } q_k = 0 \end{cases}$$

$$\text{for } k = 1, ..., K$$

$$\Omega'' = \Omega_1'' \cup \ldots \cup \Omega_K''$$

if $\Omega'' \neq \emptyset$ **then**

$$(k',l') = \underset{(k,l) \text{ such that } \mathbf{S}_k(l,l) \in \Omega''}{\operatorname{argmin}} \left\{ \mathrm{SR}_{\Psi} - \mathrm{SR}_{\Psi \cup (k,l)} \right\}$$

else
finish = TRUE
end if
end if
8.3. Continuer la sélection de flux
if finish = FALSE **then**
8.3.1. Mettre à jour
$\Psi = \Psi \cup (k',l')$, $q_{k'} = q_{k'} + 1$
8.3.2. Appliquer **Alg. 1**
8.3.4. Reconstruire Ω
$\Omega = \{ (\mathbf{S}_k)(l,l) | k = 1, ..., K \text{ and } l = 1, ..., d_k \text{ et } (k,l) \notin \Psi \}$
end if
end while

1.7 Réseaux d'interférences entièrement connectés

Dans cette section, nous proposons un algorithme pour des réseaux d'interférences entièrement connectés où des pico-cellules sont déployées à proximité les unes des autres. L'algorithme proposé pour les réseaux d'interférences entièrement connectés est développé en analysant les données collectées lors des recherches exhaustives. La construction des séquences de flux basée sur la structure régulière est exprimée une fois la recherche exhaustive expliquée.

1.7.1 Recherche exhaustive pour les réseaux hétérogènes

Bien que la recherche exhaustive soit expliquée dans les sections précédentes, il y a une contrainte supplémentaire consistant à sélectionner au moins un flux pour chaque utilisateur. Puisque l'ensemble Φ_j défini dans Eq. (1.13) inclut toutes les séquences de flux possibles, un ensemble supplémentaire est défini comme l'ensemble Π dans lequel toutes les séquences de flux, incluant au moins un flux pour chaque couple (station de base-utilisateur) sont stockées. L'ensemble Π peut se définir comme suit.

$$\begin{aligned}\Pi = \Big\{ & \pi = (\pi_1 \pi_2 \dots \pi_j) \mid \pi \in \Phi_j;\ j \geq K; \\ & \forall k, \exists m \in \{1, \dots, j\} \text{ such that } k_m = k \Big\}\end{aligned} \tag{1.15}$$

1.7.2 Algorithme (ASNSSS) de sélection successive avancée de flux

Cet algorithme est développé en analysant les données collectées par les recherches exhaustives. Il réalise la sélection d'une séquence de flux parmi un ensemble prédéterminé de séquences afin de réduire la complexité tout en respectant Eq. (1.14b). Cet ensemble prédéterminé est composé de séquences ayant la plus forte probabilité d'occurrence lors de la recherche exhaustive. Les séquences dans cet ensemble prédéterminé ont une structure régulière. La construction des séquences de flux basées sur la structure régulière est exprimée comme suit.

Les séquences de flux générées sont stockées dans l'ensemble Π_A, pouvant contenir de multiples séquences de flux initialisées avec un même pico-flux. Pour cela, nous définissons les ensembles suivants construits pour chaque pico-utilisateur $k' \in \Gamma$.

- $\Xi_{k'} = \Big\{\pi = \left(\pi_1 \pi_2 \dots \pi_{d_{k'}}\right) | \pi \in \Phi; \forall i \in \{1, \dots, d_{k'}\}, \pi_i = (k', l_i)$
  for some $l_i \in \{1, \dots, d_{k'}\}\Big\}$ (1.16)

où la définition de l'ensemble Φ est donnée dans Eq. (1.12). En d'autres termes, l'ensemble $\Xi_{k'}$ inclut des séquences de flux π qui se composent de permutations de flux de longueur $d_{k'}$ appartenant au pico-utilisateur k'. C'est pourquoi le nombre d'éléments de $\Xi_{k'}$ est $|\Xi_{k'}| = d_{k'}!$.

- $\Upsilon_{k',h'} = \Big\{\pi = \left(\pi_1 \pi_2 \dots \pi_{|\Gamma|-2}\right) \mid \pi \in \Phi;$
  $\forall i \in \{1, \dots, |\Gamma| - 2\}, k_i \in \Gamma \setminus \{k', h'\},$ and $k_i \neq k_j$ if $i \neq j\Big\}$ (1.17)

L'ensemble $\Upsilon_{k',h'}$ comporte deux indices. L'indice k' est utilisé pour isoler les flux du pico-utilisateur k' qui sont utilisés pour la construction de $\Xi_{k'}$ et l'indice h' est utilisé pour isoler les flux du pico-utilisateur h', un flux parmi ceux-ci étant considéré pour la construction de l'ensemble $\Delta_{h'}$. Le nombre d'éléments de cet ensemble est calculé comme suit.

$$\left|\Upsilon_{k',h'}\right| = (|\Gamma| - 2)! \times \prod_{i \in \Gamma \setminus \{k',h'\}} d_i \tag{1.18}$$

Notez que si $|\Gamma| = 2$, $\Upsilon_{k',h'} = \emptyset$.

- $\Lambda = \Big\{p |\ p = (k, l) \text{ and } k, l = 1\Big\}$ (1.19)

Puisque l'ensemble Λ ne contient que le flux le plus fort du macro-utilisateur, $|\Lambda| = 1$.

- $\Delta_{h'} = \Big\{p |\ p = (h', l) \text{ and } l = 1\Big\}$ (1.20)

Par ailleurs, le nombre d'éléments de cet ensemble est $|\Delta_{h'}| = 1$. C'est à dire que l'ensemble $\Delta_{h'}$ contient le flux le plus fort du pico-utilisateur restant.

D'après les ensembles ci-dessus, Π_A est construit comme suit.

$$\Pi_A = \bigcup_{k' \in \Gamma} \Xi_{k'} \times \left(\bigcup_{h' \in \Gamma \setminus \{k'\}} \Upsilon_{k',h'} \times \Lambda \times \Delta_{h'} \right) \tag{1.21}$$

En construisant l'ensemble Π_A l'alignement d'interférence est implémenté suite à la sélection de chaque flux. Après la séquence de sélection de flux dans Π_A, il peut encore être

possible d'augmenter le sum-rate en sélectionnant des flux supplémentaires. Ceci est réalisé en essayant de sélectionner le plus fort des flux depuis l'ensemble composé des flux non-sélectionnés restants et défini comme suit:

$$\Omega = \left\{ (\mathbf{S}_k)(l,l) | k = 1, ..., K,\ l = 1, ..., d_k \text{ and } (k,l) \notin \pi_A^* \right\}$$

où π_A^* est la séquence des flux sélectionnés.

L'ensemble de la procédure de l'algorithme ASNSSS est décrit dans Alg. 5.

Alg. 5 Algorithme (ASNSSS) de sélection successive avancée de noyaux de flux

Entrée: α_{kj}, $\mathbf{H}_{kj}$ $\forall k, j$
Initialiser l'ensemble Π_A
for chaque séquence de flux $\pi \in \Pi_A$ **do**
  Appliquer **Alg. 2**
end for
Sélectionner les matrices de pré- et post-codage pour la permutation qui maximise le sum-rate
  $\pi_A^* = \underset{\pi \in \Pi_A}{\text{argmax}}\ \text{SR}_\pi$
  $\mathbf{T}_k = (\mathbf{T}_k)_{\pi_A^*}$, $\mathbf{D}_k = (\mathbf{D}_k)_{\pi_A^*}$ pour $k = 1, ..., K$
Initialisation des variables
  finish = FALSE
Construire Ω
  $\Omega = \left\{ (\mathbf{S}_k)(l,l) | k = 1, ..., K \text{ and } l = 1, ..., d_k \text{ and } (k,l) \notin \pi_A^* \right\}$
while finish = FALSE **do**
  Construire l'ensemble de flux augmentant le sum-rate
    $\Omega' = \left\{ \mathbf{S}_k(l,l) \in \Omega | \ \text{SR}_{\Psi \cup (k,l)} > \text{SR}_\Psi \right\}$
  if $\Omega' \neq \emptyset$ **then**
    $(k^*, l^*) = \underset{(k,l) \text{ such that } \mathbf{S}_k(l,l) \in \Omega'}{\text{argmax}}\ \mathbf{S}_k(l,l)$
    Mettre à jour
      $\pi_A^* = \pi_A^* \cup (k^*, l^*)$
      $q_{k^*} = q_{k^*} + 1$
    Appliquer **Alg. 1**
    Reconstruire Ω
      $\Omega = \left\{ (\mathbf{S}_k)(l,l) | k = 1, ..., K \text{ and } l = 1, ..., d_k \text{ and } (k,l) \notin \pi_A^* \right\}$
  else
    finish = TRUE
  end if
  Créer les matrices de pré- et post-codage pour la séquence construite
    $\mathbf{T}_k^* = \mathbf{T}_k$, $\mathbf{D}_k^* = \mathbf{D}_k$ for $k = 1, ..., K$
end while
Sortie: $\mathbf{T}_k^*$, $\mathbf{D}_k^*$ $\forall k$

1.8 Résultats de performance pour le cas CSI parfait

Dans cette section, les performances des algorithmes proposés à la fois pour les réseaux d'interférences partiellement et entièrement connectés sont fournies en incluant un nombre différent de pico-cellules.

Nous considérons des scénarios dans lesquels il y a 2 antennes d'émission par pico-cellule et 4 antennes d'émission par macro-cellule. Chaque cellule comprend un utilisateur placé aléatoirement dans sa zone de couverture et chaque utilisateur dispose de 2 antennes de réception.

Pour étudier les résultats de performance des algorithmes proposés, les pico-cellules sont déployées en bordure d'une macro-cellule. Les emplacements des pico-cellules sont identifiés en utilisant le rapport d/R où R est le rayon de la macro-cellule et d est la distance entre la station de base macro et chaque station de base pico. De plus, le niveau d'interférence généré entre les pico-cellules est étudié en modifiant la distance L entre pico-cellules, alors que d/R reste fixe.

1.8.1 Scénarios pour les réseaux d'interférences partiellement connectés

Scénario 1.2 : d/R varie pour 2 pico-cellules

Dans ce scénario, il y a au total 6 flux dont 4 appartiennent aux pico-utilisateurs. C'est pourquoi 4 séquences de flux sont initialisées par les pico-flux.

Dans la Figure 1.1, ces méthodes sont également comparées aux méthodes d'IA existantes. La performance de l'algorithme ISNSSS est ainsi supérieure à celle des autres algorithmes d'IA.

Par ailleurs les complexités des algorithmes de sélection de flux sont comparées dans le Tableau 1.1. Il apparait que la recherche exhaustive est plus complexe par comparaison à l'algorithme ISNSSS, le nombre total de flux du réseau augmentant sensiblement.

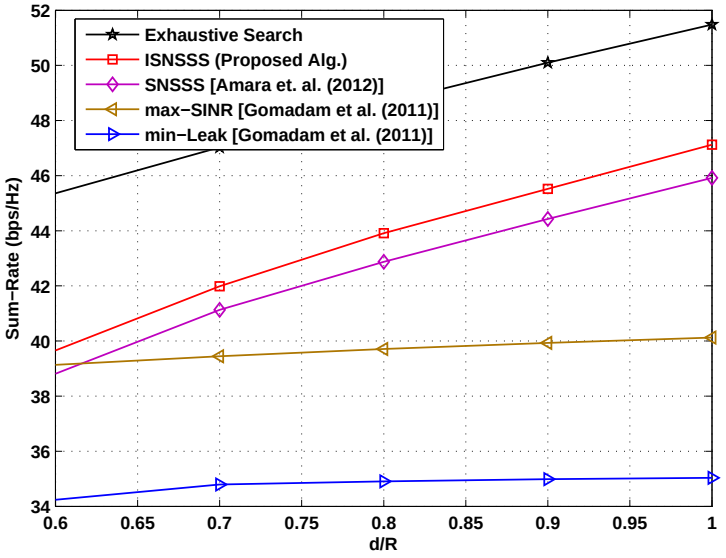

Figure 1.1: Scénario 1.2: Sum-rate moyen par rapport à d/R.

Table 1.1: Scénario 1.2: Complexité des algorithmes de sélection de flux dans le cas de 2 pico-cellules

Recherche exhaustive	**ISNSSS**	**SNSSS**
9720	24	6

1.8.2 Scénarios pour les réseaux d'interférences entièrement connectés

Scénario 2.1: d/R varie alors que L reste fixe

Afin d'évaluer l'algorithme ASNSSS pour ce scénario, les pico-cellules sont rapprochées de la bordure de la macro-cellule en modifiant le rapport d/R. La distance entre les pico-cellules reste constante avec $L = 150$m pour permettre des scénarios entièrement connectés.

Les valeurs de sum rate atteintes avec différentes approches d'IA sont fournies à la Figure 1.2. On observe que l'algorithme ASNSSS est plus performant que les méthodes de sélection de flux existantes et que les approches itératives.

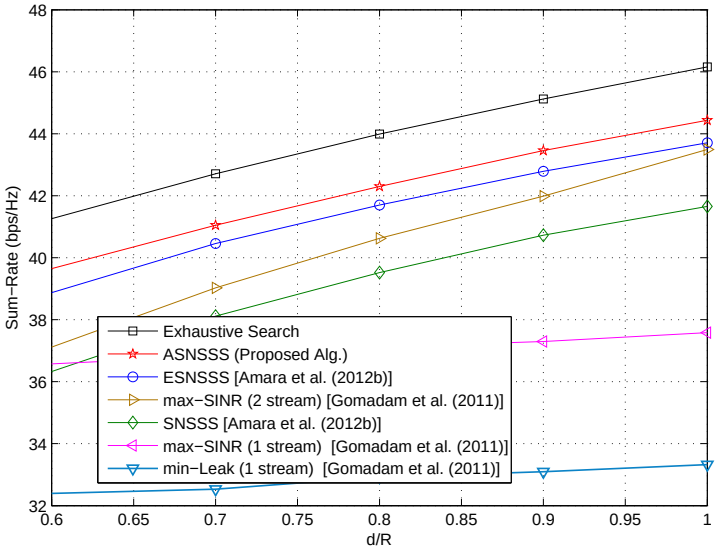

Figure 1.2: Scénario 2.1: Sum-rate moyen par rapport à d/R entre 0.6 et 1

Table 1.2: Scénario 2.1: Comparaison de la complexité pour les algorithmes de sélection de flux dans le cas de 2 pico-cellules

Recherche exhaustive	**ASNSSS**	**ESNSSS**	**SNSSS**
9720	24	36	6

Les résultats montrent que l'algorithme ASNSSS a une complexité plus faible avec une structure régulière simple par comparaison aux autres algorithmes d'IA basés sur la

sélection de flux.

1.9 Modèle du système pour le cas CSI imparfait

Les modèles pour la transmission et la quantification du canal dans le cas CSI imparfait sont donnés dans les sections suivantes.

1.9.1 Modèle de transmission

Nous modifions Eq. (1.1) pour le cas CSI imparfait et définissons le signal transmis en utilisant $\tilde{\mathbf{T}}_k$ et $\tilde{\mathbf{D}}_k$ au lieu de $\mathbf{T}_k$ et $\mathbf{D}_k$, qui sont obtenus par les algorithmes proposés dans le canal quantifié $\tilde{\mathbf{H}}_{kj}$, entre le $j^{\text{ème}}$ émetteur et le $k^{\text{ème}}$ récepteur, de dimension $N_{R_k} \times N_{T_j}$.

Le débit de données atteignable pour le $i^{\text{ème}}$ flux du $k^{\text{ème}}$ utilisateur peut être exprimé comme suit.

$$\tilde{\mathrm{R}}'_{ki} = \log_2(1 + \tilde{\gamma}'_{ki}) \tag{1.22}$$

où $\tilde{\gamma}'_k$ est le SINR atteignable pour le $i^{\text{ème}}$ flux du $k^{\text{ème}}$ récepteur et est donné par

$$\tilde{\gamma}'_{ki} = \frac{(P_k/q_k)\,\alpha_{kk}^2 \left(\tilde{\mathbf{d}}_k^i\right)^H \mathbf{H}_{kk} \tilde{\mathbf{t}}_k^i \left(\tilde{\mathbf{t}}_k^i\right)^H \mathbf{H}_{kk}^H \tilde{\mathbf{d}}_k^i}{\left(\tilde{\mathbf{d}}_k^i\right)^H \tilde{\mathbf{B}}'_{ki} \tilde{\mathbf{d}}_k^i} \qquad \forall k = 1, ..., K, \quad \forall i = 1, ..., q_k \tag{1.23}$$

La matrice de covariance interférence plus bruit du flux i du $k^{\text{ème}}$ récepteur, $\tilde{\mathbf{B}}'_{ki}$ est définie comme

$$\tilde{\mathbf{B}}'_{ki} = \sum_{\substack{l=1,\\ l\neq i}}^{q_k} \frac{P_k}{q_k} \alpha_{kk}^2 \mathbf{H}_{kk} \tilde{\mathbf{t}}_k^l \tilde{\mathbf{t}}_k^{lH} \mathbf{H}_{kk}^H + \sum_{\substack{j=1\\ j\neq k}}^{K} \sum_{q=1}^{q_j} \frac{P_j}{q_j} \alpha_{kj}^2 \mathbf{H}_{kj} \tilde{\mathbf{t}}_j^q \tilde{\mathbf{t}}_j^{qH} \mathbf{H}_{kj}^H + \sigma^2 \mathbf{I}_{N_{R_k}} \qquad \forall k = 1, ..., K, \quad \forall i = 1, ..., q_k \tag{1.24}$$

Le sum rate atteignable est calculé comme suit.

$$\tilde{\mathrm{SR}}' = \sum_{k=1}^{K} \sum_{i=1}^{q_k} \tilde{\mathrm{R}}'_{ki} \tag{1.25}$$

1.9.2 Modèle de retour limité

Dans cette section, un schéma de retour limité est présenté, reposant sur la quantification vectorielle aléatoire (RVQ). Les algorithmes d'IA proposés nécessitent tous les CSI afin d'obtenir les vecteurs de pré- et post-codage. C'est pourquoi un modèle de retour centralisé est adopté, dans lequel la station de base macro collecte tous les CSI en provenance des stations de base pico via des liens backhaul dépourvus d'erreurs et de retards. Il est supposé que le CQI est immédiatement disponible au niveau de la station de base et que les récepteurs ne renvoient que leur CDI.

1.10 Algorithme de sélection successive avancée restreinte de flux

Dans cette section, l'algorithme (RASNSSS) de sélection successive avancée restreinte de flux est présenté pour le schéma de retour limité. Lorsque le nombre de flux augmente, l'erreur de quantification augmente également pour un nombre de bits de retour donné. Autrement dit, lorsque le nombre de bits de retour est fixé, le fait de sélectionner moins de flux pour chaque utilisateur peut réduire l'interférence intra-flux dans le schéma de retour limité. Dans l'algorithme RASNSSS, une fois que les séquences de flux dans l'ensemble Π_A sont sélectionnées, il n'y a plus de sélection de flux supplémentaire, par opposition à l'algorithme ASNSSS. L'algorithme RASNSSS applique Alg. 2 en utilisant $\tilde{\mathbf{H}}_{kj}$ $\forall k, j$ au lieu de $\mathbf{H}_{kj}$ $\forall k, j$.

La construction de l'ensemble des séquences de flux,Π_A est la même que celle donnée à la Section 1.7.2.

1.11 Algorithme de sélection K-flux

Dans cette section, l'algorithme de sélection K-flux (KSS) est décrit, dans lequel une séquence de flux est sélectionnée à partir d'un ensemble prédéterminé de séquences de taille limitée. Chaque séquence de flux est construite avec différentes combinaisons des meilleurs flux de chaque utilisateur. De cette façon toutes les séquences de flux incluent un seul flux par utilisateur pour empêcher des interférences intra-flux. Chaque séquence est initialisée

avec les flux des pico-utilisateurs puisque les pico-utilisateurs sont plus susceptibles d'avoir des valeurs de SNR plus élevées en moyenne.

Chaque flux i peut être exprimé comme $\pi_i = (k_i, l_i)$ où $k_i \in \{1, \ldots, K\}$, $l_i \in \{1, \ldots, q_{k_i}\}$ et $i \in \{1, \ldots, r\}$. L'ensemble de toutes les permutations de longueur $j \in \{1, \ldots, r\}$ peut être défini comme suit.

$$\Phi_j = \left\{ \pi = (\pi_1 \pi_2 \ldots \pi_j) \,|\, \forall i, i' \in \{1, \ldots, j\},\ \pi_i \neq \pi_{i'} \text{ if } i \neq i' \right\} \tag{1.26}$$

Toutes les séquences de flux incluant au moins un flux de chaque couple (station de base-utilisateur) sont stockées dans l'ensemble Π qui peut être défini comme suit.

$$\begin{aligned} \Pi = \Big\{ & \pi = (\pi_1 \pi_2 \ldots \pi_j) \,|\, \pi \in \Phi_j;\ j \geq K; \\ & \forall k, \exists m \in \{1, \ldots, j\} \text{ such that } k_m = k \Big\} \end{aligned} \tag{1.27}$$

Les séquences de flux générées sont stockées dans l'ensemble Π_p définit comme suit.

$$\Pi_p = \left\{ \pi = (\pi_1 \pi_2 \ldots \pi_j) \,|\pi \in \Pi;\ j = K; l_1 = \ldots = l_j = 1;\ k_1 \in \Gamma \right\} \tag{1.28}$$

L'Alg. 6 décrit l'algorithme KSS qui applique Alg. 2 en utilisant $\tilde{\mathbf{H}}_{kj}\ \forall k, j$.

Alg. 6 Algorithme KSS

Entrée: α_{kj}, $\tilde{\mathbf{H}}_{kj}\ \forall k, j$
Initialiser l'ensemble Π_p tel que donné par Eq.(5.14)
for chaque séquence de flux $\pi \in \Pi_p$ **do**
  Appliquer **Alg. 2**
end for
Sélectionner les matrices de pré- et post-codage pour la permutation maximisant le sum-rate
  $\pi_p^* = \underset{\pi \in \Pi_p}{\text{argmax}}\ \tilde{\text{SR}}_\pi$
  $\tilde{\mathbf{T}}_k^* = (\tilde{\mathbf{T}}_k)_{\pi_p^*}$, $\tilde{\mathbf{D}}_k^* = (\tilde{\mathbf{D}}_k)_{\pi_p^*}$ pour $k = 1, ..., K$
Sortie: $\tilde{\mathbf{T}}_k^*$, $\tilde{\mathbf{D}}_k^*\ \forall k$

1.12 Schéma d'allocation de bit adaptatif pour CSI quantifié

Dans cette section, une allocation de bit de retour adaptative est présentée. L'objectif principal est de maximiser le sum rate moyen en optimisant le nombre de bits pour quantifier les CDI macro et pico pour chaque utilisateur. Puisque l'optimisation du nombre total

de bits pour l'ensemble du système est trop complexe, une borne supérieure est obtenue pour le débit de données de chaque utilisateur. De cette façon, le nombre total de bits de retour pour chaque utilisateur est alloué localement et de manière adaptative aux canaux.

Le problème d'optimisation de l'allocation de bit pour les algorithmes d'IA basés sur la sélection de flux peut être formulé pour le $k^{\text{ème}}$ utilisateur comme suit.

$$\begin{aligned} &\max_{B_{kj};j=1,\ldots,K} \sum_{i=1}^{q_k} \mathbb{E}\left[\tilde{\mathrm{R}}_{ki}\right] \\ &\text{s.t.} \sum_{j=1}^{K} B_{kj} \leq B_k \end{aligned} \tag{1.29}$$

Où B_k est le nombre total de bits de retour pour l'utilisateur k.

Une borne supérieure approximative est dérivée pour la solution au problème d'allocation de bit dans Eq. (1.29). La borne supérieure pour le débit de données total de chaque utilisateur est la somme des bornes supérieures des débits de chaque flux. C'est pourquoi une borne supérieure est obtenue pour chaque flux (Anand et al. [2013]). Ainsi, $\mathbb{E}\left[\tilde{\mathrm{R}}_{ki}\right]$ peut être réécrit en utilisant Eq. (1.22) comme suit.

$$\begin{aligned} &\mathbb{E}\left[\underbrace{\log_2\left(\left(P_{kk}/q_k\right)\left(\tilde{\mathbf{d}}_k^i\right)^H \mathbf{H}_{kk}\tilde{\mathbf{t}}_k^i\tilde{\mathbf{t}}_k^{iH}\mathbf{H}_{kk}^H\tilde{\mathbf{d}}_k^i\right)}_{a}\right] - \\ &\underbrace{\mathbb{E}\left[\log_2\left(\underbrace{\sum_{\substack{l=1,\\ l\neq i}}^{q_k}\left(P_{kk}/q_k\right)\left(\tilde{\mathbf{d}}_k^l\right)^H \mathbf{H}_{kk}\tilde{\mathbf{t}}_k^l\tilde{\mathbf{t}}_k^{lH}\mathbf{H}_{kk}^H\tilde{\mathbf{d}}_k^l}_{b1} + \underbrace{\sum_{\substack{j=1\\ j\neq k}}^{K}\sum_{q=1}^{q_j}\left(P_{kj}/q_j\right)\left(\tilde{\mathbf{d}}_j^q\right)^H \mathbf{H}_{kj}\tilde{\mathbf{t}}_j^q\tilde{\mathbf{t}}_j^{qH}\mathbf{H}_{kj}^H\tilde{\mathbf{d}}_j^q}_{b2} + \sigma^2\mathbf{I}_{N_{R_k}}\right)\right]}_{b} \end{aligned} \tag{1.30}$$

où P_{kj} est la puissance moyenne reçue par l'utilisateur k depuis la station de base j, calculée comme $P_{kj} = P_j\alpha_{kj}^2$.

Le problème d'optimisation peut s'exprimer comme suit pour tout flux du $k^{\text{ème}}$ utilisa-

teur.

$$\max_{B_{kj};j=1,\ldots,K} \left[\log_2 \left((P_{kk}/q_k) \left(1 - 2^{-\frac{B_{kk}}{N_{T_k} N_{R_k} - 1}} \right) \right) - \log_2 \left(\frac{P_{kk}(q_k - 1)}{q_k} 2^{-\frac{B_{kk}}{N_{T_k} N_{R_k} - 1}} + \sum_{\substack{j=1 \\ j \neq k}}^{K} P_{kj} 2^{-\frac{B_{kj}}{N_{T_j} N_{R_k} - 1}} \right) \right] \quad (1.31)$$

$$\text{s.t.} \sum_{j=1}^{K} B_{kj} \leq B_k$$

1.13 Résultats de performance pour le cas CSI imparfait

Les performances des algorithmes d'IA basés sur la sélection de flux avec CSI quantifié sont évaluées dans le Scénario 1.2 et le Scénario 2.1. Pour tous les scénarios, des schémas d'allocation de bits (BAS) différents sont réalisés pour différents nombres de bits de retour. $B_T = \sum_{k=1}^{K} B_k$, tels que $B_T = 63$ et $B_T = 120$. Les valeurs de B_1, B_2 et B_3 pour $B_T = 63$ sont BAS-3, $B_1 = 9$, $B_2 = B_3 = 27$ et BAS-4, $B_1 = B_2 = B_3 = 21$. Les valeurs de B_1, B_2 et B_3 pour $B_T = 120$ sont BAS-7,$B_1 = 10$, $B_2 = B_3 = 55$ et BAS-8, $B_1 = B_2 = B_3 = 40$.

Dans les scénarios considérés, il y a 9 canaux comprenant les canaux d'intérêt et les canaux interférents. C'est pourquoi, le nombre de bits alloués à chaque canal est 7 avec $B_T = 63$ dans le schéma d'allocation de bits égal (EBA).

1.13.1 Scénario pour des réseaux d'interférences partiellement connectés

Scénario 1.2: d/R varie pour 2 pico-cellules

Pour les réseaux d'interférences partiellement connectés, nous évaluons les algorithmes KSS et ISNSSS pour le Scénario 1.2.

Les nombres de bits alloués à chaque canal sont présentés en détail dans le Tableau 1.3 pour le schéma BAS-3 avec $B_T = 63$. Pour l'algorithme KSS, la plupart des bits sont associés aux canaux d'interférence entre la station de base macro et les pico-utilisateurs. Pour l'algorithme ISNSSS, les canaux d'intérêt des pico-utilisateurs ont plus de bits que les autres canaux afin de réduire les interférences intra-flux entre les pico-flux, puisque plusieurs flux sont sélectionnés pour les pico-utilisateurs.

Table 1.3: Scénario 1.2: Nombre moyen de bits alloués pour $B_T = 63$.

	$B_1 = 9$	$B_2 = 27$	$B_3 = 27$
KSS	$\boldsymbol{B_{11} = 4.7}$	$\boldsymbol{B_{21} = 21.8}$	$\boldsymbol{B_{31} = 21.8}$
	$B_{12} = 2.0$	$B_{22} = 5.2$	$B_{32} = 0$
	$B_{13} = 2.3$	$B_{23} = 0$	$B_{33} = 5.2$
ISNSSS	$\boldsymbol{B_{11} = 8.6}$	$B_{21} = 9.3$	$B_{31} = 9.3$
	$B_{12} = 0.2$	$\boldsymbol{B_{22} = 17.7}$	$B_{32} = 0$
	$B_{13} = 0.2$	$B_{23} = 0$	$\boldsymbol{B_{33} = 17.7}$

Les comparaisons entre le KSS, l'ISNSSS et les algorithmes existants sont présentées en Figure 1.3 pour le schéma BAS-3 avec $B_T = 63$. L'algorithme KSS est plus performant que l'ISNSSS puisqu'un seul flux est sélectionné pour chaque utilisateur, évitant ainsi l'interférence intra-flux. Les comparaisons de performance des algorithmes pour $B_T = 120$

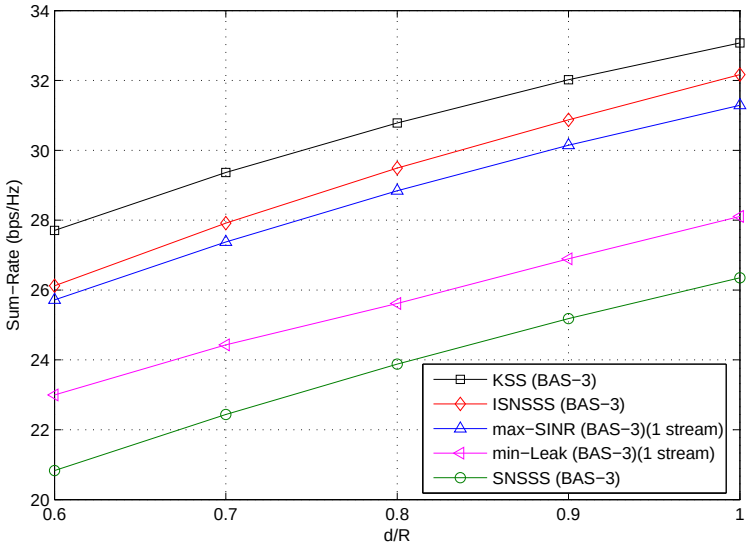

Figure 1.3: Scénario 1.2: Comparaison des différents algorithmes avec $B_T = 63$.

sont présentées en Figure 1.4. L'algorithme ISNSSS est plus performant que le KSS et les autres algorithmes existants. Puisque l'interférence intra-flux est réduite avec une erreur de quantification décroissante, sélectionner plusieurs flux améliore la performance.

Pour $B_T = 120$, l'allocation de bits détaillée pour chaque canal est donnée dans le Tableau 1.4. On remarque que le nombre de bits alloués aux canaux d'interférence entre

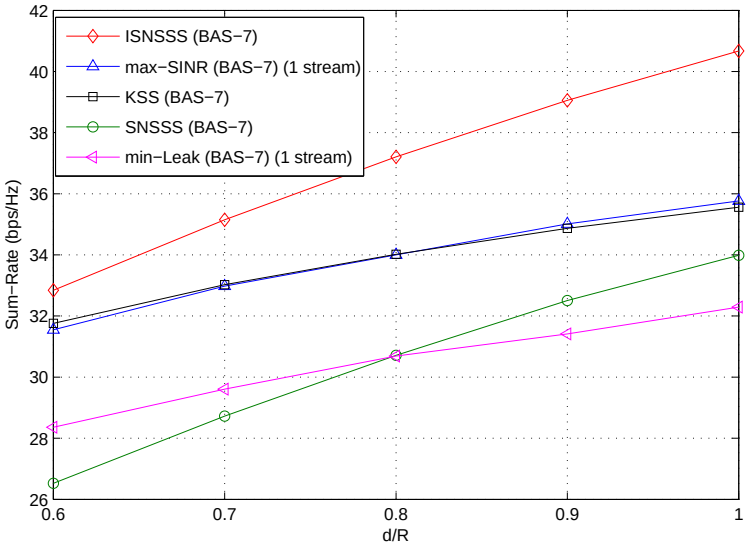

Figure 1.4: Scénario 1.2: Comparaison des différents algorithmes avec $B_T = 120$.

la station de base macro et les pico-utilisateurs est plus élevé que pour le cas où $B_T = 63$. Par ailleurs, les pico-canaux d'intérêt ont également suffisamment de bits de retour pour réduire l'interférence intra-flux entre les pico-utilisateurs.

Table 1.4: Scénario 1.2: Nombre moyen de bits alloués pour $B_T = 120$.

	$B_1 = 10$	$B_2 = 55$	$B_3 = 55$
KSS	$\boldsymbol{B_{11} = 4.8}$	$\boldsymbol{B_{21} = 49.4}$	$\boldsymbol{B_{31} = 49.4}$
	$B_{12} = 2.5$	$B_{22} = 5.2$	$B_{32} = 0.4$
	$B_{13} = 2.7$	$B_{23} = 0.4$	$B_{33} = 5.2$
ISNSSS	$\boldsymbol{B_{11} = 9.5}$	$\boldsymbol{B_{21} = 26.5}$	$\boldsymbol{B_{31} = 26.5}$
	$B_{12} = 0.2$	$\boldsymbol{B_{22} = 28.2}$	$B_{32} = 0.3$
	$B_{13} = 0.3$	$B_{23} = 0.3$	$\boldsymbol{B_{33} = 28.2}$

1.13.2 Scénario pour des réseaux d'interférences entièrement connectés

Scénario 2.1: d/R varie alors que L reste fixe

Les performances sont comparées dans la Figure 1.5 pour un schéma BAS-3 avec $B_T = 63$. Le Tableau 5.3 montre en détail le nombre moyen de bits alloués à chaque canal.

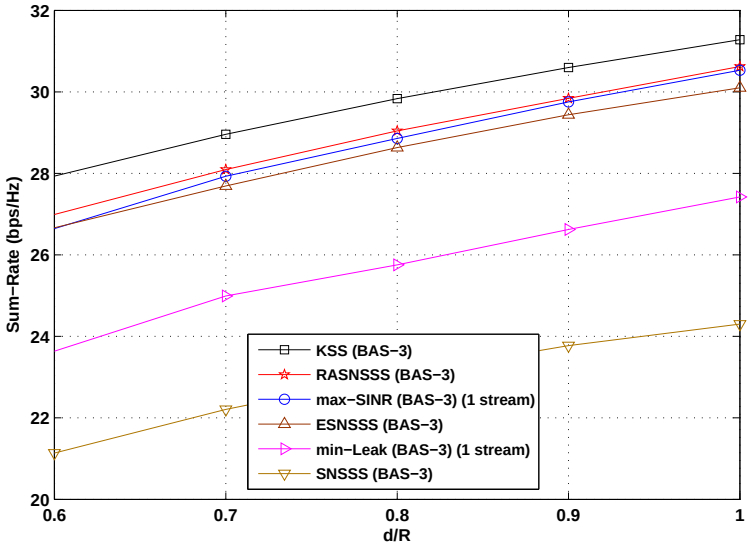

Figure 1.5: Scénario 2.1: Comparaison des différents algorithmes avec $B_T = 63$.

Pour l'algorithme KSS, puisque l'interférence générée depuis la station de base macro vers les pico-utilisateurs est fortement dominante, les canaux d'interférences entre les pico-utilisateurs et la station de base macro se voient allouer un plus grand nombre de bits, B_{21} et B_{31}. Pour l'algorithme RASNSSS, les pico-canaux d'intérêt requièrent un plus grand nombre de bits car une pico-cellule possède plus d'un flux dans l'algorithme RASNSSS. Les performances des algorithmes proposés et existants sont données à la Figure 1.6 pour

Table 1.5: Scénario 2.1: Nombre moyen de bits alloués pour $B_T = 63$.

	$B_1 = 9$	$B_2 = 27$	$B_3 = 27$
KSS	$\boldsymbol{B_{11} = 4.8}$	$\boldsymbol{B_{21} = 18.8}$	$\boldsymbol{B_{31} = 18.7}$
	$B_{12} = 2.1$	$B_{22} = 5.5$	$B_{32} = 2.8$
	$B_{13} = 2.1$	$B_{23} = 2.7$	$B_{33} = 5.5$
RASNSSS	$\boldsymbol{B_{11} = 4.8}$	$B_{21} = 9.1$	$B_{31} = 9.1$
	$B_{12} = 2.1$	$\boldsymbol{B_{22} = 16.5}$	$B_{32} = 1.1$
	$B_{13} = 2.1$	$B_{23} = 1.4$	$\boldsymbol{B_{33} = 16.8}$

le schéma BAS-7 avec $B_T = 120$. Dans ce cas, l'algorithme RASNSSS a une meilleure performance que l'algorithme KSS puisque le nombre de bits alloués est suffisant pour résoudre à la fois les canaux d'intérêt et d'interférence.

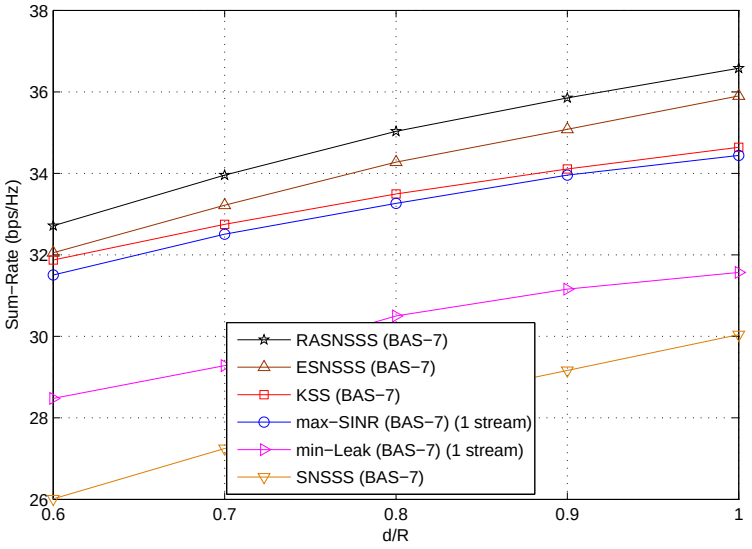

Figure 1.6: Scénario 2.1: Comparaison des différents algorithmes avec $B_T = 120$.

L'allocation de bits détaillée pour chaque canal est donnée dans le Tableau 1.6 pour le schéma BAS-7 avec $B_T = 120$. On observe que l'algorithme RASNSSS a une meilleure performance que l'algorithme KSS car les séquences de flux construites par l'algorithme RASNSSS ont une plus grande probabilité d'occurrence lors de la recherche exhaustive.

Table 1.6: Scénario 2.1: Nombre moyen de bits alloués pour $B_T = 120$.

	$B_1 = 10$	$B_2 = 55$	$B_3 = 55$
KSS	$\boldsymbol{B_{11} = 4.8}$	$\boldsymbol{B_{21} = 41.5}$	$\boldsymbol{B_{31} = 40.6}$
	$B_{12} = 2.5$	$B_{22} = 5.9$	$B_{32} = 8.5$
	$B_{13} = 2.7$	$B_{23} = 7.6$	$B_{33} = 5.9$
RASNSSS	$\boldsymbol{B_{11} = 4.8}$	$\boldsymbol{B_{21} = 23.7}$	$\boldsymbol{B_{31} = 23.6}$
	$B_{12} = 2.5$	$\boldsymbol{B_{22} = 27.3}$	$B_{32} = 4.1$
	$B_{13} = 2.7$	$B_{23} = 4.0$	$\boldsymbol{B_{33} = 27.3}$

1.14 Conclusion

Dans cette thèse, nous avons développé différents algorithmes d'IA basés sur la sélection de flux pour des réseaux hétérogènes en considérant à la fois le cas de CSI parfait et imparfait.

Pour le cas CSI parfait, deux cas différents ont été étudiés, ceux de réseaux hétérogènes partiellement et entièrement connectés. L'algorithme ISNSSS a été présenté pour le réseau d'interférence partiellement connecté et l'algorithme ASNSSS a été proposé pour les réseaux d'interférence entièrement connectés. Les résultats montrent que les algorithmes ISNSSS et ASNSSS ont de meilleures performances que les algorithmes d'IA itératifs. Par comparaison aux algorithmes d'IA basés sur la sélection de flux existants, les algorithmes proposés peuvent en moyenne allouer davantage de flux aux pico-utilisateurs tout en assurant un meilleur service et en augmentant le sum rate. Par ailleurs les algorithmes ASNSSS et ISNSSS réduisent significativement la complexité de la recherche exhaustive.

Pour le cas CSI imparfait, un schéma de retour limité a été considéré pour les algorithmes proposés. L'algorithme ASNSSS a été adapté en algorithme RASNSSS. De plus, un nouvel algorithme de sélection de flux, nommé KSS, a été proposé. Les résultats ont montré que les schémas d'allocation de bit adaptatifs améliorent les performances des algorithmes par rapport aux allocations de bits égales. On a observé qu'allouer plus de bits aux canaux d'interférence entre la station de base macro et les pico-utilisateurs donne de meilleurs résultats. Pour un nombre raisonnable de bits de retour, l'algorithme KSS a une meilleure performance que les algorithmes de sélection de flux et les algorithmes d'IA itératifs existants. D'un autre côté, lorsqu'il existe un nombre suffisant de bits pour améliorer la qualité CSI, les algorithmes RASNSSS et ISNSSS ont de meilleures performances que l'algorithme KSS. En d'autres termes, allouer plus de bits réduit l'interférence intra-flux; c'est pourquoi plus de flux peuvent être sélectionnés pour chaque utilisateur ce qui résulte en une augmentation du sum rate. Cependant, la charge de retour augmente et la conception du code-book devient plus complexe avec le nombre croissant de bits, ce qui n'est pas pratique pour un schéma à retour limité. C'est pourquoi nous proposons l'algorithme KSS pour les implémentations pratiques.

Part II

part 2

Introduction

1.15 Motivation of the Thesis

As the demand of higher data rates and the quality of service are increasing in wireless communication, innovative approaches and solutions have been investigated to increase the spectral efficiency. Drastic changes are required in wireless communication systems to maintain the quality of service (QoS) in a heavy loaded network. In order to provide the necessary capacities to support high data rate services, novel wireless system architectures will be utilized. Therefore, heterogeneous networks are considered as a promising technique for cellular networks since they provide a deployment of large number of smaller cells with different transmit power levels under the coverage of the conventional macro cell. Even if this overlaying cellular network provides a coverage extension and a capacity increase, the network topology brings up the technical challenge of the interference management. Therefore, several interference management approaches have been developed.

Interference alignment (IA) is one of the techniques to effectively mitigate the interference in wireless networks (Jafar [2011]). It has been introduced as a linear precoding technique that aligns the interfering signals in time, frequency, or space. The key idea is to align the interfering signals into one dimensional subspace at each receiver by designing precoding and postcoding vectors so that the desired signal can be obtained in the interference-free signal subspaces. In the study of Cadambe and Jafar [2008], it has been shown that all the interference can be concentrated on one half of the signal space at each receiver, leaving the other half available to the desired signal and free of interference. However, there are some problems due to the nature of interference alignment methods. For instance, the number of alignment constraints grows very rapidly as the number of the

users increases in the network, so larger signal space is required for each user to recover nearly half of it.

Closed form solutions for the IA problem are difficult to obtain for large scale networks; therefore, iterative and distributed IA approaches have been intensively studied in the literature (Gomadam et al. [2008a]). Multiple input multiple output (MIMO) IA precoders and postcoders are iteratively designed in the distributed IA solutions under the assumption of the channel state information (CSI) availability at the transmitters. One of the studied iterative IA algorithm is called the minimum interference leakage (min-Leak) algorithm in which the users reduce the interference leakage in the received signal at each iteration. Another iterative IA algorithm has been examined that maximizes the signal-to-interference-plus-noise ratio (SINR) per stream and it is called max-SINR algorithm. Only the local channel knowledge at each node is required for both iterative algorithms. In the study of Schreck and Wunder [2011], max-SINR algorithm has been adapted for the cellular networks by considering the intra-cell interference only at the receivers. Another iterative IA approach has been studied based on an alternating minimization method (Peters and Jr. [2009]). In the study of Schmidt et al. [2009], an algorithm similar to max-SINR which iteratively minimizes the sum mean square error (MSE) of all the receivers has been studied. The disadvantage of the iterative approaches is that they generally require too many iterations. Another problem in such iterative algorithms is that converging to an optimal solution has not been proven. In the study of Wilson and Veeravalli [2013], max-SINR algorithm has been modified by adding a power control step performed at each iteration to balance the received SINR at both forward and reverse direction of communication and it has been shown the algorithm converges to a local maximum.

All the aforementioned studies are based on a transmission with a fixed number of streams that depends on the feasibility conditions. It has been shown that the IA is achievable if and only if $(N_{T_k} + N_{R_k}) \geq q_k(K+1)$ where K is the number of user and the base station pair, N_{T_k} and N_{R_k} are the number of transmit and receive antennas of each user, respectively, and q_k is the number of data streams (Yetis et al. [2010]). Stream selection algorithms are able to select different number of streams for each user (Amara et al. [2011], Sun and Jorswieck [2016]). Stream selection based IA approaches are inspired

from user selection problems (Yoo and Goldsmith [2006], Sun and McKay [2010]). The idea is to mitigate the interference between the selected streams by performing orthogonal projections after selecting each stream (Amara et al. [2011], Amara et al. [2012b], Amara et al. [2012a]).

Since the stream selection based IA approaches are not iterative and they can dynamically select streams for each user, they are promising techniques. Therefore, in this thesis, we study on the stream selection based IA algorithms for heterogeneous networks. The proposed selection algorithms are based on constructing sets of stream sequences derived according to the heterogeneous network characteristics.

The most challenging drawback of the IA approach is the requirement of the CSI at the transmitters. Most of the IA algorithms are based on the perfect CSI at the transmitters and/or receivers, however this assumption is not realistic. Therefore, there are many studies that focus on CSI in IA methods and techniques to increase the accuracy of the channel (Kim et al. [2012]), (de Kerret and Gesbert [2012]), (Rao et al. [2013]), (Schreck et al. [2015]). In addition, obtaining CSI in heterogeneous networks has been investigated considering the distinctive features of the heterogeneous networks, such as the unequal number of transmit antennas and transmit power levels (Niu et al. [2014]), (Rihan et al. [2015]). Therefore, we propose stream selection based IA algorithms for the limited feedback schemes in heterogeneous networks in this thesis. Adaptive feedback bit allocation schemes are presented to improve the performance of the proposed algorithms with the imperfect CSI.

1.16 Organization of the Thesis

The organization of the thesis is given as follows.

Chapter 2 gives background knowledge for the following chapters. We first define the wireless interference channels and the concept of the interference alignment. Next, we briefly review the wireless channel models. Since CSI is very important for interference alignment, we explain the quantization procedure and CSI feedback topologies. Finally, we introduce the concept of the heterogeneous networks.

In Chapter 3, the IA algorithms that have been addressed in the thesis are presented in detail. The existing IA algorithms, including iterative and stream selection based IA, are explained and their performances are compared for K pair interference channel assuming each transmitter has equal transmit power and each user has the same location in the cell.

In Chapter 4, interference in the heterogeneous networks is handled assuming the perfect CSI is available at the transmitters. Two stream selection based IA algorithms are proposed for two different deployments of pico cells named partially connected and fully connected networks. The networks in which the interference between the pico cells can be negligible are referred as partially connected networks. To obtain a partially connected network, a scenario in which the pico cells are separately deployed is considered, so that they do not generate any interference to each other. They only receive interference from macro cell. For this kind of scenarios, the improved successive null space stream selection (ISNSSS) algorithm is proposed for the heterogeneous networks with one pico cell (Aycan et al. [2014]), two pico cells (Aycan Beyazit et al. [2015]) and three pico cells where the initial streams of the constructed stream sequences are selected among the pico streams. The networks in which the interference generated to a pico user from other pico BSs is very dominant are referred as fully connected networks. In the fully connected network scenario, pico cells are deployed closer to each other and each pico cell receives the interference generated from both the macro BS and other pico BSs. For this scenario, the advanced successive null space stream selection (ASNSSS) algorithm is proposed where the selection of a stream sequence is performed among a predetermined set of sequences (Aycan Beyazit et al. [2016a]). For the ISNSSS and the ASNSSS algorithms proposed for partially and fully connected networks, respectively, the aim is to increase the overall rate of the system while mitigating the interference and assigning at least one stream per each user.

In Chapter 5, the proposed ISNSSS and ASNSSS stream selection based IA algorithms are studied with imperfect CSI. For the partially connected interference networks, the performance of the ISNSSS algorithm is evaluated with the imperfect CSI (Aycan et al. [2015]). For the fully connected interference networks, the ASNSSS algorithm is modified for the case of limited feedback and it is called restricted ASNSSS (RASNSSS). RASNSSS does not

continue to select more streams after the stream sequence selection from a predetermined set of sequences, because continuing to select more streams generally causes a degradation in the achievable sum rate due to the quantization. In addition, a novel stream selection based IA algorithm is proposed called as K-stream selection (KSS) algorithm where the stream sequences are constructed by different stream combinations of the best streams from each user for both the partially and the fully connected interference networks. Similarly to the other proposed algorithms, stream sequences are initialized with the streams of pico users. In all cases, a centralized feedback topology is considered, because the proposed stream selection based IA algorithms require all CSI to compute all precoding and post-coding vectors. The macro BS collects all the CSIs from pico BSs through the delay free backhaul links. Different adaptive feedback bit allocation schemes are presented for the ISNSSS (Aycan Beyazit et al. [2016b]), the RASNSSS (Aycan Beyazit et al. [2016c]) and the KSS (Aycan Beyazit et al. [2016d]) algorithms in order to increase the system capacity for a fixed feedback load per user.

Finally, the major contributions are summarized and the perspectives to further develop the proposed approaches for next generation wireless networks are given in Chapter 5.7.

In Appendix A, the justification for the initialization of stream sequences with pico streams is given and statistical analysis of the exhaustive search are provided for the scenarios of the partially and the fully connected interference networks in Appendix B.

Part III

part 3

Chapter 2

Preliminaries

In this chapter, we provide a technical background which is necessary for the following chapters. Firstly, interference channels (ICs) are described to give fundamental insights on the interference alignment (IA) method since IC is a good model for communication in cellular networks. Secondly, we introduce the wireless channel model that we use for the rest of the thesis. Then, the techniques to obtain CSI are explained, because IA algorithms require CSI to be available at the transmitters and/or the receivers to design precoding and postcoding vectors. For this purpose, feedback topologies and quantization techniques are discussed in detail. Finally, heterogeneous networks are introduced since the main objective of this thesis is to mitigate the interference in the wireless heterogeneous networks.

2.1 Interference Channels

The K user interference channel is a simple network composed of K transmitters with N_{T_k} antennas and K receivers with N_{R_k} antennas, where each transmitter has a message for only one of the receivers, as shown in Figure 2.1. Each transmitter-receiver pair causes interference to the other pairs. Hence, if one of the pair achieves higher rate by increasing its signal-to-noise ratio (SNR), the link quality of the other pairs is decreased by the strong interference coming from the corresponding pair.

For the K user IC, the received signal can be described as follows (Cadambe and Jafar [2008]):

$$\mathbf{y}_k = \mathbf{H}_{k1}\mathbf{x}_1 + \mathbf{H}_{k2}\mathbf{x}_2 + ... + \mathbf{H}_{kK}\mathbf{x}_K + \mathbf{n}_k \tag{2.1}$$

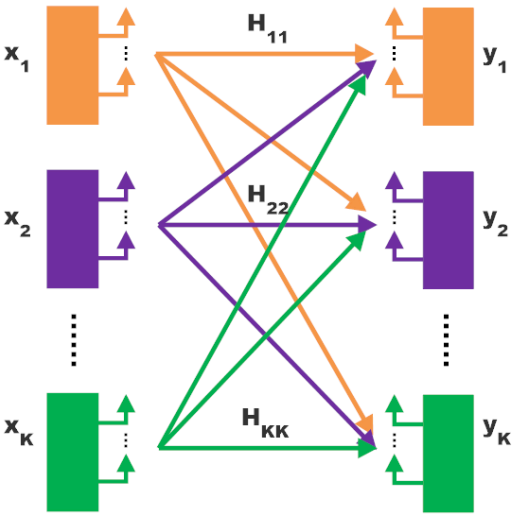

Figure 2.1: K user network interference network

where $k \in \{1, 2, ..., K\}$ is the user index, $\mathbf{y}_k$ is the output signal of the k^{th} receiver with dimension $N_{R_k} \times 1$, $\mathbf{x}_k$ is the transmitted signal from the k^{th} transmitter with dimension $N_{T_k} \times 1$, $\mathbf{H}_{kj}$ is the channel fading coefficient with dimension $N_{R_k} \times N_{T_k}$ from transmitter j to receiver k and $\mathbf{n}_k$ is the $N_{R_k} \times 1$ additive white Gaussian noise (AWGN) term. In this system model, each noise term is independent identically distributed (i.i.d.) zero-mean complex Gaussian with variance of σ^2, and channel knowledge is available at both the transmitters and the receivers.

Degrees of freedom (DoF) is the multiplexing gain and it characterizes how the achievable rate scales with transmit power as the SNR goes to infinity. In general, the spatial degrees of freedom can be considered as the number of non-interfering paths that can be obtained in an interference channel.

In a K user IC, each user can communicate with a fraction of $1/K$ DoF which is also known as a "cake-cutting" approach while IA can achieve $K/2$ DoF at each receiver. In other words, each user gets half of the cake.

IA is a linear precoding technique that aligns interfering signals in time, frequency, or space. In MIMO networks, IA uses the spatial dimension offered by multiple antennas for alignment. The key idea is that users coordinate their transmissions by using linear precoding, such that the interference signal lies in a reduced dimensional subspace at each

receiver.

The IA can be illustrated in Figure 2.2. There are three transmitter-receiver pairs. At each receiver, the undesired signals received from other transmitters are aligned onto one dimension, so that the desired signal is left out in an interference free space. For instance, $\mathbf{H}_{12}\mathbf{t}_2$ and $\mathbf{H}_{13}\mathbf{t}_3$ are aligned at the first receiver, $\mathbf{H}_{21}\mathbf{t}_1$ and $\mathbf{H}_{23}\mathbf{t}_3$ are aligned at the second receiver, and $\mathbf{H}_{31}\mathbf{t}_1$ and $\mathbf{H}_{23}\mathbf{t}_3$ are aligned at the third receiver. In this way, $\mathbf{H}_{11}\mathbf{t}_1$, $\mathbf{H}_{22}\mathbf{t}_2$ and $\mathbf{H}_{33}\mathbf{t}_3$ are obtained in an interference free space at each receiver where $\mathbf{t}_1$, $\mathbf{t}_2$ and $\mathbf{t}_3$ are the precoder vectors of transmitter 1, transmitter 2 and transmitter 3, respectively. Therefore, IA can increase the DoF, which is also known as the multiplexing gain of the

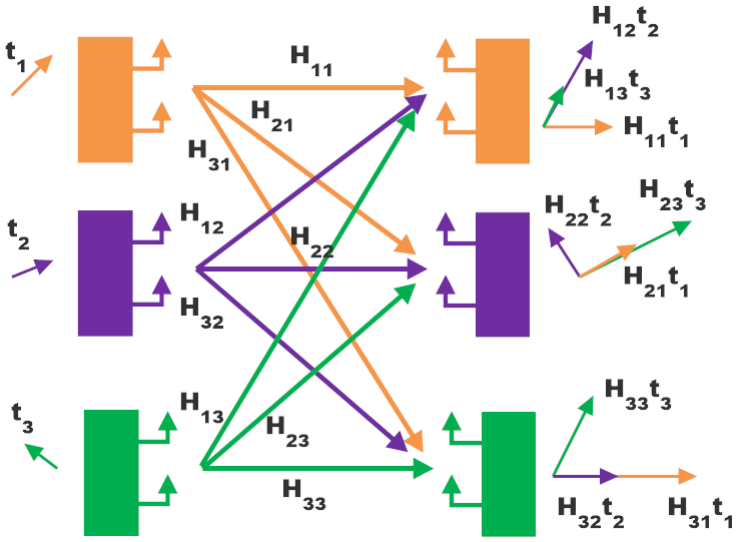

Figure 2.2: Illustration of IA for $K = 3$ with $N_{T_k} = N_{R_k} = 2$ case.

channel, so the sum rates provided by IA can approach the theoretical maximum sum capacity. Since IA can achieve maximum DoF by efficiently mitigating interference, most of the studies have been mainly focused on maximizing the sum rate of the overall system by designing and optimizing the precoders and postcoders, (Jafar and Shamai [2008]), (Cadambe and Jafar [2008]), (Gomadam et al. [2008a]), (Zhao et al. [2012]), (Fadlallah et al. [2012]), (Shi et al. [2011]), (Westreicher and Guillaud [2012]), (Amara et al. [2012b]), (Tang and Lambotharan [2013]).

The benefit of IA can be exemplified as follows. In the study of Jafar and Shamai

[2008], the DoF region D of the K user is defined as

$$D = \Big\{(d_1, d_2, ..., d_k) \in R_+^K : \forall (w_1, w_2, ..., w_k) \in R_+^K, \\ w_1 d_1 + w_2 d_2 + ... + w_k d_k \leq \limsup_{\rho \to \infty} \left[\sup_{R(\rho) \in C(\rho)} \frac{[w_1 R_1(\rho) + ... + w_k R_k(\rho)]}{log(\rho)} \right] \Big\} \tag{2.2}$$

$C(\rho)$ is the capacity region of the K-user IC, composed of the set of all achievable rate-tuples $R(\rho) = \{R_1(\rho), ..., R_K(\rho)\}$, i.e. the sets of rate tuples for which each transmitter-receiver pair is able to reliably communicate (Jafar and Shamai [2008]) and ρ defines the SNR. If the receiver is able to suppress all undesired interference, the k^{th} transmitter-receiver pair will be able to achieve d_k DoF. Finally, the number of DoF for the K user IC can be expressed as follows (Cadambe and Jafar [2008]):

$$(d_1 + d_2 + ... + d_k) \geq \frac{1}{2} \sum_{i=1}^{K} \min(N_{R_k}, N_{T_k})$$

Figure 2.3 illustrates the DoF region of the 3-user IC shown in Figure 2.2. It is seen that points A, B and C are achieved by allocating all the resources to any of the 3 users. As a result, segments AB, AC and BC can be achieved by time-sharing between any two users. However, point D can only be achieved by using IA, where each user is able to achieve 1/2 DoF, therefore maximizing the sum-rate capacity to 3/2 for the 3-user IC.

The closed form solutions to IA for both SISO and MIMO interference channels are given in the following sections.

2.1.1 K User SISO Interference Channels

For SISO channels, interference signals cannot be aligned in the space domain. However, IA is still possible in time-varying or frequency-selective fading environments.

The IA problem for the K user SISO IC can be explained by the following example. Let us consider a $K = 3$ user IC. The system model at time slot $t \in \mathbb{N}$ can be given as follows.

$$\begin{aligned} y_1(t) &= h_{11}(t)x_1(t) + h_{12}(t)x_2(t) + h_{13}(t)x_3(t) + n_1(t) \\ y_2(t) &= h_{21}(t)x_1(t) + h_{22}(t)x_2(t) + h_{23}(t)x_3(t) + n_2(t) \\ y_3(t) &= h_{31}(t)x_1(t) + h_{32}(t)x_2(t) + h_{33}(t)x_3(t) + n_3(t) \end{aligned} \tag{2.3}$$

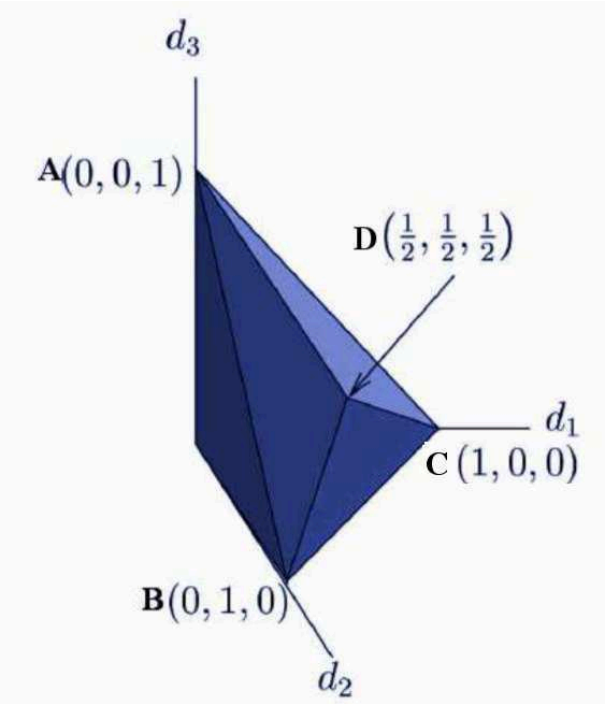

Figure 2.3: DoF region for the 3-user IC

In the study of Cadambe and Jafar [2008], since each terminal has only one antenna and there is not enough space dimension to separate interference subspace with desired signal subspace, time extension method over τ time slots is used to achieve the IA as follows.

$$\mathbf{y}'_1(t) = \mathbf{H}'_{11}(t)\mathbf{x}'_1(t) + \mathbf{H}'_{12}(t)\mathbf{x}'_2(t) + \mathbf{H}'_{13}(t)\mathbf{x}'_3(t) + \mathbf{n}'_1(t) \tag{2.4}$$

$$\mathbf{y}'_2(t) = \mathbf{H}'_{21}(t)\mathbf{x}'_1(t) + \mathbf{H}'_{22}(t)\mathbf{x}'_2(t) + \mathbf{H}'_{23}(t)\mathbf{x}'_3(t) + \mathbf{n}'_2(t) \tag{2.5}$$

$$\mathbf{y}'_3(t) = \mathbf{H}'_{31}(t)\mathbf{x}'_1(t) + \mathbf{H}'_{32}(t)\mathbf{x}'_2(t) + \mathbf{H}'_{33}(t)\mathbf{x}'_3(t) + \mathbf{n}'_3(t) \tag{2.6}$$

where $\mathbf{x}'_k(t)$ is a column vector with dimension $\tau \times 1$ representing the τ symbol extension of the input signal $x_k(t)$ and $\mathbf{y}'_k(t)$ represents the τ symbol extension of the output signal $y_k(t)$. $\mathbf{n}'_k(t)$ represents the τ symbol extension of $n_k(t)$. $\mathbf{H}'_{kj}(t)$ is the $\tau \times \tau$ dimensional diagonal extended channel matrix of the channel $h_{kj}(t)$ between the receiver k and transmitter j over the time slot t such that

$$\mathbf{H}'_{kj}(t) = \begin{bmatrix} h_{kj}(\tau(t-1)+1) & 0 & \cdots & 0 \\ 0 & h_{kj}(\tau(t-1)+2) & \cdots & 0 \\ \vdots & \vdots & \ddots & \vdots \\ 0 & 0 & \ldots & h_{kj}(\tau t) \end{bmatrix}_{\tau \times \tau} \tag{2.7}$$

This model is the so called extended IC model where each destination has a τ dimensional received signal and only the channel gain remains constant within one time slot but changes independently across different time slots.

Let $\tau = 2n+1$, where n is a positive constant. At transmitter 1, the message is encoded into $n+1$ independent data streams $s_{1,i}(t);\ i = 1, ..., n+1$. Each $s_{1,i}(t)$ is transmitted by a precoding vector t_1^i with dimension $\tau \times 1$ so that the $\mathbf{x}_1(t)$ is given as follows.

$$\mathbf{x}_1(t) = \sum_{i=1}^{n+1} s_{1,i}(t) t_1^i = \mathbf{T}_1' \mathbf{s}_1 \tag{2.8}$$

where $\mathbf{s}_1 = [s_{1,i}(t), ..., s_{1,n+1}(t)]^T$ with dimension $(n+1) \times 1$ and $\mathbf{T}_1'$ is the precoding matrix as $\mathbf{T}_1' = [t_1^1, ..., t_1^{n+1}]$ with dimension $(2n+1) \times (n+1)$. Similarly, transmitter 2 and transmitter 3 encode their messages to n independent data streams.

Since IA method aligns all the interference signals at each receiver within one half of the total received signal space and separates the desired signal to the other half interference free signal space, interference should occupy a subspace with less dimensions than the total signal space dimensions.

Thus, in order to obtain the $(n+1)$ dimensional interference-free signal, the dimension of the interference subspace should be less than or equal to n. This condition can be achieved at transmitter 1 by aligning the interference signals received from transmitter 2 and transmitter 3 as follows:

$$(\mathbf{H}_{12}'(t)\mathbf{T}_2') = (\mathbf{H}_{13}'(t)\mathbf{T}_3') \tag{2.9}$$

In addition, it should be guaranteed that the subspace spanned by the interference from transmitter 1 contains all the interference generated from the other transmitters. Therefore, to have n dimensional interference-free subspaces at receiver 2 and receiver 3, the interference signals must be aligned as:

$$\text{span}(\mathbf{H}_{23}'(t)\mathbf{T}_3') \subset \text{span}(\mathbf{H}_{21}'(t)\mathbf{T}_1') \tag{2.10}$$

$$\text{span}(\mathbf{H}_{32}'(t)\mathbf{T}_2') \subset \text{span}(\mathbf{H}_{31}'(t)\mathbf{T}_1') \tag{2.11}$$

where span($\mathbf{A}$) represents the space spanned by the column vectors of matrix $\mathbf{A}$. By satisfying these conditions, $\frac{3n+1}{2n+1}$ DoF is achieved, which converges to 3/2 as $n \to \infty$.

Different precoding matrices can be constructed using the conditions above; one set of solutions that meets these conditions are given as follows (Cadambe and Jafar [2008]):

$$\mathbf{T}'_1 = [\mathbf{u}', \mathbf{L}'\mathbf{u}', \ldots, \mathbf{L}'^{n}\mathbf{u}'] \tag{2.12}$$

$$\mathbf{T}'_2 = \mathbf{H}'^{-1}_{32}(t)\mathbf{H}'_{31}(t)[\mathbf{u}', \mathbf{L}'\mathbf{u}', \ldots, \mathbf{L}'^{n-1}\mathbf{u}'] \tag{2.13}$$

$$\mathbf{T}'_3 = \mathbf{H}'^{-1}_{23}(t)\mathbf{H}'_{21}(t)[\mathbf{L}'\mathbf{u}', \mathbf{L}'^{2}\mathbf{u}', \ldots, \mathbf{L}'^{n}\mathbf{u}'] \tag{2.14}$$

where $\mathbf{L}' = \mathbf{H}'_{12}(t)\mathbf{H}'^{-1}_{21}(t)\mathbf{H}'_{23}(t)\mathbf{H}^{-1}_{32}(t)\mathbf{H}'_{31}(t)\mathbf{H}'^{-1}_{13}(t)$ and $\mathbf{u}' = [1 \ldots \ 1]^T$ is a column vector with dimension $(2n+1) \times 1$.

In case of $K > 3$, the signals from transmitter 1 should be aligned at receivers $2, \ldots, K$. As the alignment restrictions increase, the number of constraints on $\mathbf{T}'_1$ increase. This situation can be generalized as follows.

IA problem is transformed to a problem of finding common non-trivial invariant subspaces of all $\mathbf{L}'^{(i)}$ with the above deductions. However finding common non-trivial invariant subspaces is an infeasible approach due to the following reasons:

- $\mathbf{L}'^{(i)}$'s are determined by the channel coefficients, therefore there is no control over their construction.
- Generic linear transformations do not have non-trivial common invariant subspaces.

The solution given in the study of Cadambe and Jafar [2008] is based on the assumption that the linear transformations $\mathbf{L}'^{(i)}$ are commutative with respect to multiplication. This assumption is valid for the channel matrices that have a diagonal structure, such as those that are obtained by time extension over time varying channels. However, the desired signals must be aligned separately from the interference signals at each receiver. Therefore, the trivial common invariant subspaces of diagonal matrices can not solve the IA problem.

As a conclusion, IA solutions based on symbol extensions are necessary when we are dealing with SISO networks.

2.1.2 K User MIMO Interference Channels

In the previous section, symbol extension has been explained to increase the dimensionality of the vector space in K user SISO IC since the number of antennas is insufficient

to achieve IA. In this section, we assume that there are multiple antennas at both transmitters and receivers, so that the spatial domain can be used to perform IA. If the SISO is expanded to $N_{T_k} > 1$, $N_{R_k} > 1$ case with the assumption of $N_{T_k} = N_{R_k} = M$ (when all nodes have the same number of antennas), total DoF will become $KM/2$, because it can be simply thought as splitting each node into M separate nodes. Then, K user $M \times M$ MIMO IC is transformed into the KM user 1×1 IC.

In this section, the precoding matrix $\mathbf{T}_k$ of the k^{th} transmitter is obtained for $K = 3$ MIMO IC case where $N_{T_k} = N_{R_k} = M$ to show that the dimension of interference is equal to $M/2$ at all the receivers without symbol extension (Cadambe and Jafar [2008]).

In order to obtain $M/2$ data streams, the interference at each receiver should have at maximum $M/2$ dimensions in M dimensional signal space. The interference alignment constraints that should be satisfied by designing $\mathbf{T}_k$, $\forall k$ can be expressed as follows.

$$\text{At receiver 1:} \quad \text{span}(\mathbf{H}_{12}\mathbf{T}_2) = \text{span}(\mathbf{H}_{13}\mathbf{T}_3) \tag{2.15}$$

$$\text{At receiver 2:} \quad \text{span}(\mathbf{H}_{21}\mathbf{T}_1) = \text{span}(\mathbf{H}_{23}\mathbf{T}_3) \tag{2.16}$$

$$\text{At receiver 3:} \quad \text{span}(\mathbf{H}_{31}\mathbf{T}_1) = \text{span}(\mathbf{H}_{32}\mathbf{T}_2) \tag{2.17}$$

As a consequence, the interference signals only occupy an $M/2$-dimensional subspace (Cadambe and Jafar [2008]). The above equations can be rewritten by substituting $\mathbf{T}_2$ and $\mathbf{T}_3$ into the first equation as follows.

$$\text{span}(\mathbf{T}_1) = \text{span}(\mathbf{E}\mathbf{T}_1) \tag{2.18}$$

$$\text{span}(\mathbf{T}_2) = \text{span}(\mathbf{H}_{32}^{-1}\mathbf{H}_{31}\mathbf{T}_1) \tag{2.19}$$

$$\text{span}(\mathbf{T}_3) = \text{span}(\mathbf{H}_{23}^{-1}\mathbf{H}_{21}\mathbf{T}_1) \tag{2.20}$$

where $\mathbf{E} = (\mathbf{H}_{31})^{-1}\mathbf{H}_{32}(\mathbf{H}_{12})^{-1}\mathbf{H}_{13}(\mathbf{H}_{23})^{-1}\mathbf{H}_{21}$. Let us define the eigenvectors of $\mathbf{E}$ as $\mathbf{e}_1 \dots \mathbf{e}_M$, then $\mathbf{T}_1 = [\mathbf{e}_1 \dots \mathbf{e}_{M/2}]$. So that $\mathbf{T}_2$ and $\mathbf{T}_3$ can be solved as follows.

$$\mathbf{T}_2 = (\mathbf{H}_{32})^{-1}\mathbf{H}_{31}[\mathbf{e}_1 \dots \mathbf{e}_{M/2}] \tag{2.21}$$

$$\mathbf{T}_3 = (\mathbf{H}_{23})^{-1}\mathbf{H}_{21}[\mathbf{e}_1 \dots \mathbf{e}_{M/2}] \tag{2.22}$$

In this example, each transmitter can transmit a single stream by performing IA and the receivers can retrieve the desired message from the received signal by designing postcoding

matrices with zero forcing. If the IA conditions given above are fulfilled, then the precoding and the postcoding matrices satisfy the following conditions.

$$\mathbf{D}_k^H \mathbf{H}_{kj} \mathbf{T}_j = 0, \quad \forall j \neq k \tag{2.23}$$
$$\text{rank}(\mathbf{D}_k^H \mathbf{H}_{kk} \mathbf{T}_k) = M/2, \quad \forall k$$

where $\mathbf{D}_k$ is the postcoding matrix of the k^{th} receiver.

It is clear that the explained closed form solutions are difficult to find for the large scale networks. Therefore, different IA solutions have been investigated in the literature (Gomadam et al. [2008b]), (Aycan et al. [2014]), (Akitaya and Saba [2013]),(Westreicher and Guillaud [2012]).

Furthermore, the CSI must be available at the transmitters and/or receivers to compute the closed form expressions. We will discuss methods for obtaining CSI in the next sections.

2.2 Wireless Channel Models

The characteristic of a wireless channel model can be defined depending on the factors that affect the received signal power. Main factors are explained as follows.

Path Loss:

The path loss depends on the distance between the transmitter and the receiver. If the signal travels along a straight line where there is no obstacle between the transmitter and the receiver, then the received signal is called a line-of-sight (LOS) signal. The power loss in the received signal is inversely proportional to the square of the distance between the transmitter and receiver which is also known as free-space path loss. Path loss is usually represented by traveling distance and path loss exponent which depends on the signal propagation environment (Goldsmith [2005]).

Since the path loss increases with the distance between the transmitter and the receiver, the path loss experienced by a small cell user is comparatively smaller than the macro user.

Shadowing:

The reason for shadowing is the presence of obstacles between the transmitter and the receiver that attenuate signal power through absorption, reflection, scattering, and diffrac-

tion. The variation is referred as large-scale propagation effects since the variation due to the shadowing occurs over large distances. The most common model for the shadowing effect is log-normal shadowing (Goldsmith [2005]).

Fading:

The reason of the fading is the multi-path propagation due to the scattered, reflected and diffracted components of the received signal. The variation caused by the fast fading is referred as small-scale propagation effects since the variation due to the multipath occurs over short distances. Multipath fading effect can make the received signal either stronger or weaker due to the different phases of the received rays, and is modeled as Rayleigh or Rician distribution. Different power delay profiles are standardized for pedestrian or vehicular to characterize different environment for multipath fading (Goldsmith [2005]).

2.3 Channel State Information

IA methods can achieve high number of DoF by designing the precoding and postcoding vectors to align the interfering terms on the same signal space at each receiver. However, IA algorithms require CSI to be available at the transmitters and/or receivers to calculate precoders and postcoders to align the interference generated by each transmitter. This assumption is problematic for practical systems; therefore, two methods are used to obtain CSI, which are reciprocity and feedback.

In time division duplexed systems (TDD), forward and reverse transmission share the same frequency spectrum, but they are separated in time. The channels are reciprocal in such systems, so that the channel responses are the same in both directions. Uplink channel measurements are used to obtain precoders with the reciprocity property of the networks. However, this technique has a number of potential drawbacks. The reciprocity requires tightly calibrated RF devices in TDD systems (Love et al. [2008]). On the other hand, exploiting reciprocity of the channel in frequency division duplexed (FDD) system is not possible, since the uplink and the downlink channels are separated in frequency. Therefore, the feedback schemes have been implemented for FDD systems.

CSI feedback methods are based on sending the CSI to the transmitters through feed-

back channels (Özbek and Le Ruyet [2014b]). In these systems, receivers estimate the forward channels by using the training sequences. After the estimation of the forward channels, receivers quantize the CSI, and feedback it to the transmitters, so that the precoders and postcoders can be calculated to align the interference. However, quantization procedure introduces some distortion on the CSI. Therefore, there are studies that have focused on designing quantized feedback strategies with low distortion in CSI for IA (de Kerret et al. [2013b]), (Rao et al. [2013]), (Chen and Yuen [2014]).

2.3.1 Quantization

The fundamental idea behind the limited feedback is to quantize the normalized channel which is also known as channel direction information (CDI) and channel quality indicator (CQI) at each receiver due to the limited bandwidth of the feedback channel. The CDI is obtained by normalizing the channel matrix using its Frobenius norm as $\bar{\mathbf{H}}_{kj} = \frac{\mathbf{H}_{kj}}{\|\mathbf{H}_{kj}\|_F}$, $\forall k,\ \forall j$, where $\|\mathbf{H}_{kj}\|_F$ is the channel gain which is assumed to be perfectly known at all transmitters and all receivers. The quantized CDI is fed back to the corresponding transmitters. However, quantization process introduces some distortion on the CSI.

There are different channel quantization methods implemented in the literature related with limited feedback approaches for IA, such as Grassmannian line packing (Krishnamachari and Varanasi [2010]) and random vector quantization (RVQ) (Chen and Yuen [2014]). Although RVQ is not a practical solution, it is generally used for the analytical approaches. It has been shown to be asymptotically optimal for the point-to-point MIMO link as the number of antennas tends to infinity both at the transmitter and the receiver sides (Santipach and Honig [2009]).

In case of RVQ, codewords in codebook are randomly generated for a given number of feedback bits and the CDI is quantized by selecting the codeword with the minimum distance. The distance metric used in the quantization of the CDI is an indicator of the quantization error, because distortion is caused when the CDI is replaced by the selected codeword. Chordal distance is the most utilized distance metric to obtain the quantized CDI (Rao et al. [2013], Chen and Yuen [2014]). Different channel quantization strategies have been studied to design the feedback channels for IA (Aycan et al. [2015]).

As the size of the codebook increases, the distortion caused by the limited feedback decreases, but the feedback overhead increases in the network. Therefore, the number of bits should be optimized depending on the channel conditions.

Codebook Design:

For RVQ, each codebook contains $2^{B_{kj}}$ codewords which are randomly generated, where B_{kj} is the number of quantization bits to quantize the channel between the j^{th} transmitter and the k^{th} receiver. The codewords are independent and isotropically distributed over the unit sphere.

Quantization Metrics:

First, the CDI is obtained by normalizing the channel matrix using its Frobenius norm as $\bar{\mathbf{H}}_{kj} = \frac{\mathbf{H}_{kj}}{\|\mathbf{H}_{kj}\|_F}$, $\forall k,\ \forall j$, where $\|\mathbf{H}_{kj}\|_F$ is the channel gain which is perfectly known at all transmitters and all receivers. Afterwards, $\bar{\mathbf{H}}_{kj}$ is vectorized as $\bar{\mathbf{h}}_{kj} = \text{vec}(\bar{\mathbf{H}}_{kj})$ by stacking the columns of $\bar{\mathbf{H}}_{kj}$ where $\bar{\mathbf{h}}_{kj} \in \mathbb{C}^{N_{T_k} N_{R_k} \times 1}$.

Then, the codebook for each transmitter and receiver pair is generated using RVQ as $\mathbf{W}_{kj} = \left\{ \mathbf{c}_{kj}^1 \dots \mathbf{c}_{kj}^i \dots \mathbf{c}_{kj}^{2^{B_{kj}}} \right\}$ where $\left\| \mathbf{c}_{kj}^i \right\| = 1$, $\forall i$ and $\mathbf{c}_{kj}^i \in \mathbb{C}^{N_{T_k} N_{R_k} \times 1}$. The codeword $\mathbf{c}_{kj}^{i*}$ that minimizes the given distance metric is selected as the quantized CDI, $\tilde{\bar{\mathbf{h}}}_{kj} = \mathbf{c}_{kj}^{i*}$. Then, $\mathbf{c}_{kj}^{i*}$ is reshaped to a matrix form as $\mathbf{C}_{kj}^{i*} \in \mathbb{C}^{N_{R_k} \times N_{T_k}}$. Accordingly, the quantized channel $\tilde{\mathbf{H}}_{kj}$ is calculated as $\tilde{\mathbf{H}}_{kj} = \mathbf{C}_{kj}^{i*} \times \|\mathbf{H}_{kj}\|_F$.

Chordal distance and the Euclidean distance metrics are explained as follows.

1. Chordal Distance Metric **(M1)**: The codeword $\mathbf{c}_{kj}^{i*}$ that minimizes the Chordal distance metric is chosen by

$$\mathbf{c}_{kj}^{i*} = \min d_c(\bar{\mathbf{h}}_{kj}, \mathbf{c}_{kj}^i) \tag{2.24}$$

where $d_c(\bar{\mathbf{h}}_{kj}, \mathbf{c}_{kj}^i) = \sqrt{1 - \left| \bar{\mathbf{h}}_{kj}^H \mathbf{c}_{kj}^i \right|^2}$.

2. Euclidean Distance Metric **(M2)**: The codeword $\mathbf{c}_{kj}^{i*}$ that minimizes the Euclidean distance metric is chosen by

$$\mathbf{c}_{kj}^{i*} = \min d_e(\bar{\mathbf{h}}_{kj}, \mathbf{c}_{kj}^i) \tag{2.25}$$

where $d_e(\bar{\mathbf{h}}_{kj}, \mathbf{c}_{kj}^i) = \left\| \bar{\mathbf{h}}_{kj} - \mathbf{c}_{kj}^i \right\|$.

The quantization error caused by RVQ can be modeled as follows (Cho et al. [2012], Ravindran and Jindal [2008]).

$$\begin{aligned} \tilde{\bar{\mathbf{h}}}_{kk} &= \cos\theta_{kk}\bar{\mathbf{h}}_{kk} + \sin\theta_{kk}\ \mathbf{z}_{kk} \\ &= \sqrt{1-e_{kk}}\bar{\mathbf{h}}_{kk} + \sqrt{e_{kk}}\mathbf{z}_{kk} \end{aligned} \tag{2.26}$$

where θ_{kk} is the angle between $\bar{\mathbf{h}}_{kk}$ and $\tilde{\bar{\mathbf{h}}}_{kk}$ and $e_{kk} \triangleq \sin^2\theta_{kk}$. $\mathbf{z}_{kk}$ is the unit vector representing the direction of the quantization error vector and it is isotropically distributed in the null space of $\bar{\mathbf{h}}_{kk}$. e_{kk} is the minimum of $2^{B_{kk}}$ independent $\beta((N_{t_k}N_{r_k}-1),1)$ random variables (Jindal [2006]). Accordingly, Eq. (2.26) can be expressed in matrix form using the channel matrix as follows.

$$\begin{aligned} \tilde{\bar{\mathbf{H}}}_{kk} &= \cos\theta_{kk}\bar{\mathbf{H}}_{kk} + \sin\theta_{kk}\ \mathbf{Z}_{kk} \\ &= \sqrt{1-e_{kk}}\bar{\mathbf{H}}_{kk} + \sqrt{e_{kk}}\mathbf{Z}_{kk} \end{aligned} \tag{2.27}$$

where $\mathbf{Z}_{kk} \in \mathbb{C}^{N_{R_k} \times N_{T_k}}$ is reshaped as matrix using the vector $\mathbf{z}_{kk} \in \mathbb{C}^{N_{R_k}N_{T_k} \times 1}$.

In order to generate values for $Z = e_{kk}$, the following cumulative distribution function (CDF) can be used in inverse transform sampling (Jindal [2006]).

$$F_Z(z) = P(Z \leq z) = 1 - (1 - z^{N_{R_k}N_{T_k}-1})^{2^{B_{kk}}} \tag{2.28}$$

2.3.2 Feedback Topologies

CSI can be shared using centralized or distributed feedback topologies. In the centralized topologies, IA precoding and postcoding vectors are computed in a central unit and then, these vectors are transmitted to the related nodes. In the distributed topologies, on the other hand, IA precoding and postcoding vectors are computed locally at each transmitter or receiver.

There are advantages and disadvantages of both centralized and distributed CSI feedback topologies. For instance, centralized topologies can cause feedback delay. On the other hand, in the distributed feedback systems, the precoding and postcoding vectors are separately calculated at each related terminals. However, designing an efficient exchange mechanism between transmitters and receivers is still an open issue.

Centralized Feedback Topologies:

There are different kinds of centralized topologies depending on the network structure. For example, an additional central unit is introduced to the network or one particular transmitter can be selected as a central unit with backhaul connections only to the transmitters (Cho et al. [2012]).

An example for a centralized topology can be shown in Figure 2.4 (Rao et al. [2013]).

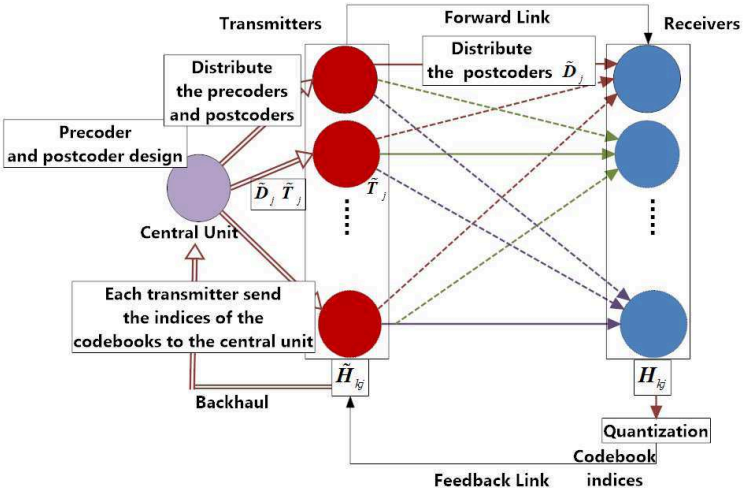

Figure 2.4: Centralized Feedback Topology

This feedback scheme adapting IA can be explained as follows.

- Each receiver quantizes all the CSI belonging to all transmitters.
- The codeword indices are fed back to the associated transmitters using feedback link.
- Transmitters forward the indices to the centralized unit through the backhaul link.
- Based on the collected information from all transmitters, centralized unit computes all the precoding and postcoding vectors.
- Centralized unit distributes the precoding and the postcoding vectors to the transmitters.
- Each transmitter forwards the postcoding vectors to its receiver using the forward control link.

The feedback overhead in Figure 2.4 can be calculated as $\underbrace{K \times K \times B_{kj}}_{\substack{\text{from receivers} \\ \text{to transmitters}}}$.

Another centralized feedback topology is based on selecting one particular transmitter as a central unit that collects all the codeword indices from all other transmitters through the backhaul as shown in Figure 2.5 (Rao and Lau [2014]).

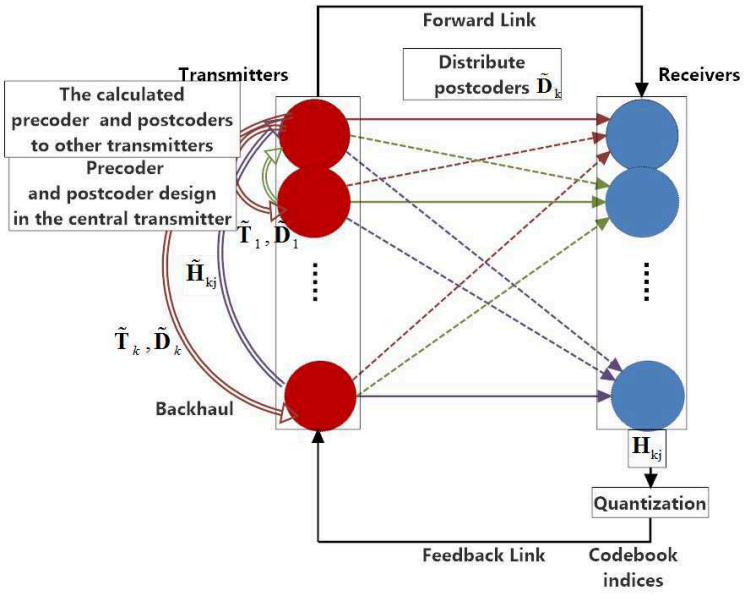

Figure 2.5: Centralized Feedback Topology

Distributed Feedback Topologies:

In the distributed CSI feedback topologies, receivers broadcast their quantized codeword indices (for the CSI), so that all the transmitters can have all the indices from all the receivers. Then the transmitters can locally calculate their own precoders and postcoders.

In comparison to the centralized feedback topology, the adaptation of the distributed feedback topology eliminates the information exchange step between the transmitters and the centralized unit. The feedback scheme illustrated in Figure 2.6 can be summarized as follows.

- Each receiver sends its codeword indices for the quantized CSI through the feedback channels.

- All the transmitters compute the precoding and postcoding vectors in a distributed manner.
- The transmitters transmit the postcoding vectors to the corresponding receivers.

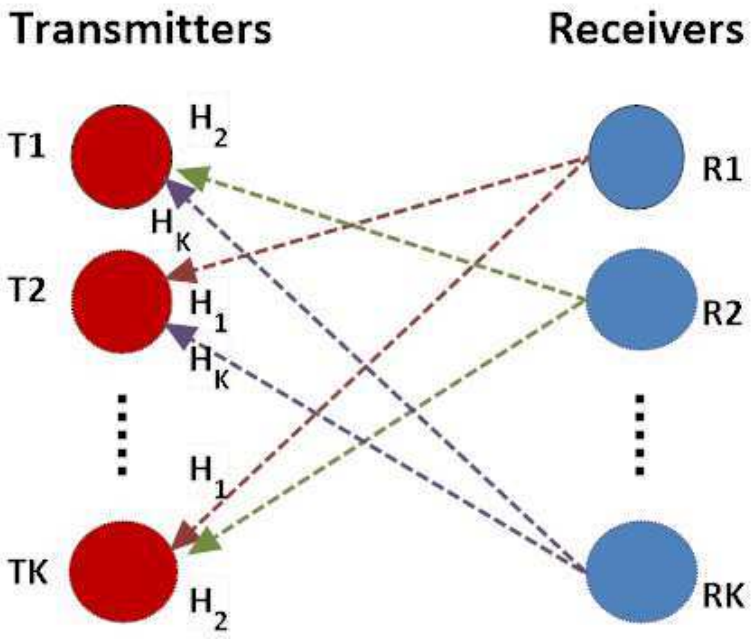

Figure 2.6: Distributed Feedback Strategy

Another distributed feedback topology has been studied using transmitter cooperation in the study of de Kerret et al. [2013a]. In this topology, each transmitter receives its own CSI and then all the transmitters cooperatively share their received information.

In addition, there are studies to decrease the feedback overhead for the distributed feedback topology. In case of having incomplete knowledge of the CSI at the transmitters, the problem of robust precoding and poscoding schemes with the partial CSI has been investigated in the literature (de Kerret and Gesbert [2012], de Kerret et al. [2013b]).

2.4 Heterogeneous Networks

Heterogeneous networks are one of the next generation network structures since they provide coverage extension and spectral efficiency (Sambo et al. [2014], Han et al. [2015]). There is a large number of base station deployment of small cells with different power levels

(micro, pico or femto cells) in the coverage of the conventional macro cell using the same spectrum. These small cells are categorized according to their transmit powers, antenna sizes, access types, and the backhaul connection to the existing cells. The goal of using low power nodes is to offload the traffic from macro cells, enhance indoor coverage, and increase the spectral efficiency in the cell edges (Zou et al. [2015]). In addition, the cost of deploying small cells is lower than the conventional macro cell.

A heterogeneous cellular network composed of micro, pico, femto and macro cell is illustrated in Figure 2.7. Solid green lines show useful signals and red dashed lines show interference signals.

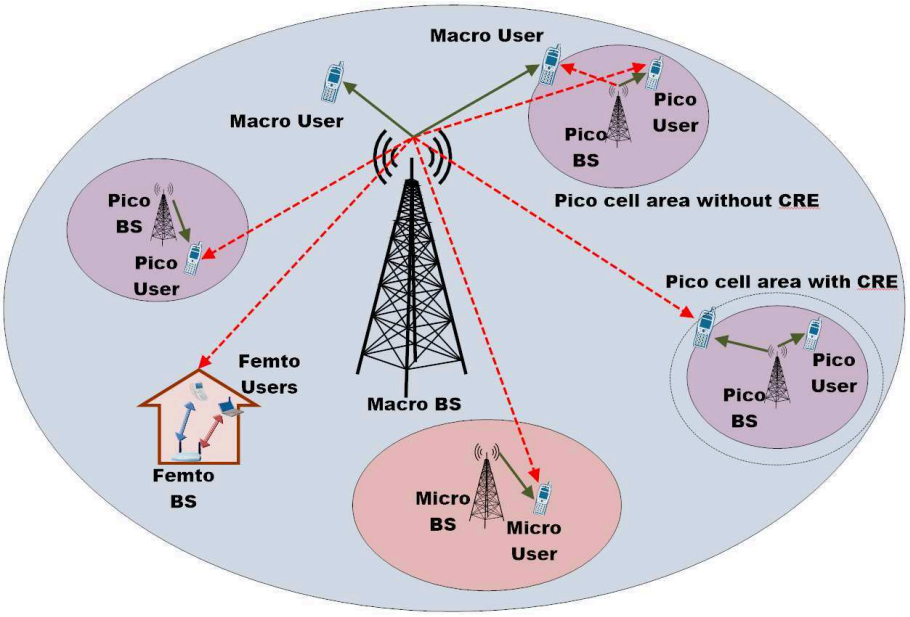

Figure 2.7: Heterogeneous network architecture.

The evaluation of the heterogeneous network technology started in the beginning of 4th generation mobile communication system that offers different services in different radio environments. The number of studies on this type of network is increasing to achieve the network densification without any wireless communication limitations, i.e. limited spectrum, limited power. Network densification is composed of dense deployment of small cells and dense radio spectrum in diverse frequency bands. This wireless evolution is called 5th generation where many different radio access technologies have the interoperability mechanisms.

Deployment Scenarios

There are different types of small cells that are targeted at different types of environments and traffic. These small cells are classified as follows.

- **Pico cells:** They are low power cells deployed indoors or outdoors often in a planned manner in hot-spots or cell-edge areas of the macrocells. Their transmit power ranges between 23dBm and 30dBm and they can cover 300m or less (Lopez-Perez et al. [2011]). Pico cells serve an Open Subscriber Group (OSG) and can be accessed by any user.
- **Femto cells:** They can be also called as home base station (BS). Their transmit power is less than 23dBm and they can cover at most 50m (Lopez-Perez et al. [2011]). They can serve a Closed Subscriber Group (CSG) or OSG.

Since there are many ways to build a heterogeneous network, some important points about small cells must be considered while planning the deployment of pico or macro BSs. These points can be listed as follows:

- Transmit power: It should be chosen considering the requirement of both signal quality and interference management.
- Location: The distance between the small cells and the macro cell should be properly chosen.
- Deployment density: Since the amount of interference coming from other small cells is an important factor in the signal quality of the users, the distance between small cells and their densities should be carefully planned.

The answers of where and how many nodes should be deployed play an important role in increasing the system throughput (Tian et al. [2012]). On the other hand, the unplanned deployment of femto cells increases the interference in the heterogeneous cellular networks (Zhang et al. [2015]). These problems have been investigated in the study of Obaid and Czylwik [2013] by implementing an adaptive power control among the macro and the pico cells.

Another critical challenge is the offloading from the macro cell to the small cells. Many metrics such as signal strength, distance, SNR, bit error rate (BER), traffic load, quality indicator and some combination of these indicators can be used in order to decide offloading. In addition, a balanced user association can reduce the load on the macrocell to provide better services to the macro users.

User association to the cells increases the Quality of Service (QoS) for users and balances the system load (Park et al. [2013]). Existing cell selection schemes have been mainly based on the received signal strength interference (RSSI), signal-to-interference-plus-noise ratio (SINR) or the distance from the nearby BSs to achieve a successful cell association for each user (Yang et al. [2015]).

In general, pico cells are aimed to be deployed in areas where macro signal is weak. Therefore, it is more efficient to place the pico cells at the cell edge zones rather than to place in the cell center of the macro cell (Landstrom et al. [2011]). However, even if there are small nodes at the cell edges, most users in the network continue to receive the strongest signal from the macrocell BSs.

In order to overcome the disparity between the transmit power levels of macro and small cell BSs, and make a fairer cell association, users can be shifted to the lightly loaded small cells by cell range expansion (CRE) techniques (Okino et al. [2011]), (X.Chu and Gunnarsson [2013]). The traffic of the macro cell is offloaded to pico cells by adding a bias to the pico received powers, so that the network capacity is increased by achieving a fairer user association among the cells. However, shifting macro users to the pico cells increases the inter-cell interference, since the shifted users still receive strong signal from the macro BS.

Accordingly, in the context of heterogeneous networks, interference management has become more critical to overcome the inter-cell interference problem.

Interference Management

There are two types of interference in HetNets as follows:

- Co-layer Interference: Co-layer interference is the interference generated from a node to another node which belongs to the same type of cell in the downlink or uplink (Lopez-Perez et al. [2009]). For instance, a pico BS generates co-layer interference to other pico users that are in other pico cells.

- Cross-layer Interference: Cross-layer interference is the interference generated from a node to another node which belongs to a different type of cell in the downlink or uplink (Lopez-Perez et al. [2009]). For instance, a pico BS generates cross-layer interference to a macro user.

So far there are different kinds of interference mitigation approaches which are investigated in a multi cell environment. These mitigation approaches are classified into two major categories:

- Interference Cancellation: It is based on receiver processing. The main aim is to minimize the effects of interference at the receiver part. Interfering signal characteristics are estimated, such as phase, amplitude, angle of arrival. After these estimations, interference can be canceled at the receiving system by using antenna arrays (Rahman et al. [2009], Osman et al. [2010]).

- Interference Avoidance: It is based on resource usage in terms of resource partitioning and power allocation (Bernardo et al. [2010]). In general interference avoidance techniques are based on resource allocation methods such as frequency allocation (Tan et al. [2011]; Cao et al. [2010]), sub-channel allocation (Jung and Lee [2011, 2010]; Cao et al. [2011]), spectrum allocation and frequency reuse methods (Rahman and Yanikomeroglu [2010]; Lee et al. [2010]; Akoum et al. [2010]). These techniques also can be implemented as a combination.

In addition, self configuration and self-adaptation techniques give promising and effective results in the absence of the synchronization mechanisms among small cells (X.Chu and Gunnarsson [2013]). Power control approach is one of these methods that small cells can dynamically adapt their transmission power according to the network situation. Moreover, resource allocation can also improve the power efficiency of the network and perform

the interference control keeping the interference in an acceptable level in the heterogeneous networks (Bu et al. [2015]).

Interference alignment is also interference mitigation technique that has been implemented for heterogeneous networks to handle the problems caused by the coexistence of macro and small cells. In the study of Lv et al. [2010], a spectral transmission scheme for femtocell networks, which includes an adaptive subband partition method and an adaptive IA transceiver has been introduced. Another IA approach on femtocellular networks has been given in the studies of Guler and Yener [2011] and Guler and Yener [2014] where the uplink interference is aligned caused by the macro cell users to the closest femtocell by satisfying the required QoS. Clustering the pico cells based on the strength of inter-pico interference has been studied to eliminate the interference in the clusters (Seno et al. [2015]). In the study of Shin et al. [2012], beamforming matrices have been sequentially determined for small cells and macro cells in order to mitigate interference in the heterogeneous networks. Beamforming vectors are designed based on the number of antennas in each base station and it is assumed that the number of antennas of macro base station is higher than those of pico cells. The transmit beamforming matrices are successively constructed according to the ascending order of the number of transmit antennas in order to align the interference vectors in a small dimensional space. However, this method has been implemented for 2 pico cells, which is a problem in dense deployment of small cells. This problem has been handled and hierarchical IA has been extended to more than 2 pico cells by multi stage alignment process with a decrease in per user capacity performance (Akitaya and Saba [2013]).

In addition, resource allocation and IA methods have been compared for a femto cellular network (Lertwiram et al. [2012]). Limited spectrum resources are divided into two groups for each method. The results indicate that the highest sum-rate can be achieved by performing resource allocation in low SNR regions. On the other hand, performing IA maximizes the sum-rate in the high SNR regions.

Furthermore, partial and fully connected interference networks have been investigated for IA approach to increase the performance of heterogeneous networks due to the random and distributed deployment of femto cells (Liu et al. [2015]).

In Chapter 4 and Chapter 5, we study stream selection based IA algorithms for the heterogeneous networks for the perfect and the imperfect CSI cases.

Part IV

part 4

Chapter 3

Interference alignment algorithms

3.1 Introduction

Interference alignment is an interference mitigation technique that aligns the interfering signals by exploiting the available signaling dimensions provided by time slots, frequency blocks, or antennas. In MIMO networks, IA uses the spatial dimension offered by multiple antennas for alignment. The key idea is that users coordinate their transmissions by using linear precoding, such that the interference signal lies in a reduced dimensional subspace at each receiver.

Since finding the closed form IA solutions can be difficult for large networks, distributed IA approaches based on iterative schemes in which MIMO IA precoders and postcoders are iteratively designed have been studied (Gomadam et al. [2008a], Gomadam et al. [2011], Schreck and Wunder [2011], Zhao et al. [2012]). However, the convergence to the global minimum is not always guaranteed and these algorithms generally require too many iterations in high SNR regions. In addition, these algorithms can allocate a fixed number of streams to each user.

In order to overcome the disadvantages of the iterative algorithms, different IA solutions based on stream selection have been presented in the studies of Amara et al. [2011], Amara et al. [2012b] and Amara et al. [2012a]. IA is achieved by performing successive orthogonal projections after the stream selection. Hence, as the stream selection continues, the channel of each selected stream is guaranteed to become orthogonal to the channels of the previously selected streams.

In this chapter, the iterative IA algorithms and stream selection based IA algorithms that have been addressed in this thesis are presented in detail. First, the system model is specified for K-pair MIMO interference network. Then, the existing iterative and the stream selection based IA algorithms are explained. The chapter is concluded by comparing the performances of the presented IA algorithms.

3.2 System Model

In this chapter, a K-pair interference channel is considered with N_{T_k} transmit and N_{R_k} receive antennas as illustrated in Figure 3.1. In this chapter, it is assumed that perfect CSI is available at all transmitters and receivers.

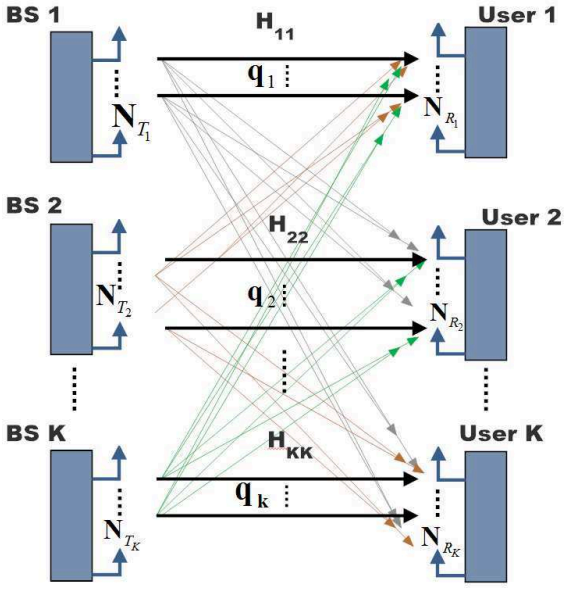

Figure 3.1: System Model for K-pair IC.

The output signal at user k is defined as follows.

$$\mathbf{y}_k = \alpha_{kk}\mathbf{H}_{kk}\mathbf{x}_k + \sum_{\substack{j=1,\\ j\neq k}}^{K} \alpha_{kj}\mathbf{H}_{kj}\mathbf{x}_j + \mathbf{n}_k \tag{3.1}$$

where, $\alpha_{kj}\mathbf{H}_{kj}$ is the channel matrix between transmitter j and receiver k with dimension $N_{R_k} \times N_{T_j}$. Each element of $\mathbf{H}_{kj}$ includes fading which is modeled as an independent and identically distributed complex Gaussian random variable with $\mathcal{CN}(0,1)$. α_{kj} denotes the

pathloss and shadowing. For each receiver k, $\mathbf{n}_k$ is a $N_{R_k} \times 1$ vector. Each element of $\mathbf{n}_k$ represents additive white Gaussian noise with zero mean and variance of σ^2. $\mathbf{x}_k$ is the transmitted signal from the k^{th} transmitter with dimension $N_{T_k} \times 1$ and it is calculated as follows.

$$\mathbf{x}_k = \sqrt{P_k}\mathbf{T}_k\mathbf{s}_k \tag{3.2}$$

where P_k is the transmit power of BS k. $\mathbf{T}_k$ is the unitary precoding matrix of transmitter k with dimension $N_{T_k} \times q_k$, and transmitter k can transmit q_k independent streams with $q_k \leq d_k$ where $d_k = \min(N_{R_k}, N_{T_k})$. $\mathbf{s}_k$ is the symbol vector with dimension of $q_k \times 1$ and denoted as $\mathbf{s}_k = [s_{k,1} \ ... \ s_{k,q_k}]^T$ where $\mathbb{E}\left[\|\mathbf{s}_k\|^2\right] = 1$, and it is assumed that the transmit power is equally shared between the symbols, $\mathbb{E}\left[|s_{k,n}|^2\right] = 1/q_k$, $n = 1, ..., q_k$. In addition, the maximum total number of streams in the network is calculated as follows.

$$r = \sum_{k=1}^{K} d_k \tag{3.3}$$

Desired signals are obtained by multiplying $\mathbf{y}_k$ with the postcoding vector, $\mathbf{D}_k$ with a size of $N_{R_k} \times q_k$. The obtained decoded data symbols can be written as

$$\hat{\mathbf{y}}_k = \mathbf{D}_k^H \mathbf{y}_k \tag{3.4}$$

The data rate for the i^{th} stream of the k^{th} user can be expressed as follows.

$$\mathrm{R}_{ki} = \log_2(1 + \gamma_{ki}) \tag{3.5}$$

where γ_{ki} is the SINR for the i^{th} stream of the k^{th} user and it is calculated as

$$\gamma_{ki} = \frac{(P_k/q_k)\alpha_{kk}^2 \mathbf{d}_k^{iH}\mathbf{H}_{kk}\mathbf{t}_k^i\mathbf{t}_k^{iH}\mathbf{H}_{kk}^H\mathbf{d}_k^i}{\mathbf{d}_k^{iH}\mathbf{B}_{ki}\mathbf{d}_k^i} \qquad \forall k = 1, ..., K, \quad \forall i = 1, ..., q_k \tag{3.6}$$

where $\mathbf{t}_k^i$ is the i^{th} column vector of the precoding matrix $\mathbf{T}_k$ with dimension $N_{T_k} \times 1$, and $\mathbf{d}_k^i$ is the i^{th} column vector of postcoding matrix $\mathbf{D}_k$ with dimension $N_{R_k} \times 1$. Furthermore, $\mathbf{B}_{ki}$ is defined as the interference plus noise covariance matrix for the i^{th} stream of the k^{th} receiver and it is given by

$$\mathbf{B}_{ki} = \sum_{\substack{l=1,\\ l\neq i}}^{q_k} \frac{P_k}{q_k}\alpha_{kk}^2\mathbf{H}_{kk}\mathbf{t}_k^l(\mathbf{t}_k^l)^H\mathbf{H}_{kk}^H + \sum_{\substack{j=1\\ j\neq k}}^{K}\sum_{q=1}^{q_j} \frac{P_j}{q_j}\alpha_{kj}^2\mathbf{H}_{kj}\mathbf{t}_j^q(\mathbf{t}_j^q)^H\mathbf{H}_{kj}^H + \sigma^2\mathbf{I}_{N_{R_k}} \qquad \forall k = 1, ..., K, \quad \forall i = 1, ..., q_k \tag{3.7}$$

Accordingly, the sum rate (SR) is calculated as follows.

$$\mathrm{SR} = \sum_{k=1}^{K} \sum_{i=1}^{q_k} \log_2(1 + \gamma_{ki}) \tag{3.8}$$

3.3 Iterative IA Algorithms

The study of Gomadam et al. [2008b] has presented the first distributed solution exploiting channel reciprocity to find MIMO IA precoders and postcoders. The idea of designing the precoding and postcoding matrices to achieve IA is that at each iteration, the users minimize the interference leakage which their signal leaks into the desired signal subspaces of the other users. After the algorithm converges, the IA condition that is defined as $\mathbf{D}_k^H \mathbf{H}_{kj} \mathbf{T}_j = 0$, $\forall j, k$ and $j \neq k$ should be satisfied and the desired signal spaces should be free of interference. While the algorithm performs well at high SNR, it can be far from optimal at low SNR values. This algorithm is also known as minimum interference leakage (min-Leak) in the literature. Since this algorithm deals with only minimizing the interference, another algorithm has been studied that iteratively maximizes the per stream SINR. In the proposed algorithm, perfect alignment conditions are relaxed by eliminating the assumption that all the precoders are orthogonal to each other. By this relaxation max-SINR algorithm performs better at moderate SNR levels.

Many IA algorithms in the literature are based on the iterative IA approaches. However, the disadvantage of the iterative approaches is that they generally require many iterations in high SNR regimes. Besides, the assumption that the wireless channel remains unchanged during the data exchange between the transmitters and receivers is unrealistic.

The mentioned iterative algorithms are described in detail in the following sections. The notation $\overleftarrow{\mathbf{x}}$ indicates the value of vector $\mathbf{x}$ in the reciprocal channel.

3.3.1 Min-Interference Leakage Algorithm

The minimum interference leakage algorithm iteratively reduces interference by designing the postcoding vectors to minimize the remaining interference in the desired signal subspace at each receiver within each network. While the algorithm exploits channel reci-

procity to perform the iteration, it can also be performed in a centralized node using a centralized topology explained in Section 2.3.2. This iterative procedure is given in Alg. 7.

Alg. 7 Min-Leak Algorithm

Input: α_{kj}, $\mathbf{H}_{kj}$ $\forall k, j$

Step 1. Start with arbitrary precoding matrices $\mathbf{T}_j$, $\forall j = 1, ..., K$, with the constraint that the column vectors of each precoding matrices are orthonormal to each other.

Step 2. Compute the interference covariance matrix $\mathbf{Q}_k$ (Eq. (3.11)), $\forall k = 1, ..., K$ at each receiver.

Step 3. Compute the postcoding matrix $\mathbf{D}_k$ column by column (Eq. (3.13)), $\forall k = 1, ..., K$ at each receiver.

Step 4. Reverse the communication direction, passing to the reciprocal network and set $\overleftarrow{\mathbf{T}}_k = \mathbf{D}_k$, $\forall k = 1, ..., K$ at each receiver.

Step 5. In the reciprocal network, compute the interference covariance matrix $\overleftarrow{\mathbf{Q}}_j$ (Eq. (3.12)), $\forall j = 1, ..., K$ at each transmitter which becomes receiver of the reciprocal channel.

Step 6. In the reciprocal network, compute the interference suppression matrix column by column $\overleftarrow{\mathbf{D}}_j$ (Eq.(3.14)), $\forall j = 1, ..., K$ at each transmitter which becomes receiver of the reciprocal channel.

Step 7. Reverse the communication direction, returning to the original network, and set $\mathbf{T}_j = \overleftarrow{\mathbf{D}}_j$, $\forall j = 1, ..., K$ at each transmitter.

Step 8. Repeat from Step 2 until convergence.

Output: $\mathbf{T}_k$, $\mathbf{D}_k$ $\forall k$

The main aim is to minimize the total interference leakage at each receiver and can be expressed as follows.

$$\min_{\mathbf{D}_k} I_k \tag{3.9}$$

where I_k is the total interference leakage at receiver k due to all undesired transmitters ($j \neq k$) is expressed as follow.

$$I_k = Tr[\mathbf{D}_k^H \mathbf{Q}_k \mathbf{D}_k] \tag{3.10}$$

$\mathbf{Q}_k$ is the interference covariance matrix at receiver k

$$\mathbf{Q}_k = \sum_{j=1, j\neq k}^{K} P_j \alpha_{kj}^2 \mathbf{H}_{kj} \mathbf{T}_j \mathbf{T}_j^H \mathbf{H}_{kj}^H \tag{3.11}$$

For the reciprocal network,

$$\overleftarrow{\mathbf{Q}}_j = \sum_{k=1, k\neq j}^{K} \overleftarrow{P}_k \, \alpha_{jk}^2 \, \overleftarrow{\mathbf{H}}_{jk} \overleftarrow{\mathbf{T}}_k \overleftarrow{\mathbf{T}}_k^H \overleftarrow{\mathbf{H}}_{jk}^H \tag{3.12}$$

where $\overleftarrow{\mathbf{H}}_{jk} = \mathbf{H}_{kj}^H$.

$$\mathbf{d}_k^i = \nu_i[\mathbf{Q}_k] \quad \forall i = 1, ..., q_k \tag{3.13}$$

where $\nu_i[\mathbf{A}]$ denotes the eigenvector corresponding to the i^{th} smallest eigenvalue of the matrix $\mathbf{A}$. For the reciprocal network,

$$\overleftarrow{\mathbf{d}}_j^i = \nu_i[\overleftarrow{\mathbf{Q}}_j] \quad \forall i = 1, ..., q_j \tag{3.14}$$

3.3.2 Max-SINR Algorithm

Instead of minimizing the interference power at each iteration, SINR is iteratively maximized in max-SINR algorithm. In this method, perfect alignment conditions are relaxed by eliminating the condition that all the precoders are strictly orthogonal to each other. At each step, the algorithm updates the postcoding matrices in the considered network and then the communication direction is inverted. In the following step the postcoding matrices used in the previous iteration become the new precoding matrices and the postcoding matrices are set as the precoding matrices used in the previous step. The algorithm continues until the convergence is achieved. This method is summarized in Alg. 8.

$\overleftarrow{\mathbf{B}}_{ki}$ is the interference plus noise covariance matrix in the reverse channel and it is calculated as follows.

$$\begin{aligned} \overleftarrow{\mathbf{B}}_{ki} = & \sum_{\substack{l=1, \\ l\neq i}}^{q_k} \frac{P_k}{q_k} \alpha_{kk}^2 \, \overleftarrow{\mathbf{H}}_{kk} \overleftarrow{\mathbf{t}}_k^l \, (\overleftarrow{\mathbf{t}}_k^l)^H (\overleftarrow{\mathbf{H}}_{kk})^H + \\ & \sum_{\substack{j=1 \\ j\neq k}}^{K} \sum_{q=1}^{q_j} \frac{P_j}{q_j} \alpha_{kj}^2 \, \overleftarrow{\mathbf{H}}_{kj} \overleftarrow{\mathbf{t}}_j^q \, (\overleftarrow{\mathbf{t}}_j^q)^H (\overleftarrow{\mathbf{H}}_{ki})^H + \sigma^2 \mathbf{I}_{N_{R_k}}, \; \forall k = 1, ..., K, \quad \forall i = 1, ..., q_k \end{aligned} \tag{3.15}$$

where $\overleftarrow{\mathbf{H}}_{jk} = \mathbf{H}_{kj}^H$.

The column vectors of the interference suppression matrix that maximizes the SINR of the i^{th} stream of the k^{th} receiver are given as

$$\mathbf{d}_k^i = \frac{(\mathbf{B}_{ki})^{-1} \mathbf{H}_{kk} \mathbf{t}_k^i}{\left\| (\mathbf{B}_{ki})^{-1} \mathbf{H}_{kk} \mathbf{t}_k^i \right\|} \quad k = 1, ..., K, \quad i = 1, ..., q_k \tag{3.16}$$

Alg. 8 Max-SINR algorithm

Input: α_{kj}, $\mathbf{H}_{kj}$ $\forall k, j$

Step 1. Start with arbitrary precoding matrices $\mathbf{T}_j$, $\forall j = 1, ..., K$, so that the column vectors of each precoding matrix are linearly independent.

Step 2. Compute the interferences plus noise covariance matrix $\mathbf{B}_{ki}$ for stream i of receiver k (Eq. (3.15)), $\forall k = 1, ..., K$, $\forall i = 1, ..., q_k$ at each receiver.

Step 3. Compute the postcoding matrix (interference suppression matrices) $\mathbf{D}_k$ column by column (Eq.(3.16)), $\forall k = 1, ..., K$ at each receiver.

Step 4. Reverse the communication direction, passing to the reciprocal network and set $\overleftarrow{\mathbf{T}}_k = \mathbf{D}_k$, $\forall k = 1, ..., K$ at each receiver.

Step 5. In the reciprocal network, compute the interference plus noise covariance matrix $\overleftarrow{\mathbf{B}}_{ki}$ (Eq.(3.15)), $\forall j = 1, ..., K$, $\forall i = 1, ..., q_j$ at each transmitter which becomes receiver of the reciprocal channel.

Step 6. In the reciprocal network, compute the interference suppression matrix $\overleftarrow{\mathbf{D}}_j$ column by column, $\forall j = 1, ..., K$, $\forall i = 1, ..., q_j$ (similar to step 3) at each transmitter which becomes receiver of the reciprocal channel.

Step 7. Reverse the communication direction, returning to the original network, and set $\mathbf{T}_j = \overleftarrow{\mathbf{D}}_j$, $\forall j = 1, ..., K$ at each transmitter.

Step 8. Repeat from Step 2 until convergence.

Output: $\mathbf{T}_k$, $\mathbf{D}_k$ $\forall k$

In Figure 3.2 and Figure 3.3, the convergence of the iterative algorithms is illustrated for low SNR and high SNR values, respectively. It is observed that as the SNR increases, the number of required iteration increases.

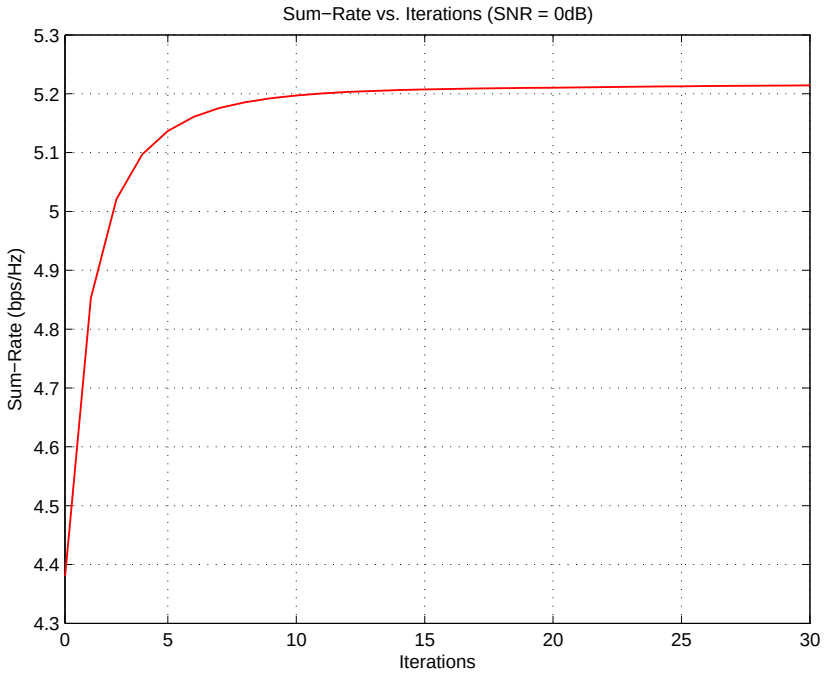

Figure 3.2: Sum rate vs. number of iterations for SNR = 0dB for $N_{T_k} = 4, N_{R_k} = 2$ and $K = 2$

Max-SINR algorithm has been interpreted in the study of Schmidt et al. [2009] as a variation of an algorithm that minimizes the sum Mean Squared Error (MSE) for single stream per user. In order to maximize the sum utility that depends on rate or SINR metrics, a weighted sum MSE beamforming objective function is used to compute the beams. The weights are updated according to the sum utility objective function. A distributed approach as in the max-SINR algorithm is implemented by pricing the interference coming from the other transmitters. To maximize the utility objective function, the MSE weights are adapted according to the user priorities. So that the maximization is achieved in a two stage algorithm. In the first stage, beams are adapted in an inner loop with fixed weights and in the second stage these weights are updated to minimize a weighted sum MSE objective.

Another study on IA that maximizes the network sum rate is given in the study of Shi et al. [2011]. A distributed linear transceiver design approach has been implemented by the weighted minimum mean square error (WMMSE) algorithm to utilize maximization in an interfering broadcast channel. Interference is treated as noise coming from the other cells and the weighted sum-rate is maximized. The main goal is to find the precoding and the postcoding matrices $\{\mathbf{T}, \mathbf{D}\}$ that maximize the system utility. The utility maximization

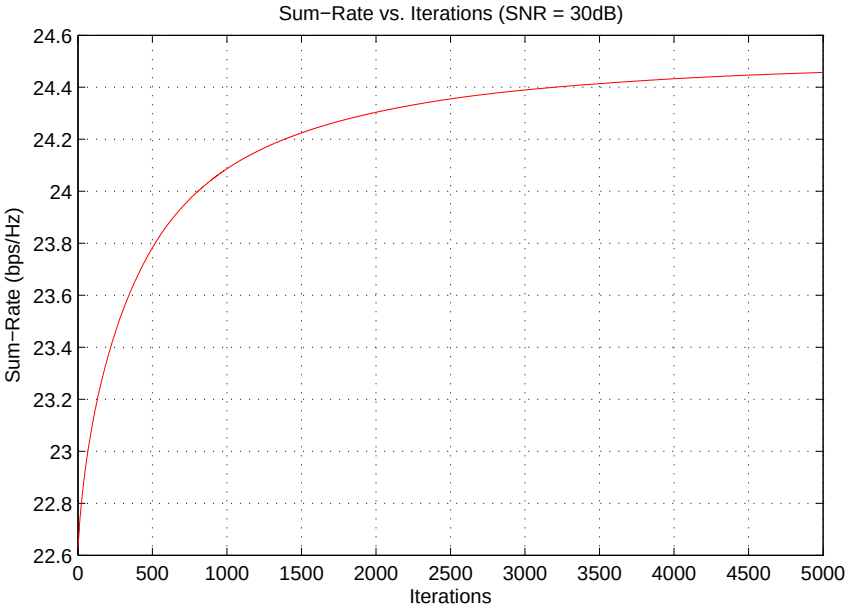

Figure 3.3: Sum rate vs. number of iterations for SNR = 30dB for $N_{T_k} = 4, N_{R_k} = 2$ and $K = 2$

problem is the weighted sum rate maximization that can be formulated as follows.

$$\max_{\mathbf{T},\mathbf{D}} \sum_{k=1}^{K} \sum_{i=1}^{q_k} w_{ki} \log_2(1 + \gamma_{ki})$$

where w_{ki} denotes the weight for the priority of the i^{th} stream of the k^{th} user. This problem formulation is transformed to an equivalent sum-MSE cost minimization problem by defining a weight matrix. The solution is based on an iterative approach which requires only local channel knowledge and converges to a stationary point of the weighted sum rate maximization problem.

In the study of Zhao et al. [2012], max-SINR algorithm has been used as an initial step to determine the precoding vectors. Distributed convex optimization based on IA method has been studied in both single and multi-beam cases to maximize the weighted sum rate problem given in Eq. (3.17). Since the rate function is non-concave, this formulation is hard to solve. Therefore, linear receiver filters as auxiliary optimization variables have been introduced and this problem is transformed into a convex problem. In order to solve this convex optimization problem, an algorithm consisting of two stages is implemented, as IA phase and post-alignment optimization phase. The output of the first stage is used as the input for the second stage.

The first study IA solution for cellular networks is given in the study of Suh et al. [2010]. The authors apply sub-space IA approach to cellular systems in order to increase the throughput of the network considering the cell-edge area. In the study of Schreck and Wunder [2011], max-SINR algorithm (Gomadam et al. [2011]) is extended for the cellular

networks. In this study, degrees of freedom are analyzed for MIMO cellular systems for different number of antennas per base station.

A different family of IA is based on successive stream selection where the least interfering stream is selected in the null space of the previously selected streams at each step (Amara et al. [2011], Amara et al. [2012b]). Such approaches have been inspired from user selection problems (Yoo and Goldsmith [2006], Sun and McKay [2010]). They are not iterative, since they perform IA by successively selecting the streams as long as the total sum rate increases.

3.4 Stream Selection Algorithms

In stream selection based IA algorithms, each stream is selected in the null space of the previously selected streams at each step where streams are computed from the singular value decomposition (SVD) of all the channels, $(\alpha_{kk}\mathbf{H}_{kk}) = \mathbf{U}_k\mathbf{S}_k\mathbf{V}_k^H$. In addition, the l^{th} column vector of $\mathbf{V}_k$ and $\mathbf{U}_k$ are denoted as $\mathbf{v}_k^l$ and $\mathbf{u}_k^l$, respectively. The interference is aligned after each stream selection step using orthogonal projections.

There are two kinds of interference between the streams. The first one is the interference from the selected stream to the unselected streams and the second one is the interference to the selected stream from the unselected streams. Therefore, two types of virtual channels are defined as Virtual Receiving Channels (VRCs) and Virtual Transmitting Channels (VTCs) (Amara et al. [2012b]). These can be expressed as follows.

- Virtual Receiving Channel: VRC is the channel between the transmitter k and the receiver k^* including the postcoding vector of the selected stream l^*, $\mathbf{u}_{k^*}^{l^*}$.

$$\mathbf{VRC}_{k^*k}^{l^*} = (\mathbf{u}_{k^*}^{l^*})^H\mathbf{H}_{k^*k} \tag{3.17}$$

- Virtual Transmitting Channel: VTC is the channel between the transmitter k^* and the receiver k including the precoding vector of the selected stream l^*, $\mathbf{v}_{k^*}^{l^*}$.

$$\mathbf{VTC}_{kk^*}^{l^*} = \mathbf{H}_{kk^*}\mathbf{v}_{k^*}^{l^*} \tag{3.18}$$

For each selected stream, multiple VRCs and VTCs are designed by using the precoder and decoder vectors, respectively. These vectors are obtained from the SVD procedure. Precoding and postcoding matrices are constructed from the precoding and postcoding vectors corresponding to the selected streams, and they are expressed as $\mathbf{T}_{k^*} = [\mathbf{v}_{k^*}^1, \mathbf{v}_{k^*}^2, ..., \mathbf{v}_{k^*}^{q_k}]$ and $\mathbf{D}_{k^*} = [\mathbf{u}_{k^*}^1, \mathbf{u}_{k^*}^2, ..., \mathbf{u}_{k^*}^{q_k}]$, respectively.

Therefore, after the virtual channels of user k^* are obtained, the impact of the selected stream of user k^* to the unselected streams is reduced by orthogonal projections. More precisely, the space spanned by the unselected potential precoding and postcoding of each user $k \neq k^*$ is projected orthogonally to the corresponding VRC and VTC of the selected stream l^* belonging to user k^*. Projected matrices are denoted by $\mathbf{H}_{kk}^{\perp}$ and, initially, $\mathbf{H}_{kk}^{\perp} = \mathbf{H}_{kk}$.

The vectors of the projected matrices $\mathbf{H}_{kk}^{\perp}$, $\forall k \neq k^*$, are in the null space of the VRC and VTC of all previously selected streams. The projection procedure is implemented in

two steps. In the first step the interference coming from the remaining streams to the selected stream is reduced by projecting the channel matrices $\mathbf{H}_{kk}^{\perp}$ generated orthogonally to the **VRC**, $(\mathbf{u}_{k^*}^{l^*})^H\mathbf{H}_{k^*k}$, and it is calculated as

$$\mathbf{H}_{kk}^{\perp} = \mathbf{H}_{kk}^{\perp}\mathbf{P}^{\perp}_{((\mathbf{u}_{k^*}^{l^*})^H\mathbf{H}_{k^*k})} \tag{3.19}$$

where $\mathbf{P}^{\perp}_{(\mathbf{u}_{k^*}^{l^*H}\mathbf{H}_{k^*k})}$ is the orthogonal projection matrix parallel to matrix $(\mathbf{u}_{k^*}^{l^*})^H\mathbf{H}_{k^*k}$ and can be expressed as

$$\mathbf{P}^{\perp}_{((\mathbf{u}_{k^*}^{l^*})^H\mathbf{H}_{k^*k})} = \mathbf{I}_{N_{T_k}} - \frac{((\mathbf{u}_{k^*}^{l^*})^H\mathbf{H}_{k^*k})^H((\mathbf{u}_{k^*}^{l^*})^H\mathbf{H}_{k^*k})}{\left\|((\mathbf{u}_{k^*}^{l^*})^H\mathbf{H}_{k^*k})\right\|^2}. \tag{3.20}$$

The second step of the projection procedure is to reduce the interference generated to the remaining streams and consists in projecting the channel matrices $\mathbf{H}_{kk}^{\perp}$ generated to the **VTC**, $\mathbf{H}_{kk^*}\mathbf{v}_{k^*}^{l^*}$, and it is calculated as

$$\mathbf{H}_{kk}^{\perp} = \mathbf{P}^{\perp}_{(\mathbf{H}_{kk^*}\mathbf{v}_{k^*}^{l^*})}\mathbf{H}_{kk}^{\perp} \tag{3.21}$$

where $\mathbf{P}^{\perp}_{(\mathbf{H}_{kk^*}\mathbf{v}_{k^*}^{l^*})}$ is the orthogonal projection matrix parallel to matrix $\mathbf{H}_{kk^*}\mathbf{v}_{k^*}^{l^*}$ and can be mathematically expressed as

$$\mathbf{P}^{\perp}_{(\mathbf{H}_{kk^*}\mathbf{v}_{k^*}^{l^*})} = \mathbf{I}_{N_{R_k}} - \frac{(\mathbf{H}_{kk^*}\mathbf{v}_{k^*}^{l^*})(\mathbf{H}_{kk^*}\mathbf{v}_{k^*}^{l^*})^H}{\left\|(\mathbf{H}_{kk^*}\mathbf{v}_{k^*}^{l^*})\right\|^2}. \tag{3.22}$$

An illustration of the explained interference alignment process is given in Figure 3.4. In this figure, it is assumed that the first stream of the first user is selected. The channel of the second user is orthogonally projected to both VTC and VRC of the selected stream. In this way, when another stream is to be selected, its channel is guaranteed to become orthogonal to the channels of the previously selected streams and, thus, it does not generate any interference to them.

The main objective is to mitigate the interference while finding the best stream sequence. The stream selection scheme which maximizes the total sum rate given in Eq. (3.8) of the network can be formulated as follows.

$$\{(\mathbf{T}_k^*, \mathbf{D}_k^*)\}_{k\in[1,\ldots,K]} = \underset{\mathbf{T}_k,\mathbf{D}_k}{\operatorname{argmax}}\,(\mathrm{SR}) \tag{3.23}$$

The interference alignment procedure for a given selected stream l^* of user k^* is summarized in Alg. 9. The worst case computational complexity of Alg. 9 is calculated as follows (Golub and Van Loan [1996]), (Rosen [2002]).

$$\mathcal{O}(K(NM^2 + N^2M + M^3)) \tag{3.24}$$

where $M = \max_{\forall k}(N_{T_k})$ and $N = \max_{\forall k}(N_{R_k})$ are the maximum number of transmitter and receiver antennas, respectively.

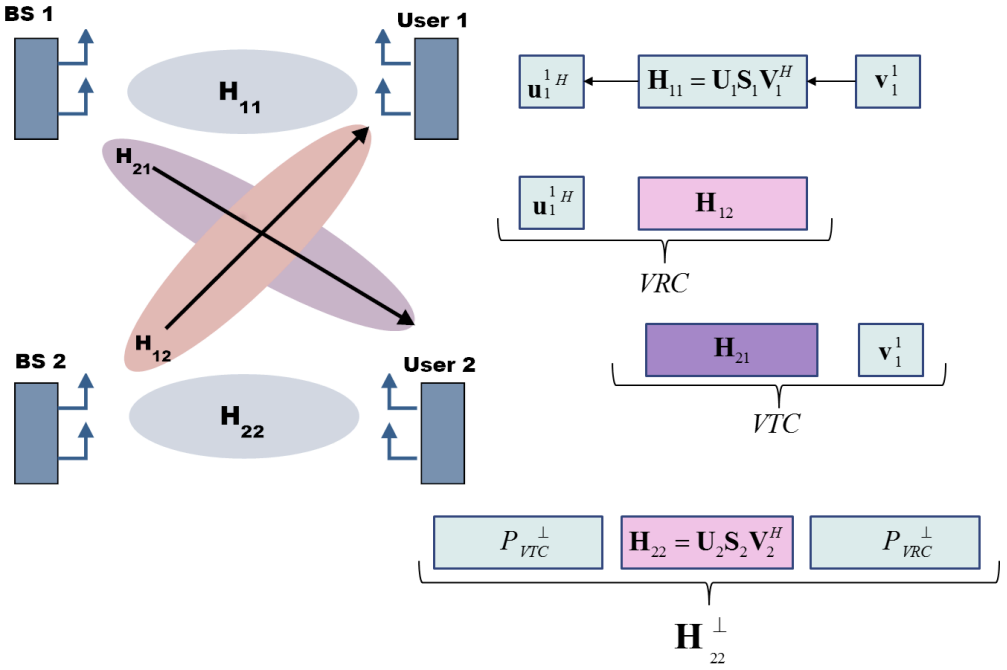

Figure 3.4: The visualization of the interference alignment process for $K = 2$ MIMO network.

Alg. 9 Interference Alignment Algorithm

Input: α_{kk}, $\mathbf{H}_{kk}^{\perp}$, $\mathbf{H}_{kk^*}$ and $\mathbf{H}_{k^*k}$ $\forall k$; $\mathbf{v}_{k^*}^{l^*}$, $\mathbf{u}_{k^*}^{l^*}$, $\mathbf{T}_{k^*}$, $\mathbf{D}_{k^*}$

Project orthogonally to **VRC**, $(\mathbf{u}_{k^*}^{l^*})^H \mathbf{H}_{k^*k}$

$\mathbf{H}_{kk}^{\perp} = \mathbf{H}_{kk}^{\perp} \mathbf{P}^{\perp}_{\mathbf{u}_{k^*}^{l^*H} \mathbf{H}_{k^*k}}$ for $k = 1, ..., K$ where $k \neq k^*$

Project orthogonally to **VTC**, $\mathbf{H}_{kk^*} \mathbf{v}_{k^*}^{l^*}$

$\mathbf{H}_{kk}^{\perp} = \mathbf{P}^{\perp}_{\mathbf{H}_{kk^*} \mathbf{v}_{k^*}^{l^*}} \mathbf{H}_{kk}^{\perp}$ for $k = 1, ..., K$ where $k \neq k^*$

Compute the SVD of projected matrices

$(\alpha_{kk} \mathbf{H}_{kk}^{\perp}) = \mathbf{U}_k \mathbf{S}_k \mathbf{V}_k^H$ for $k = 1, ..., K$

Update

$\mathbf{T}_{k^*} = [\mathbf{T}_{k^*} \ \mathbf{v}_{k^*}^{l^*}]$

$\mathbf{D}_{k^*} = [\mathbf{D}_{k^*} \ \mathbf{u}_{k^*}^{l^*}]$

Output: $\mathbf{H}_{kk}^{\perp}$, $\mathbf{V}_k$, $\mathbf{U}_k$ and $\mathbf{S}_k$ $\forall k$; $\mathbf{T}_{k^*}$, $\mathbf{D}_{k^*}$

3.4.1 Exhaustive Search of Successive Null Space Stream Selection

The objective of the stream selection algorithms is to select the streams successively while maximizing the sum rate. The best stream sequence among all the possible stream sequences can be found by an exhaustive search (Amara et al. [2012b]). Streams, stream sequences and the related sets are defined as follows.

Each stream i can be expressed as $\pi_i = (k_i, l_i)$ where $k_i \in \{1, \ldots, K\}$, $l_i \in \{1, \ldots, q_{k_i}\}$ and $i \in \{1, \ldots, r\}$. The set of all possible stream sequences can be defined as follows.

$$\Phi = \Phi_1 \cup \ldots \cup \Phi_j \cup \ldots \cup \Phi_r \tag{3.25}$$

where Φ_j is the set of all permutations of length $j \in \{1, \ldots, r\}$ given by

$$\begin{aligned} \Phi_j = \Big\{ & \pi = (\pi_1 \pi_2 \ldots \pi_j) \mid \\ & \forall i, i' \in \{1, \ldots, j\}, \ \pi_i \neq \pi_{i'} \text{ if } i \neq i' \Big\} \end{aligned} \tag{3.26}$$

The number of elements of the set Φ is calculated as follows.

$$|\Phi| \leq \sum_{i=K}^{r} \binom{r}{i}$$

where $\binom{x}{y}$ is the number of y permutations of x elements.

Alg. 10 determines the precoding and the postcoding matrices for a given stream sequence π. It also calculates the sum-rate achieved by the selection of this sequence.

Using Alg. 10, Alg. 11 performs an exhaustive search which tries all relevant stream sequences and finds the sequence that yields the greatest sum-rate.

The most challenging drawback of the exhaustive search is the complexity that depends on the number of streams. The total number of calls to Alg. 9 in the exhaustive search algorithm can be formulated as follows.

$$\sum_{i=1}^{r} \Big(\underbrace{\left(\frac{r!}{(r-i)!} \right)}_{\substack{\text{The total number of} \\ \text{stream sequences of length } i}} \times \underbrace{i}_{\substack{\text{The number of times Alg. 9} \\ \text{is called for each stream sequence}}} \Big) \tag{3.27}$$

Since this brute force approach is too complex to implement in systems with large number of streams, an approach that has a lower complexity and a closer performance to the exhaustive search is required.

3.4.2 Successive Null Space Stream Selection (SNSSS)

In this algorithm, only one stream sequence is constructed by successively selecting the streams having the highest singular values (i.e., the strongest streams) (Amara et al. [2012b]). While the streams are selected, their sum rate contributions are checked whether

Alg. 10 Stream Selection Algorithm

Input: α_{kj}, $\mathbf{H}_{kj}$ $\forall k, j$, π

Initialize the variables

$\mathbf{T} = \emptyset$; $\mathbf{D} = \emptyset$; $i = 1$; $q_k = 0$ and $\mathbf{H}_{kk}^{\perp} = \mathbf{H}_{kk}$ for $k = 1, ..., K$

Compute the SVD of all the channels

$(\alpha_{kk}\mathbf{H}_{kk}^{\perp}) = \mathbf{U}_k\mathbf{S}_k\mathbf{V}_k^H$ for $k = 1, ..., K$

while $i \leq |\pi|$ **do**

Pick the ith stream in π

$(k^*, l^*) = \pi_i$

Update

$q_{k^*} = q_{k^*} + 1$

Apply **Alg. 9**

Increment i

$i = i + 1$

end while

Calculate the sum-rate SR_π given in Eq. (3.8)

Set the variables for the selected streams

$(\mathbf{T}_k)_\pi = \mathbf{T}_k$, $(\mathbf{D}_k)_\pi = \mathbf{D}_k$ for $k = 1, ..., K$

Output: $(\mathbf{T}_k)_\pi$, $(\mathbf{D}_k)_\pi$ $\forall k$

Alg. 11 Exhaustive Search

Input: α_{kj}, $\mathbf{H}_{kj}$ $\forall k, j$

Initialize the set Φ

for each stream sequence $\pi \in \Phi$ **do**

Apply **Alg. 10**

end for

Select the best stream sequence according to Eq. (3.23)

$\pi^* = \underset{\pi \in \Pi}{\operatorname{argmax}}\ \mathrm{SR}_\pi$

$\mathbf{T}_k^* = (\mathbf{T}_k)_{\pi^*}$, $\mathbf{D}_k^* = (\mathbf{D}_k)_{\pi^*}$ for $k = 1, ..., K$

Output: $\mathbf{T}_k^*$, $\mathbf{D}_k^*$ $\forall k$

the system throughput increases or not. Since the transmit power is equally shared between the streams, adding a stream to a user already served does not necessarily increase the total sum-rate. The maximum singular value that increases the sum rate is chosen at each iteration from the set Ω, where Ω is the set which keeps track of the eigenvalues of the available streams. In addition, the constructed stream sequence at the end of the algorithm is denoted as Ψ.

The whole procedure is described in Alg. 12.

The complexity in terms of the number of calls to Alg. 9 by SNSSS is r. This algorithm has a very low complexity, and is a suboptimal solution due to the searching of only one stream sequence which is one of the searched stream sequence by the exhaustive search.

3.4.3 Enhanced Successive Null Space Stream Selection (ESNSSS)

In the SNSSS algorithm, just one specific path is constructed by choosing the largest singular value that increases the sum rate. However, this strategy can lead to a suboptimal solution. Therefore, constructing different initializations rather than the maximum stream value can give a higher sum rate values.

In order to decrease the complexity of exhaustive search and to overcome the suboptimality of SNSSS algorithm, ESNSSS algorithm introduces different initialization points for the search process of the streams. Each stream sequence is initialized by all possible streams which are initially computed singular values and they are kept in set Ω_0. This algorithm can be summarized as in Alg. 13 (Amara et al. [2012b]).

The complexity in terms of the number of calls to Alg. 9 by ESNSSS is r^2.

3.5 Performance Evaluation

The iterative and the stream selection based IA algorithms, such as max-SINR, min-Leak, SNSSS and ESNSSS have been implemented for K-pair MIMO interference channels (Gomadam et al. [2011], Amara et al. [2011], Amara et al. [2012b]). The comparison of these algorithms is given in Figure 3.5 for $K = 3$ and $N_{T_k} = N_{R_k} = 2$. It is assumed that the transmit power for all the BSs and the received SNR for all the users are the same.

Figure 3.5 shows that the exhaustive search has the best performance in terms of the average sum rate in high SNR regions. On the contrary, SNSSS algorithm has the lowest performance. The reason is that starting with the best stream does not always yields the higher sum-rate. In addition, it can be observed that ESNSSS, minimum interference leakage (min-Leak) and maximum SINR (max-SINR) algorithms have the same performances in higher SNR regions.

The average number of selected streams is given in Table 3.1. It can be observed that the exhaustive search selects more streams than ESNSSS and SNSSS algorithms while SNSSS selects fewer stream on the average. In addition, the average total number of streams selected by the max-SINR and the min-Leak algorithms is 3, since they select a fixed number of streams per user as 1 for the considered configuration. Although the

Alg. 12 Successive Null Space Stream Selection

Input: α_{kj}, $\mathbf{H}_{kj}$ $\forall k, j$

Initialize

$\Psi = \emptyset$; $\mathbf{T} = \emptyset$; $\mathbf{D} = \emptyset$; $q_k = 0$ and $\mathbf{H}_{kk}^{\perp} = \mathbf{H}_{kk}$ for $k = 1, ..., K$;
$SR_{\Psi} = 0$; finish = FALSE

Compute the SVD of all the channels

$(\alpha_{kk}\mathbf{H}_{kk}^{\perp}) = \mathbf{U}_k\mathbf{S}_k\mathbf{V}_k^H$ for $k = 1, ..., K$

Construct Ω

$\Omega = \{(\mathbf{S}_k)(l,l) | k = 1, ..., K \text{ and } l = 1, ..., d_k\}$

while finish = FALSE **do**
Construct the set of streams which increases the sum-rate

$\Omega' = \left\{\mathbf{S}_k(l,l) \in \Omega |\ \mathrm{SR}_{\Psi\cup(k,l)} > \mathrm{SR}_{\Psi}\right\}$

if $\Omega' \neq \emptyset$ **then**

$$(k^*, l^*) = \underset{(k,l) \text{ such that } \mathbf{S}_k(l,l)\in\Omega'}{\operatorname{argmax}} \mathbf{S}_k(l,l)$$

Update

$\Psi = \Psi \cup (k^*, l^*)$

$q_{k^*} = q_{k^*} + 1$

Apply **Alg. 9**

Reconstruct Ω

$\Omega = \{(\mathbf{S}_k)(l,l) | k = 1, ..., K \text{ and } l = 1, ..., d_k \text{ and } (k,l) \notin \Psi\}$

else

finish = TRUE
end if

end while

Set the precoding and the postcoding matrices for the constructed sequence

$\mathbf{T}_k^* = \mathbf{T}_k$, $\mathbf{D}_k^* = \mathbf{D}_k$ for $k = 1, ..., K$

Output: $\mathbf{T}_k^*$, $\mathbf{D}_k^*$ $\forall k$

Alg. 13 Enhanced Successive Null Space Stream Selection

Input: α_{kj}, $\mathbf{H}_{kj}$ $\forall k, j$

Initialize the set of all streams

$\Omega_0 = \{(k,l)|k = 1, ..., K \text{ and } l = 1, ..., d_k\}$

for each stream $(k^*, l^*) \in \Omega_0$ **do**

Initialize the variables to perform stream selection starting with (k^*, l^*)

$\Psi = \emptyset$; $\mathbf{T} = \emptyset$; $\mathbf{D} = \emptyset$; $q_k = 0$ and $\mathbf{H}_{kk}^{\perp} = \mathbf{H}_{kk}$ for $k = 1, ..., K$; finish = FALSE

Compute the SVD of all the channels

$(\alpha_{kk}\mathbf{H}_{kk}) = \mathbf{U}_k\mathbf{S}_k\mathbf{V}_k^H$ for $k = 1, ..., K$

Set the stream to be selected initially (k^*, l^*)

$\Psi = \Psi \cup (k^*, l^*)$

$q_{k^*} = q_{k^*} + 1$

Apply **Alg. 9**

Construct Ω

$\Omega = \{(\mathbf{S}_k)(l,l)|k = 1, ..., K \text{ and } l = 1, ..., d_k\}$

Run **While** loop of **Alg. 12**

Compute $(\mathbf{T}_k)_\Psi$, $(\mathbf{D}_k)_\Psi$ and SR_Ψ for the stream sequence Ψ

end for

Select the best stream sequence according to Eq. (3.23)

$\Psi^* = \underset{\Psi}{\text{argmax}}\, SR_\Psi$

$\mathbf{T}_k^* = (\mathbf{T}_k)_{\Psi^*}$, $\mathbf{D}_k^* = (\mathbf{D}_k)_{\Psi^*}$ for $k = 1, ..., K$

Output: $\mathbf{T}_k^*$, $\mathbf{D}_k^*$ $\forall k$

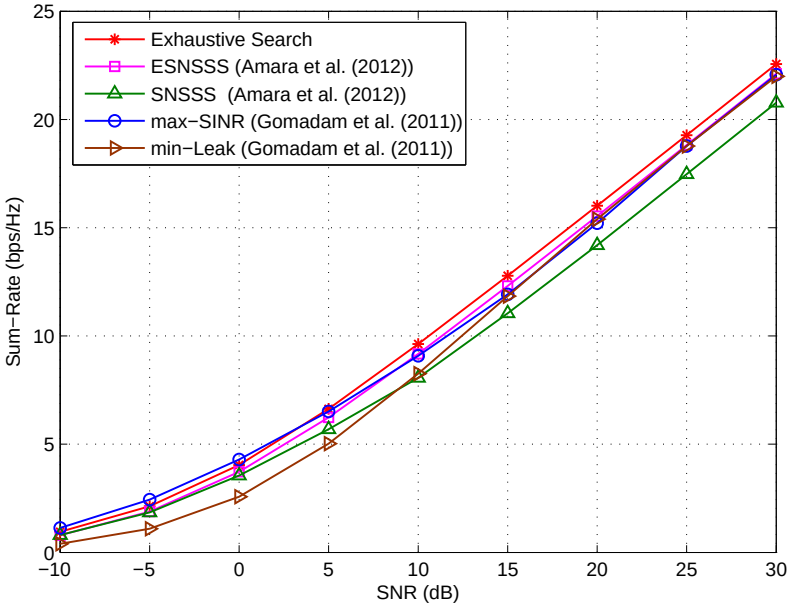

Figure 3.5: Sum rate vs. SNR for $K = 3$, $N_{T_k} = N_{R_k} = 2$

average total number of selected streams by the iterative IA algorithms is higher than those of stream selection based algorithms, the performances of the ESNSSS and the iterative algorithms are almost the same in higher SINR regions. This can be explained by the fact that the stream selection based algorithms can select different number of streams for each user at each channel realization which is not the case for the iterative algorithms. For the

Table 3.1: The average total number of selected streams

SNR(dB)	**Exhaustive Search**	**ESNSSS**	**SNSSS**
-10	4.89	4.36	4.21
5	2.71	2.50	2.41
30	2.10	2.02	2.00

stream selection based IA algorithms, it is possible that no stream is selected for a user in some cases. Mostly, this behavior is undesired; therefore, in the following chapters, we will propose solutions to avoid this drawback.

3.6 Conclusion

In this chapter, both iterative and stream selection based interference alignment algorithms have been explained for K-pair MIMO interference channels for the same received SNR.

In the iterative algorithms, namely min-Leak and max-SINR, the precoding and postcoding matrices are obtained at the end of the iterations; whereas, in the stream selection based algorithms, the column vectors of the precoding and postcoding matrices are constructed after each stream selection. Furthermore, iterative algorithms either minimize the interference or maximize the SINR; however, stream selection based IA algorithms aim to achieve both at the same time. The interference is mitigated by performing orthogonal projections and the sum-rate is maximized by selecting a stream which increases the sum-rate at each stream selection.

The comparison of the algorithms demonstrates that the max-SINR performs better in lower SNR regions. In higher SNR regions, the performances of max-SINR, min-Leak and ESNSSS algorithms are almost the same. In addition, ESNSSS can achieve better performance than SNSSS with an extra complexity while getting closer to the performance obtained by the exhaustive search. Furthermore, stream selection based IA algorithms can adaptively select different number of streams depending on the selection criteria while iterative IA algorithms always select a fixed number of streams.

Part V

part 5

Chapter 4

Stream selection based interference alignment for heterogeneous networks

4.1 Introduction

In this chapter, stream selection based IA methods are investigated for heterogeneous networks with different deployment scenarios for the pico cells. Since the purpose of using pico cells is to enhance the spectral efficiency or to increase the capacity in areas of high demand, pico cells can be deployed very close to each other or far away from each other. Therefore, both the partial and fully connected interference networks (Liu et al. [2015]) have been investigated for the stream selection based IA approaches to increase the performance of the heterogeneous networks by selecting at least one stream for each user.

In this context, two different scenarios are considered in this chapter. In the first scenario, the pico cells are deployed far away from each other where the interference is weak among the pico cells. In the second scenario, the pico cells are deployed closer to each other where the interference is strong among the pico cells. Therefore, we propose two different stream selection based IA algorithms for these two different scenarios. The objective of stream selection algorithm is to select a stream sequence composed of streams depending on the selection criteria.

In the fist part, a partial connected interference network is considered. The interference generated from each pico cell to the users of other pico cells is negligible in this scenario, since the pico cells are separately deployed from each other. Therefore, interference alignment algorithm, Alg.9, is not performed among the pico BSs. For this kind of scenarios, the ISNSSS algorithm is proposed where the initial streams of the constructed stream sequences are selected among the pico streams. In other words, to build the set of tentative stream sequences, the streams are initially selected from the users of pico cells, continuing with the strongest streams that increase the sum rate. If it is not possible to select a stream that positively contributes to the sum rate, a stream that decreases the sum rate the least is selected. The process is repeated until each user receives at least one stream.

The constructed stream sequences are compared and the sequence leading to the greatest sum rate is chosen. The main aim is to increase the overall rate of the system by designing the precoding and decoding matrices while mitigating the interference and assigning at least one stream per each user. The performance of the ISNSSS algorithm is evaluated for one pico cell (Aycan et al. [2014]), two pico cell (Aycan Beyazit et al. [2015] and three pico cell cases.

In the second part, the pico cells are deployed closer to each other. Therefore, a fully connected interference network between pico cells is considered where the mutual interference between pico cells is very strong. Therefore, IA is performed between all pico cells. In such networks, the best stream sequence achieving the highest sum-rate can be found with exhaustive search by considering all possible combinations. However, exhaustive search is too complex due to the large search space. Thus, the main goal of this study is to decrease this search space. To that end, we propose the advanced successive null space stream selection (ASNSSS) algorithm which decreases the complexity significantly while keeping the performance relatively close to that of the exhaustive search (Aycan Beyazit et al. [2016a]). In addition, the proposed algorithm is designed in such a way that it guarantees the selection of at least one stream from each user while mitigating the interference among the selected streams. The performance of the ASNSSS algorithm is evaluated in different scenarios composed of one, two and three pico cells which are deployed close to each other.

In this chapter, we first introduce the system model in Section 4.2. Then, we propose the ISNSSS algorithm for the partially connected interference networks in Section 4.3 and we propose the ASNSSS algorithm for the fully connected interference networks in Section 4.4. Next, we evaluate the performance of the proposed algorithms in Section 4.5. Finally, we conclude the chapter in Section 4.6.

4.2 System Model

A K-pair heterogeneous network is considered composed of pico cells and a macro cell as illustrated in Figure 4.1. Each pair k has N_{T_k} transmitter antennas and N_{R_k} receiver antennas. In addition, the transmit power of the macro and pico BSs are different. For the sake of simplicity, macro BS - macro user pair is defined as the pair $k = 1$, and pico BS - pico user pairs are kept in the set $k \in \Gamma = \{2, ..., K\}$. It is assumed that the required CSI is available at the transmitters in a centralized topology as explained in Section 2.3.2.

The system model used in this chapter is the same as the system model given in Chapter 3. For instance, the received signal at user k, the SINR of the i^{th} stream of the k^{th} receiver and the total sum rate (SR) can be calculated using Eq. (3.2), Eq. (3.6), Eq. (3.8), respectively.

The main objective of the stream selection based IA algorithms is given in Chapter 3 by Eq. (3.23). Due to the heterogeneity, such as different transmit power levels, there can be an unfair stream selection for the pico cell users. To avoid this problem, an additional constraint which allows allocating at least one stream to each user is introduced to the main objective. The stream selection scheme which maximizes the total sum rate of the

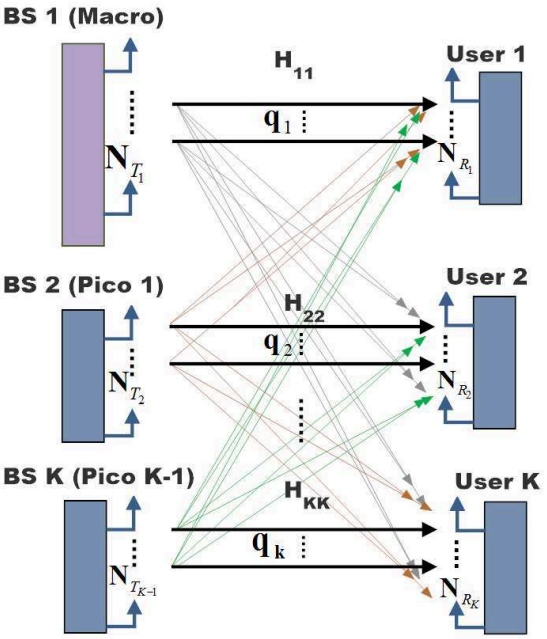

Figure 4.1: System model for MIMO heterogeneous network

network while guaranteeing at least one stream selection from each user can be formulated as follows.

$$\{(\mathbf{T}_k^*, \mathbf{D}_k^*)\}_{k=1,\ldots,K} = \underset{\mathbf{T}_k, \mathbf{D}_k}{\operatorname{argmax}} \, (\mathrm{SR}) \tag{4.1a}$$

$$\text{s.t.} \quad q_k \geq 1, \quad \forall k \tag{4.1b}$$

4.3 Partially Connected Interference Networks

In this section, we propose the ISNSSS algorithm for the partially connected interference networks. The algorithm only considers the stream sequence starting with a pico stream. After a pico stream is selected, the strongest streams with a contribution to the sum rate are selected. In each selection step, we perform successive orthogonal projections to the null space of the selected stream. The key point of this approach is to determine the stream sequences that give the highest sum rate among all the stream combination paths initialized by the pico streams. In the following, improved stream selection is explained in detail.

Improved Successive Null Space Stream Selection (ISNSSS) Algorithm

ISNSSS algorithm first constructs stream sequences starting with a pico stream, since the average SNR of the pico users is higher than the macro user. The related justification is given in Appendix A.

The initialization set that only includes pico user streams is Ξ. After the first stream is selected from pico streams, stream with the maximum singular value which increases the sum rate is chosen from the set Ω, which keeps the track of all the available streams. If there is no such a stream, a stream that causes the minimum sum-rate decrease is selected from a user with no selected streams. The construction of the stream sequence continues until no more streams can be selected. The constructed stream sequence at the end of the algorithm is denoted as Ψ.

The whole procedure is described in Alg. 14.

Alg. 14 Improved Successive Null Space Stream Selection (ISNSSS)

Input: α_{kj}, $\mathbf{H}_{kj}$ $\forall k, j$

Construct the initialization set Ξ

$\Xi = \{(k,l)|\ k \in \Gamma \text{ and } l = 1, ..., d_k\}$

for each stream $(k^*, l^*) \in \Xi$ **do**

1. Initialize the variables

$\Psi = \emptyset$; $\mathbf{T} = \emptyset$; $\mathbf{D} = \emptyset$; $q_k = 0$ and $\mathbf{H}_{kk}^{\perp} = \mathbf{H}_{kk}$ for $k = 1, ..., K$; finish = FALSE

2. Compute the SVD of all the channels

$(\alpha_{kk}\mathbf{H}_{kk}) = \mathbf{U}_k\mathbf{S}_k\mathbf{V}_k^H$ for $k = 1, ..., K$

3. Set the stream to be selected initially (k^*, l^*)

$\Psi = \Psi \cup (k^*, l^*)$

$q_{k^*} = q_{k^*} + 1$

4. Apply **Alg. 9**

6. Construct

$\Omega = \{(\mathbf{S}_k)(l,l)|k = 1, ..., K \text{ and } l = 1, ..., d_k\}$

8. Continue selecting streams (This step is in the following page)

9. Compute $(\mathbf{T}_k)_\Psi$, $(\mathbf{D}_k)_\Psi$ and SR_Ψ for the stream sequence Ψ

end for

Select the best stream sequence according to Eq. (3.23)

$\Psi^* = \underset{\Psi}{\text{argmax}}\ \mathrm{SR}_\Psi$

$\mathbf{T}_k^* = (\mathbf{T}_k)_{\Psi^*}$, $\mathbf{D}_k^* = (\mathbf{D}_k)_{\Psi^*}$ for $k = 1, ..., K$

Output: $\mathbf{T}_k^*$, $\mathbf{D}_k^*$ $\forall k$

---

8. Continue selecting streams

while finish = FALSE **do**

8.1. Compute the SR_{Ψ}

8.2. Select a stream

Construct the set of streams which increases the sum-rate

$$\Omega' = \left\{\mathbf{S}_k(l,l) \in \Omega |\ \mathrm{SR}_{\Psi\cup(k,l)} > \mathrm{SR}_{\Psi}\right\}$$

if $\Omega' \neq \emptyset$ **then**

$$(k',l') = \underset{(k,l) \text{ such that } \mathbf{S}_k(l,l)\in\Omega'}{\operatorname{argmax}} \mathbf{S}_k(l,l)$$

else

Construct the set of streams which decreases the sum-rate the least from the users with no stream

$$\Omega_k^{''} = \begin{cases} \emptyset, & \text{if } q_k \neq 0 \\ \left\{\mathbf{S}_k(l',l') |\ l' = \underset{l}{\operatorname{argmin}} \left\{\mathrm{SR}_{\Psi} - \mathrm{SR}_{\Psi\cup(k,l)}\right\}\right\}, & \text{if } q_k = 0 \end{cases}$$

$$\text{for } k = 1, ..., K$$

$$\Omega^{''} = \Omega_1^{''} \cup \ldots \cup \Omega_K^{''}$$

if $\Omega^{''} \neq \emptyset$ **then**

$$(k',l') = \underset{(k,l) \text{ such that } \mathbf{S}_k(l,l)\in\Omega''}{\operatorname{argmin}} \left\{\mathrm{SR}_{\Psi} - \mathrm{SR}_{\Psi\cup(k,l)}\right\}$$

else

finish = TRUE

end if

end if

8.3. Continue stream selection

if finish = FALSE **then**

8.3.1. Update

$\Psi = \Psi \cup (k',l')$, $q_{k'} = q_{k'} + 1$

8.3.2. Apply **Alg. 9**

8.3.4. Reconstruct Ω

$\Omega = \{(\mathbf{S}_k)(l,l) | k = 1, ..., K \text{ and } l = 1, ..., d_k \text{ and } (k,l) \notin \Psi\}$

end if

end while

The Complexity of the ISNSSS Algorithm

An upper bound on the number of Alg. 9 calls in the ISNSSS algorithm can be formulated as follows.

$$\underbrace{\sum_{k=2}^{K} d_k}_{\substack{\text{The total number of} \\ \text{stream sequences}}} \times \underbrace{r}_{\substack{\text{Maximum number of times Alg. 9} \\ \text{is called for each stream sequence}}} \tag{4.2}$$

4.4 Fully Connected Interference Networks

In this section, we propose an algorithm for the fully connectivity interference networks where pico cells are deployed closer to each other.

The proposed algorithm for the fully connected interference networks is developed by analyzing the data collected from extensive exhaustive searches. It performs the selection of a stream sequence among a predetermined set of sequences in order to reduce the complexity while guaranteeing at least one stream selection from each user as given in Eq. (4.1b).

The construction of the stream sequences based on the regular structure is expressed after the exhaustive search is explained.

4.4.1 Exhaustive Search for Heterogeneous Networks

Even if the exhaustive search is explained in the previous chapter, there is an additional constraint which is selecting at least one stream for each user. Since the set Φ_j defined in Eq. (3.26) includes all possible stream sequences, an additional set is defined as the set Π in which all stream sequences including at least one stream from each BS-user pair are kept. The set Π can be defined as follows.

$$\begin{aligned} \Pi = \Big\{ & \pi = (\pi_1 \pi_2 \dots \pi_j) \,|\, \pi \in \Phi_j;\ j \geq K; \\ & \forall k, \exists m \in \{1, \dots, j\} \text{ such that } k_m = k \Big\} \end{aligned} \tag{4.3}$$

In other words, π is a stream sequence of length j which is constructed by including at least one stream from each user k. The maximum number of stream sequences in the set Π is calculated as follows.

$$|\Pi| \leq \sum_{i=K}^{r} \binom{r}{i} \tag{4.4}$$

The algorithm is the same as Alg. 11 in Chapter 3 with only a difference in the construction of the sets. The main drawback of the exhaustive search is its complexity that depends on the number of streams. An upper bound on the number of Alg. 9 calls by the

exhaustive search can be formulated as follows.

$$\sum_{i=K}^{r} \Bigg(\underbrace{\left(\frac{r!}{(r-i)!} \right)}_{\substack{\text{An upper bound on the number of} \\ \text{stream sequences of length } i}} \times \underbrace{i}_{\substack{\text{The number of times Alg. 9 is} \\ \text{called for each stream sequence}}} \Bigg) \tag{4.5}$$

4.4.2 Advanced Successive Null Space Stream Selection (ASNSSS) Algorithm

The algorithm is developed by analyzing the data collected from extensive exhaustive searches. It performs the selection of a stream sequence among a predetermined set of sequences in order to reduce the complexity while satisfying Eq. (4.1b). This predetermined set is composed of the sequences with the highest probability of occurrence while performing the exhaustive search. The sequences in this predetermined set have a regular structure which can be achieved by selecting the initial streams from the users that have higher SNR values. Consequently, the proposed stream selection approach starts with pico streams, because pico users are more likely to have higher SNR values on average as justified in the appendix. The construction of the stream sequences based on the regular structure is expressed as follows.

Generated stream sequences are kept in set Π_A in which there can be multiple stream sequences initialized with the same pico stream. For this purpose, we define the following sets constructed for each pico user $k' \in \Gamma$.

- $\Xi_{k'} = \Big\{ \pi = \left(\pi_1 \pi_2 \dots \pi_{d_{k'}}\right) | \pi \in \Phi; \forall i \in \{1, \dots, d_{k'}\}, \pi_i = (k', l_i)$
  for some $l_i \in \{1, \dots, d_{k'}\} \Big\}$ (4.6)

where the definition of the set Φ is given in Eq. (3.25).

In other words, the set $\Xi_{k'}$ includes stream sequences π which are composed of stream permutations of length $d_{k'}$ that belong to pico user k'. Therefore, the number of elements of $\Xi_{k'}$ is $|\Xi_{k'}| = d_{k'}!$

- $\Upsilon_{k',h'} = \Big\{ \pi = \left(\pi_1 \pi_2 \dots \pi_{|\Gamma|-2}\right) \mid \pi \in \Phi;$
  $\forall i \in \{1, \dots, |\Gamma| - 2\}, k_i \in \Gamma \setminus \{k', h'\},$ and $k_i \neq k_j$ if $i \neq j \Big\}$ (4.7)

The set $\Upsilon_{k',h'}$ has two indices. Index k' is used to leave out the streams of pico user k' which are considered in construction of $\Xi_{k'}$ and index h' is used to leave out the streams of pico user h' one of which is considered in construction of set $\Delta_{h'}$. The number of elements of this set is calculated as follows:

$$\left|\Upsilon_{k',h'}\right| = (|\Gamma| - 2)! \times \prod_{i \in \Gamma \setminus \{k',h'\}} d_i \tag{4.8}$$

Note that if $|\Gamma| = 2$, $\Upsilon_{k',h'} = \emptyset$.

- $\Lambda = \Big\{ p |\ p = (k,l) \text{ and } k,l = 1 \Big\}$ (4.9)

Since set Λ only includes the strongest stream of the macro user, $|\Lambda| = 1$.

- $\Delta_{h'} = \Big\{ p |\ p = (h',l) \text{ and } l = 1 \Big\}$ (4.10)

In addition, the number of elements of this set is $|\Delta_{h'}| = 1$. That is to say, the set $\Delta_{h'}$ includes the strongest stream of the remaining pico user.

Based on the above sets, Π_A is constructed as follows:

$$\Pi_A = \bigcup_{k' \in \Gamma} \Xi_{k'} \times \left(\bigcup_{h' \in \Gamma \setminus \{k'\}} \Upsilon_{k',h'} \times \Lambda \times \Delta_{h'} \right) \tag{4.11}$$

Furthermore, the number of elements of set Π_A is computed as follows.

$$|\Pi_A| = \sum_{k' \in \Gamma} q_{k'}! \times \left(\sum_{h' \in \Gamma \setminus \{k'\}} (|\Gamma| - 2)! \times \prod_{i \in \Gamma \setminus \{k',h'\}} d_i \right) \tag{4.12}$$

While constructing set Π_A, interference alignment is implemented after the selection of each stream. Following the selection of a stream sequence from Π_A, it might still be possible to increase the sum-rate further by selecting additional streams. This is realized by attempting to select the strongest streams from the set which is composed of the remaining unselected streams and defined as follows:

$$\Omega = \Big\{ (\mathbf{S}_k)(l,l) | k = 1,...,K,\ l = 1,...,d_k \text{ and } (k,l) \notin \pi_A^* \Big\}$$

where π_A^* is the sequence of the selected streams.

The whole procedure of the algorithm ASNSSS is explained in Alg. 15.

The Complexity of the ASNSSS Algorithm

The number of Alg. 9 calls at each stream selection step of the proposed algorithm can be formulated as follows:

$$\Bigg(\underbrace{\sum_{k' \in \Gamma} d_{k'}! \times \sum_{\substack{h' \in \Gamma \\ h' \neq k'}} (|\Gamma| - 2)! \times \prod_{\substack{i \in \Gamma \\ i \neq k', i \neq h'}} d_i}_{\text{Total number of stream sequences}} \times \underbrace{r}_{\substack{\text{Maximum number of times} \\ \text{Alg. 9 is called}}} \Bigg) \tag{4.13}$$

Alg. 15 Advanced Successive Null Space Stream Selection

Input: α_{kj}, $\mathbf{H}_{kj}$ $\forall k, j$

Initialize the set Π_A

for each stream sequence $\pi \in \Pi_A$ **do**

Apply **Alg. 10**

end for

Select the precoding and postcoding matrices for the permutation that maximizes the sum-rate

$\pi_A^* = \underset{\pi \in \Pi_A}{\text{argmax}}\ \text{SR}_\pi$

$\mathbf{T}_k = (\mathbf{T}_k)_{\pi_A^*}$, $\mathbf{D}_k = (\mathbf{D}_k)_{\pi_A^*}$ for $k = 1, ..., K$

Initialize the variables

finish = FALSE

Construct Ω

$\Omega = \left\{ (\mathbf{S}_k)(l,l) | k = 1, ..., K \text{ and } l = 1, ..., d_k \text{ and } (k,l) \notin \pi_A^* \right\}$

while finish = FALSE **do**

Construct the set of streams which increases the sum-rate

$\Omega' = \left\{ \mathbf{S}_k(l,l) \in \Omega |\ \text{SR}_{\Psi \cup (k,l)} > \text{SR}_\Psi \right\}$

if $\Omega' \neq \emptyset$ **then**

$(k^*, l^*) = \underset{(k,l) \text{ such that } \mathbf{S}_k(l,l) \in \Omega'}{\text{argmax}} \mathbf{S}_k(l,l)$

Update

$\pi_A^* = \pi_A^* \cup (k^*, l^*)$

$q_{k^*} = q_{k^*} + 1$

Apply **Alg. 9**

Reconstruct Ω

$\Omega = \left\{ (\mathbf{S}_k)(l,l) | k = 1, ..., K \text{ and } l = 1, ..., d_k \text{ and } (k,l) \notin \pi_A^* \right\}$

else

finish = TRUE

end if

Set the precoding and the postcoding matrices for the constructed sequence

$\mathbf{T}_k^* = \mathbf{T}_k$, $\mathbf{D}_k^* = \mathbf{D}_k$ for $k = 1, ..., K$

end while

Output: $\mathbf{T}_k^*$, $\mathbf{D}_k^*$ $\forall k$

4.5 Performance Results

In this section, the performances of the proposed algorithms for both fully and partially connected interference networks are given with different scenarios including different number of pico cells.

We consider scenarios where there are 2 transmit antennas for each pico cell and 4 transmit antennas for the macro cell. Each cell has one user that is randomly placed inside its coverage area and there are 2 receive antennas at each user.

In order to study the performance results of the proposed algorithms, pico cells are deployed at the cell edge regions under the coverage of a macro cell. System behavior is observed by varying the locations of the pico BSs with respect to macro BS. More precisely, pico BSs are initially placed relatively close to the macro BS and they are shifted together with the pico users from the inner area to cell edge area of the macro BS which is fixed at location $(0, 0)$. Locations of the pico cells are identified using the ratio d/R where R is the macro cell radius and d is the distance between the macro BS and each pico BS. Since, in practice, pico cells are generally deployed closer to the cell edge areas of the macro cells, the ratio ranges from 0.6 to 1. In addition, the interference level between pico cells generated to each other is investigated by changing the distance between the pico cells, L, while d/R is fixed. Simulations are carried out using the system parameters listed in Table 4.1.

Table 4.1: System Parameters

Parameter Name	**Parameter Value**
Macro BS Power	43dBm
Pico BS Power	24dBm
Bandwidth	10MHz
Carrier Frequency	2.1GHz
Noise Power	-174dBm/Hz
Macro Cell Radius	1000m
Pico Cell Radius	100m
Path loss (macro)	$128.1 + 37.6\text{log10}(R_m(\text{km}))$dB
Path loss (pico)	$140.7 + 36.7\text{log10}(R_p(\text{km}))$dB
Shadowing std. dev. (macro)	8dB
Shadowing std. dev. (pico)	10dB

The received SINR by the macro user is illustrated in Figure 4.2.

Table 4.2: Received SNR (dB) and SINR (dB) of the Macro User for Different d_m Values.

$d_m = 150$m		$d_m = 200$m		$d_m = 250$m	
SNR	**SINR**	**SNR**	**SINR**	**SNR**	**SINR**
26.31	25.40	27.61	26.63	28.92	28.03

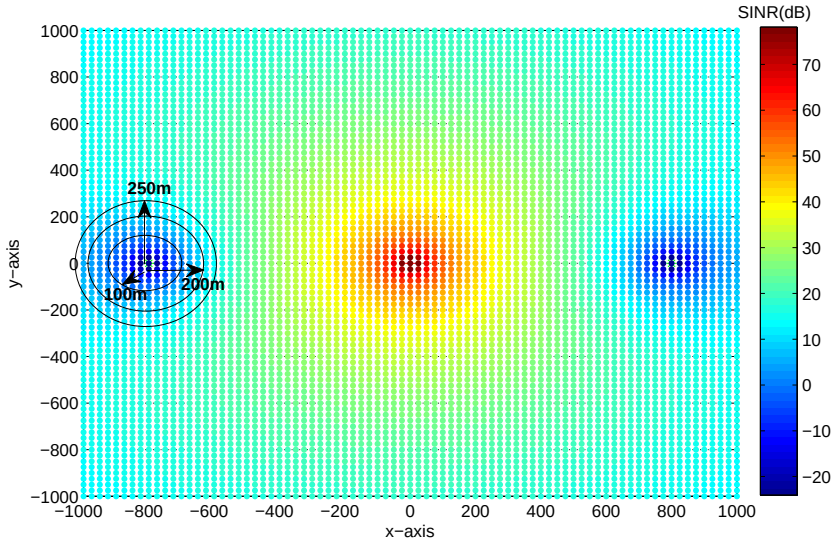

Figure 4.2: Received SINR of the macro user when pico BSs at $d/R = 0.8$

The received SNR and SINR of the macro user are given in Table 4.2 for different distances between the macro user and a pico BS, d_m. It can be observed that the macro user receives negligible interference from the pico BSs for $d_m > 250$m. Therefore, IA algorithm, Alg. 9, is applied to mitigate the interference generated from pico BSs to the macro user when $d_m \leq 250$m. Since the SNR and the SINR can vary with the different transmit power values, this condition on d_m may change for different transmit power values.

4.5.1 Scenarios for Partially Connected Interference Networks

For partially connected interference networks, we evaluate the algorithm ISNSSS considering three different scenarios including different number of pico cells. These scenarios are explained in detail in the following.

Scenario 1.1: d/R is changing for 1 Pico Cell

In Scenario 1.1, there is only 1 pico cell deployed at the cell edge regions under the coverage of a macro cell as illustrated in Figure 4.3.

In order to analyze the behavior of the stream selection algorithms, the selection probabilities of the stream sequences in the exhaustive search with their average sum rate are given in Figure B.1 in Appendix B. It can be observed that the probability of selecting the first stream from the pico user is greater than selecting it from the macro user.

Since there are two pico streams in this scenario, Alg. 14 constructs two stream sequences by selecting the first streams from these pico streams. The obtained stream paths

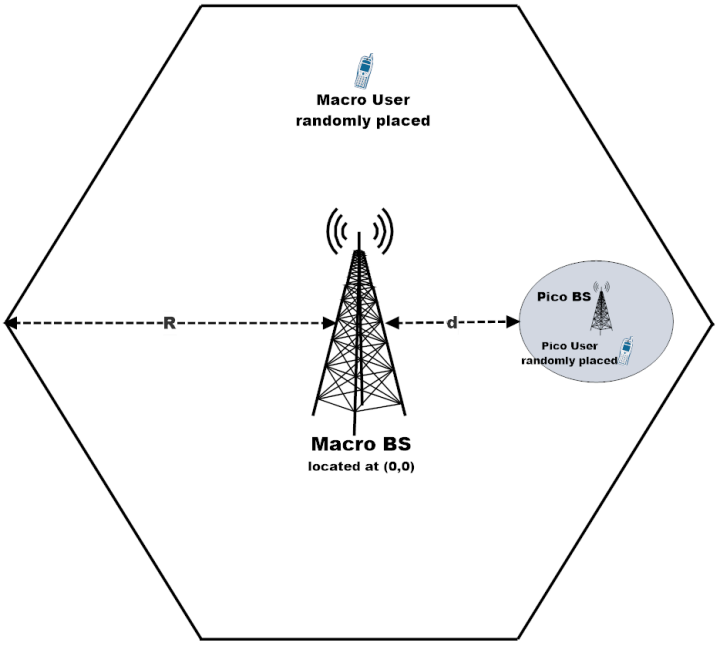

Figure 4.3: Scenario 1.1: One Pico cell is deployed under the coverage of a macro cell

are compared in terms of their sum rates and the path with the highest sum rate is selected.

In Figure 4.4, ISNSSS algorithm is also compared to the existing IA methods, max-SINR and min-Leak explained in the Chapter 3. The performance of the min-Leak algorithm with one stream per user case is very poor compared to the stream selection algorithms and max-SINR algorithm with one stream per user case. The comparison of the number of selected streams for each user for different distance ratios can be listed in Table 4.3. The results confirm that the proposed method allocates more streams to the users while increasing the sum rate.

Table 4.3: Scenario 1.1: The Average Number of the Selected Streams Per User

	d/R=0.6	d/R=0.8	d/R=1
Macro User (ISNSSS)	1.89	1.9	1.92
Macro User (SNSSS (Amara et al. [2012b]))	1.79	1.83	1.85
Pico User (ISNSSS)	1.5	1.55	1.58
Pico User (SNSSS (Amara et al. [2012b]))	1.5	1.47	1.42

In addition, the complexities of the stream selection algorithms are compared in Table 4.4. It can be seen that the exhaustive search is very complex when compared to the ISNSSS and the SNSSS algorithms. On the other hand, the ISNSSS algorithm provides better performance than the SNSSS algorithm with a small increase in complexity.

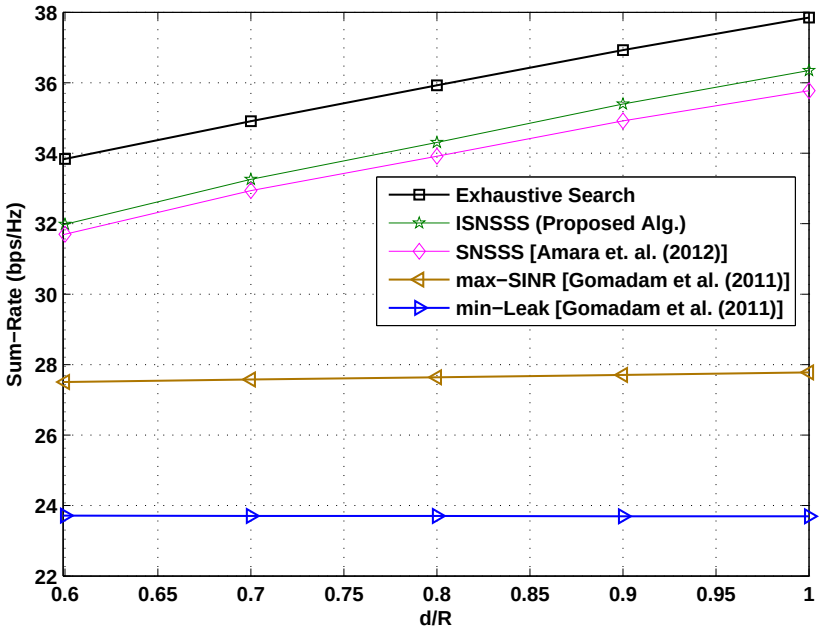

Figure 4.4: Scenario 1.1: Average sum rate vs. distance ratio d/R comparison with existing IA methods

Table 4.4: Scenario 1.1: Complexity Comparison of Stream Selection Algorithms for 1 Pico Case

Exhaustive Search	**ISNSSS**	**SNSSS**
240	8	4

Scenario 1.2: d/R is changing for 2 Pico Cells

In Scenario 1.2 there are 2 pico cells deployed at the cell edge regions under the coverage of a macro cell as illustrated in Figure 4.5.

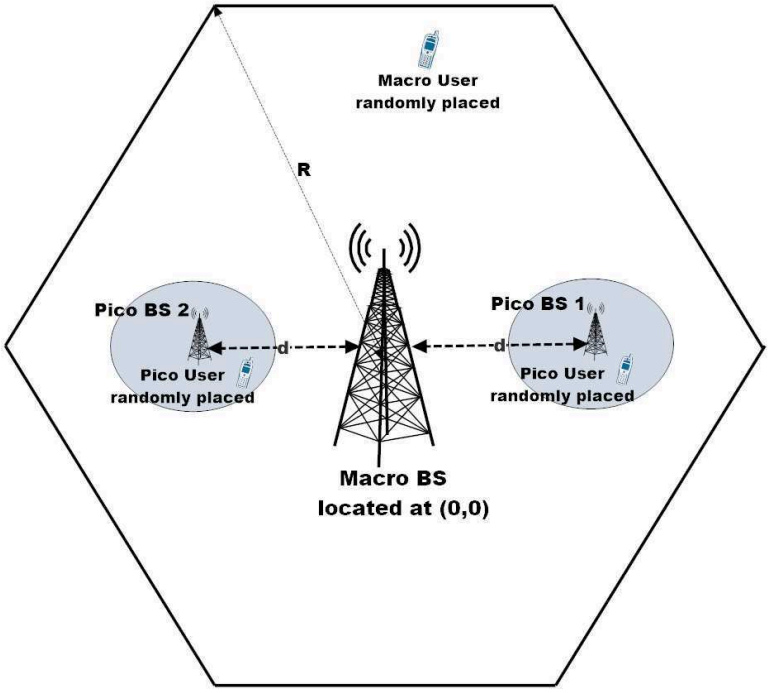

Figure 4.5: Scenario 1.2: Two Pico cells are deployed under the coverage of a macro cell

In this scenario, there are 6 streams in total and there are 4 streams that belong to the pico users. Therefore, 4 stream sequences are constructed initialized by the pico streams.

Figure B.2 given in Appendix B justifies the initial streams of the selected stream sequences in the form of trees. Each node in a given tree contains a total probability and a total weighted sum rate of the constructed stream sequences which are initialized by the corresponding initial stream. It can be seen that the stream sequences initialized by the pico streams have higher sum rate values comparing to the stream sequences initialized by the macro streams.

In Figure 4.6, these methods are also compared to the existing IA methods. Exhaustive search gives the upper bound. The performance of the ISNSSS algorithm also higher than the other IA algorithms.

The comparison of the number of selected streams for each user for different distance ratios can be listed in Table 4.5. The results confirm that the proposed method allocates more streams on average to pico users while ensuring better service to the users and increasing the sum rate.

Furthermore, the complexities of the stream selection algorithms are compared in Ta-

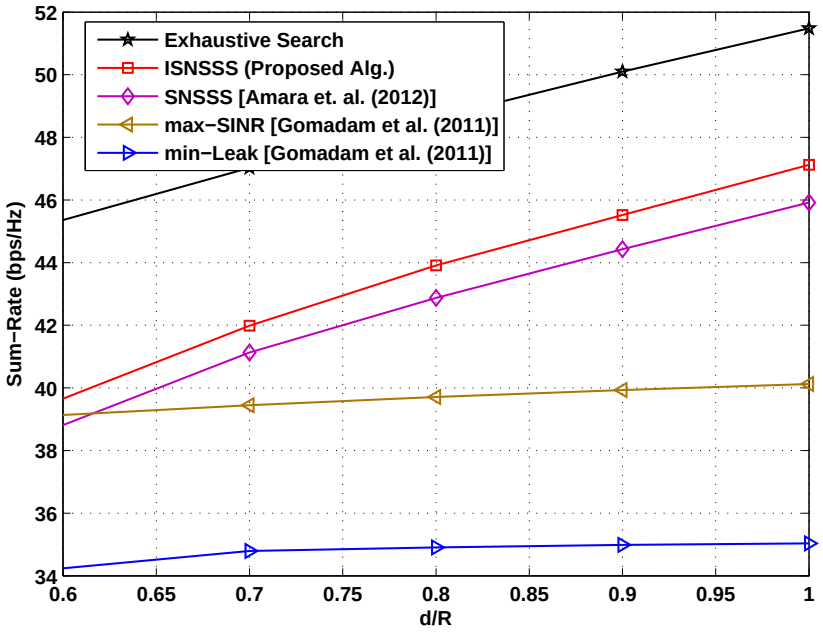

Figure 4.6: Scenario 1.2: Average sum rate vs. distance ratio d/R comparison with existing IA methods

Table 4.5: Scenario 1.2: The Average Number of the Selected Streams

	d/R=0.8	d/R=1
Macro User (ISNSSS)	1.82	1.85
Macro User (SNSSS (Amara et al. [2012b]))	1.82	1.84
Pico 1 User (ISNSSS)	1.55	1.58
Pico 1 User (SNSSS (Amara et al. [2012b]))	1.53	1.52
Pico 2 User (ISNSSS)	1.59	1.61
Pico 2 User (SNSSS (Amara et al. [2012b]))	1.58	1.57

ble 4.6. Once again, it can be seen that the exhaustive search is more complex when compared to the ISNSSS algorithm as the total number of streams increases in the network.

Table 4.6: Scenario 1.2: Complexity Comparison of Stream Selection Algorithms for 2 Pico Case

Exhaustive Search	ISNSSS	SNSSS
9720	24	6

Scenario 1.3: d/R is changing for 3 Pico Cells

In Scenario 1.3, there are 3 pico cells deployed at the cell edge regions as shown in Figure 4.7.

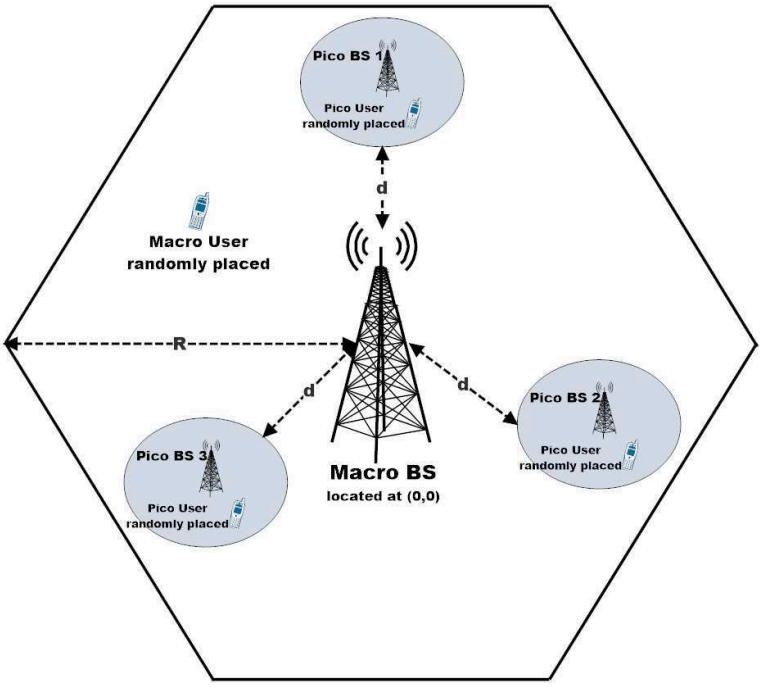

Figure 4.7: Scenario 1.3: Three pico cells are deployed with an equal distance to each other.

Figure B.3 given in Appendix B illustrates the initial streams of the selected stream sequences for Scenario 1.3. It can be seen that the total weighted sum rates ($P \times SR$) of the stream sequences initialized by the pico streams have higher values than those of the stream sequences initialized by the macro streams.

In Figure 4.8, these methods are compared to the existing iterative and stream selection based IA algorithms.

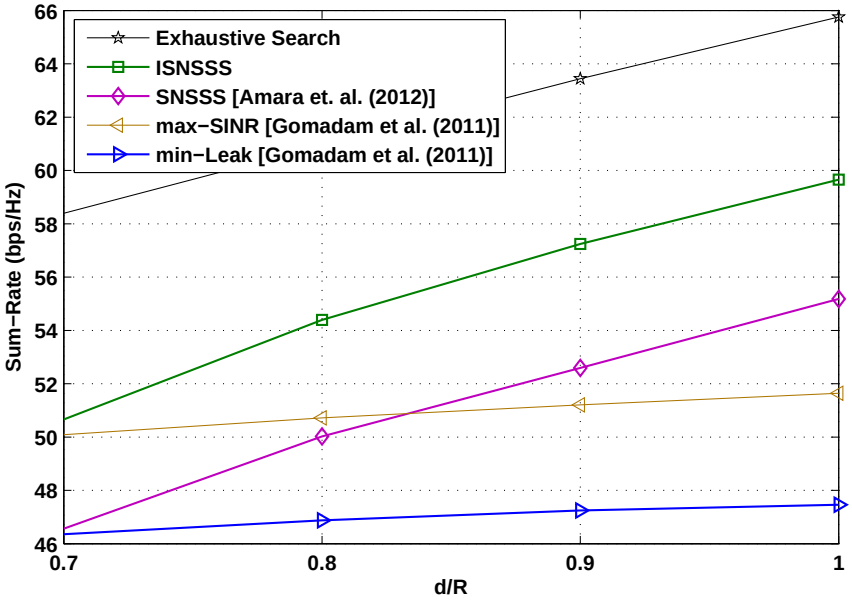

Figure 4.8: Scenario 1.3: Average sum rate vs. distance ratio d/R comparizon with existing IA methods

Furthermore, the complexities of the stream selection algorithms are compared in Table 4.7. It can be seen that the difference between the complexities of the ISNSSS and the SNSSS algorithms is insignificant when compared to the exhaustive search, but the performance of the ISNSSS algorithm is approximately 5bps/Hz higher than the SNSSS algorithm.

Table 4.7: Scenario 1.3: Complexity Comparison of Stream Selection Algorithms for 3 Pico Case

Exhaustive Search	**ISNSSS**	**SNSSS**
766080	48	8

4.5.2 Scenarios for Fully Connected Interference Networks

The scenario for fully connected interference network is realized by four different scenarios to evaluate the performance of the proposed algorithm in the following sections. In Scenarios 2.1 and 2.2, two pico cells are deployed at the cell edge regions of the macro cell as illustrated in Figure 4.9. In Scenarios 2.3 and 2.4, three pico cells are symmetrically deployed with respect to the macro cell as illustrated in the Figure 4.10. The number of N_{T_k} and N_{R_k} are same as in Scenarios 2.1 for each pico cell and for macro cell.

The related exhaustive search analysis for the scenarios of the fully connected interfer-

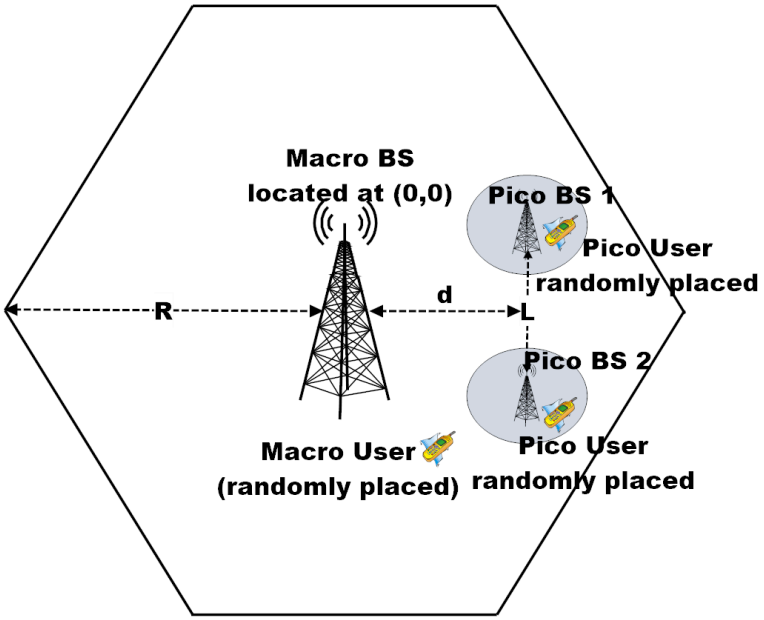

Figure 4.9: Scenario 2.1 and 2.2: Two pico cell case with different values of d and L

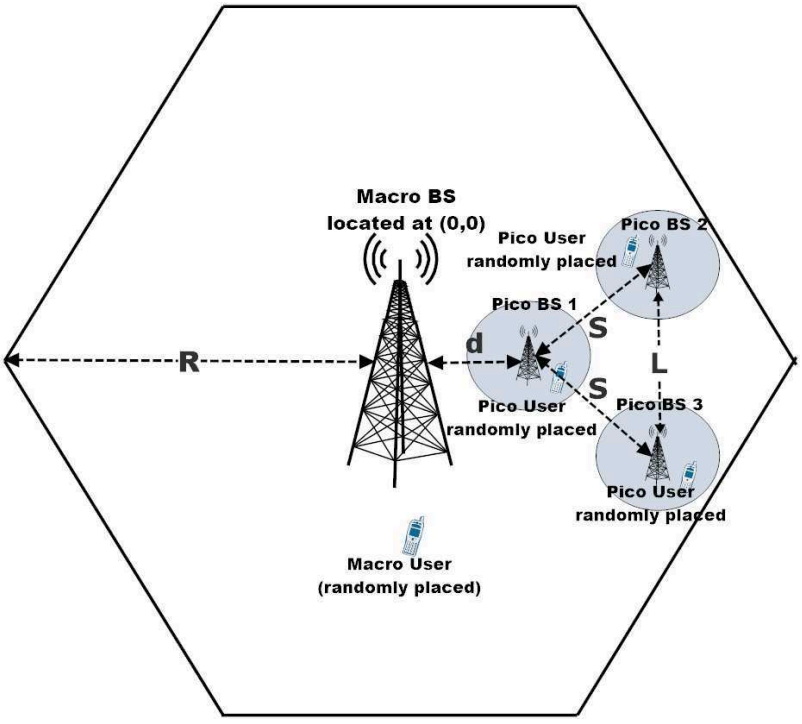

Figure 4.10: Scenario 2.3 and 2.4: Three pico cell case with different values of d and L.

ence networks is given in Appendix B. Using the given analysis, the proposed algorithm builds the set of stream sequences having a regular structure.

Scenario 2.1: d/R is changing while L is fixed

In order to evaluate the ASNSSS algorithm for this scenario, pico cells are shifted towards to the cell edge of the macro cell by changing the ratio d/R. The distance between the pico cells is constant and it is $L = 150$m to have fully connected scenarios.

The sum rate values achieved by different IA approaches are given in Figure 4.11. It can be seen that the ASNSSS algorithm outperforms the existing stream selection methods and iterative approaches.

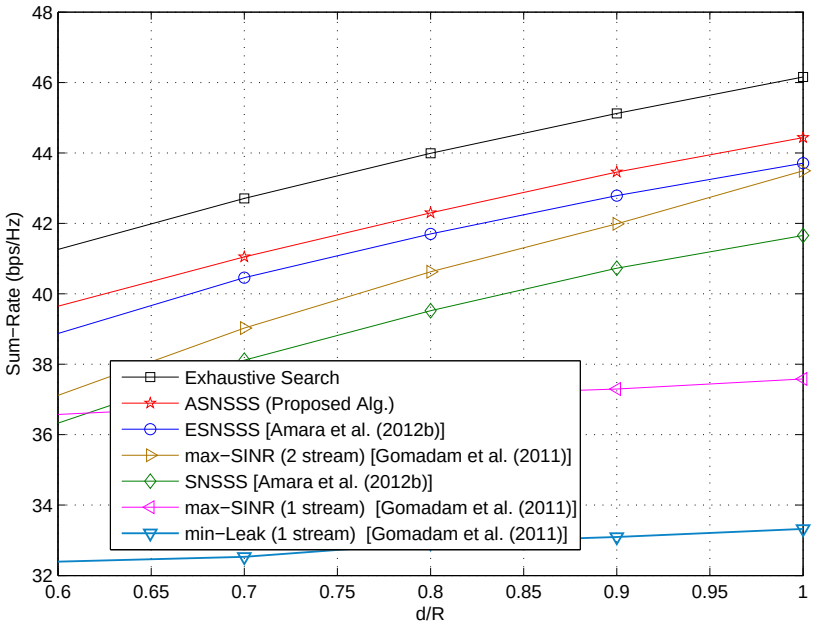

Figure 4.11: Scenario 2.1: Sum-Rate vs d/R between 0.6 and 1

The comparison of the number of selected streams for each user for different distance ratios can be seen in Table 4.8. The results confirm that the proposed method allocates more streams to pico users at the cell edge regions while increasing the sum rate.

Table 4.8: Scenario 2.1: The Average Number of the Selected Streams.

	d/R=0.6	d/R=0.8	d/R=1
Macro User (ASNSSS)	1.59	1.63	1.7
Macro User (ESNSSS (Amara et al. [2012b]))	1.67	1.74	1.81
Macro User (SNSSS (Amara et al. [2012b]))	1.91	1.89	1.93
Pico 1 User (ASNSSS)	1.47	1.46	1.5
Pico 1 User (ESNSSS (Amara et al. [2012b]))	1.18	1.2	1.25
Pico 1 User (SNSSS (Amara et al. [2012b]))	1.34	1.30	1.29
Pico 2 User (ASNSSS)	1.58	1.59	1.56
Pico 2 User (ESNSSS (Amara et al. [2012b]))	1.28	1.26	1.24
Pico 2 User (SNSSS (Amara et al. [2012b]))	1.31	1.30	1.29

Scenario 2.2: d/R is fixed while L is changing

In this scenario, pico cells are shifted away from each other along the y-axis while the x-axis is fixed for the pico cells. The distance between the pico cells is kept maximum $L = 400$m to be ensure to have fully connected network.

The SNR and SINR values of each pico user are listed in Table 4.9 and Table 4.10 for $L = 100$m and $L = 400$m, respectively. These values are obtained when there is only pico BSs generating interference to each other at different distances. Since the received SNR and SINR of the pico users are close to each other when $L = 400$m, the generated interference can be negligible between the pico cells. Therefore, the distance between the pico cells is kept maximum $L = 400$m in the scenarios.

Table 4.9: Scenario 2.2: Received SNR (dB) and SINR (dB) of the Pico Users when $L = 100$m.

	SNR	SINR
Pico 1 User	40.50	26.38
Pico 2 User	40.00	25.87

Table 4.10: Scenario 2.2: Received SNR (dB) and SINR (dB) of the Pico Users when $L = 400$m.

	SNR	SINR
Pico 1 User	40.50	39.42
Pico 2 User	40.00	39.07

Figure 4.12 shows the performance comparison between the proposed algorithm and the existing algorithms. It can be seen that the gap between the exhaustive search and the proposed ASNSSS algorithm is very small, only approximately 1.3 bps/Hz; and ASNSSS algorithm outperforms the existing stream selection methods and iterative approaches.

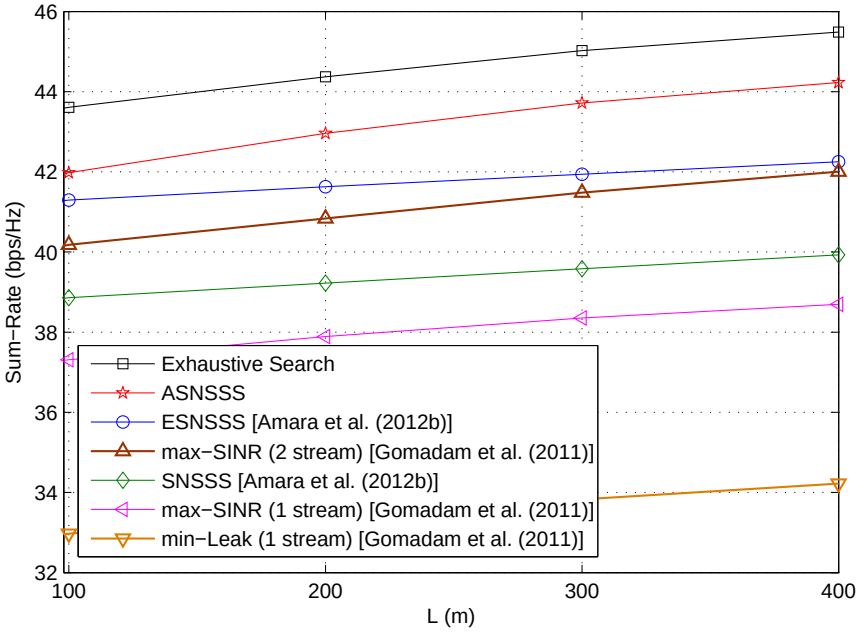

Figure 4.12: Scenario 2.2: Sum-Rate vs Distance L between 100m and 400m

Complexity Comparison of the Stream Selection Algorithms for Scenario 2.1 and Scenario 2.2:

The complexity of the stream selection algorithms are calculated in terms of the number calls to Alg. 9 and the comparison is given in Table 4.11 for Scenario 2.1 and Scenario 2.2, since the total number of streams is same in scenarios with the same network configurations. It can be observed that Alg. 9 is called by the ASNSSS algorithm at most 24 times which is much fewer than the number of calls to Alg. 9 by the exhaustive search and the ESNSSS algorithm. It should be noted that these results represent upper bounds for the given algorithms as given in Eq. (4.13), since different stream sequences constructed with the different number of streams can be selected by the stream selection algorithms. In the exhaustive search, although the number of the searched stream sequences is fixed, it is difficult to obtain the exact number of the stream sequences and, thus, the exact number of calls to Alg. 9 due to the constraint defined in Eq. (4.1b). Therefore, an upper bound is also calculated for the exhaustive search using Eq. (4.5).

Further simulations are performed to compare the complexities of the stream selection algorithms. The average number of calls to Alg. 9 is calculated when pico cells are located

Table 4.11: Scenario 2.1 and Scenario 2.2: Complexity Comparison of Stream Selection Algorithms for 2 Pico Case

Exhaustive Search	**ASNSSS**	**ESNSSS**	**SNSSS**
9720	24	36	6

at $d/R = 0.8$ and $L = 150$m. The related results are shown using histograms for SNSSS, ASNSSS, ESNSSS algorithms in Figure 4.13. The number of calls to Alg. 9 is fixed which is equal to 9216 for the exhaustive search. In addition, the average number of calls to Alg. 9 does not change with either d/R or L as illustrated in Figures 4.14.

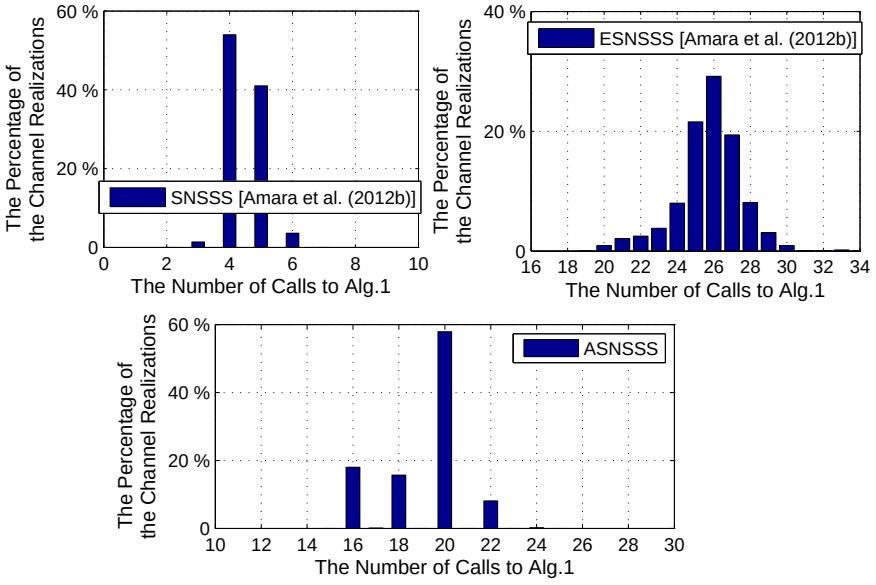

Figure 4.13: Comparisons of the Average Number of Calls to Alg. 9 at d/R=0.8 and L=150m for two pico cell case

The results demonstrate that the ASNSSS algorithm has a lower complexity with a simple regular structure when compared to the other stream selection based IA algorithms.

Scenario 2.3: d/R is changing while L is fixed

In this scenario, pico cells are shifted towards to the cell edge of the macro cell by changing the ratio d/R while the distances between the pico cells are kept fixed as $L = 200$m and $S = 200$m.

The sum rate values achieved by different approaches for the first case of this scenario are given in Figure 4.15. It is shown that the performance of the proposed algorithm is quite close to the one of the exhaustive search; and the gap is approximately 1 bps/Hz.

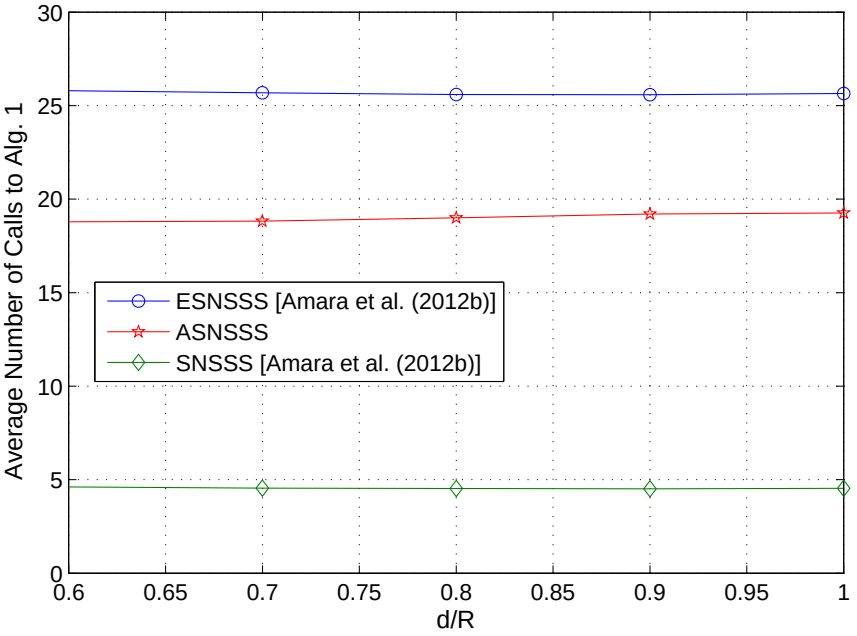

Figure 4.14: Scenario 2.1: Comparisons of the Average Number of Calls to Alg. 9 vs d/R between 0.6 and 1

Additionally, the ASNSSS algorithm shows better performance than the other existing stream selection approaches.

Scenario 2.4: d/R is fixed while L is changing

In this scenario, Pico cell 2 and Pico cell 3 are shifted away from each other along the y-axis while Pico cell 1 is fixed.

The performances of the proposed and the existing algorithms for this case is shown in Figure 4.16. Similar to the previous cases, the performance of the proposed algorithm is quite close to that of the exhaustive search; and the gap is approximately 1 bps/Hz while its performance is better than the other existing algorithms.

Complexity Comparison of the Stream Selection Algorithms for Scenario 2.3 and Scenario 2.4:

To evaluate the complexities, once again, the number calls to Alg. 9 is considered for Scenario 2.3 and Scenario 2.4. To compute the maximum numbers of calls to Alg. 9, Eq. (4.5) and Eq. (4.13) are used and the results are given in Table 4.12. As in the two pico

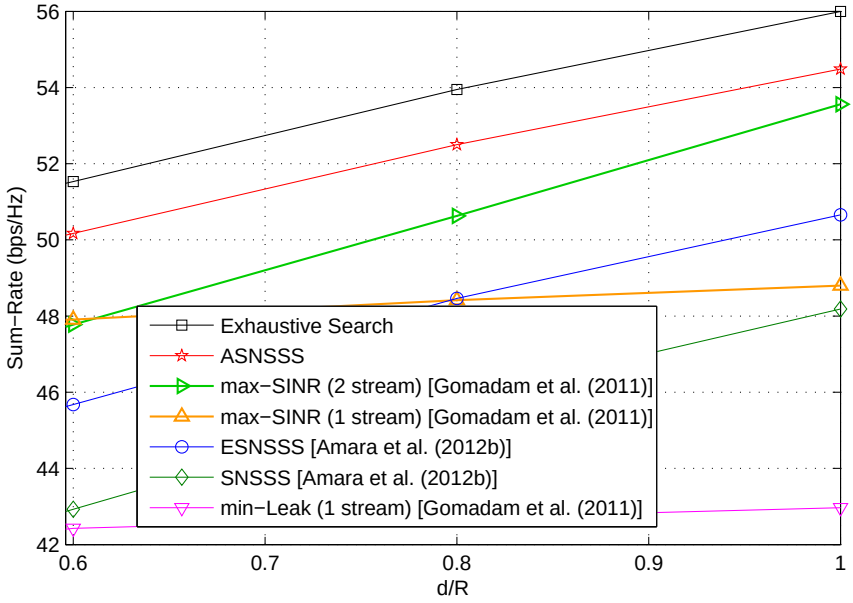

Figure 4.15: Scenario 2.3: Sum-Rate vs d/R between 0.6 and 1

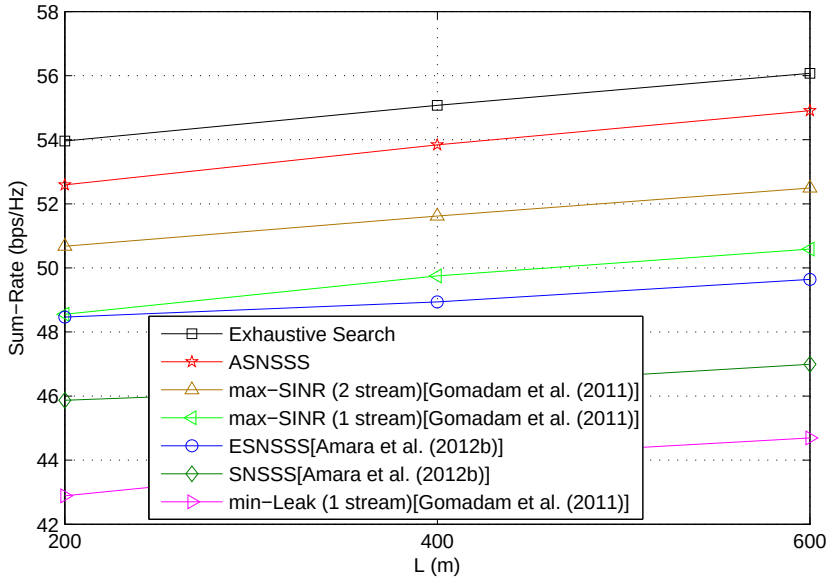

Figure 4.16: Scenario 2.4: Sum-Rate vs Distance L between 200m and 600m

cell case, given results represents the upper bounds for the given algorithms. In other words, the results given in the table can be obtained when the selected stream sequence includes all the streams. On the other hand, the upper bound for the exhaustive search is obtained due to the difficulty in computing the exact number of the stream sequences considering the constraint defined in Eq. (4.1b). Therefore, an upper bound is also calculated for the exhaustive search even if the number of the searched stream sequences is fixed.

Table 4.12: Scenario 2.3 and Scenario 2.4: Complexity Comparison of Stream Selection Algorithms for 3 Pico Case

Exhaustive Search	**ASNSSS**	**ESNSSS**	**SNSSS**
766080	192	64	8

It can be observed that there is a significant complexity reduction by performing the ASNSSS algorithm. In addition, although ESNSSS and SNSSS algorithms have lower complexities, the ASNSSS algorithm can achieve almost the same performance with the exhaustive search.

Furthermore, histograms of the numbers of calls to Alg. 9 are obtained for SNSSS, ASNSSS and ESNSSS algorithms as seen in Figure 4.17 for $d/R = 0.8$ and $L = 150$m. Since the number of calls to Alg. 9 is fixed for the exhaustive search and it is equal to 729216, it is not shown in Figure 4.17.

In addition, the average number of calls to Alg. 9 does not change with either d/R or L for the ASNSSS, ESNSSS and SNSSS algorithms and it is illustrated in Figure 4.18.

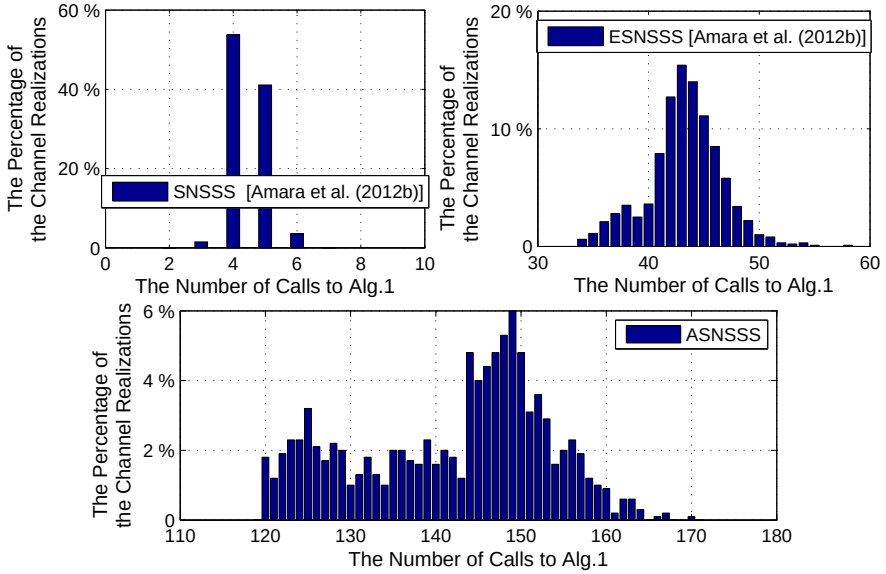

Figure 4.17: Comparisons of the Average Number of Calls to Alg. 9 at d/R=0.8 and L=150m for three pico cell case

The results demonstrates a clear advantage of the ASNSSS algorithm compared to

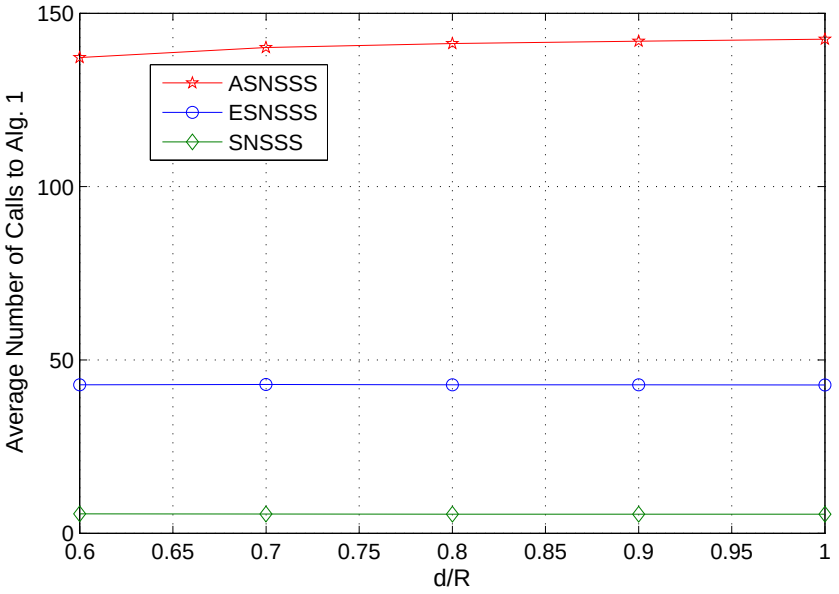

Figure 4.18: Scenario 2.3: Comparisons of Average Number of Calls to Alg.1 vs d/R between 0.6 and 1

the exhaustive search in terms of complexity and applicability due to the fact that the ASNSSS algorithm avoids from searching all stream paths by making use of a simple regular structure. In addition, as the number of the pico cells increases, the performance of the ASNSSS algorithm gets closer to the performance of the exhaustive search.

4.6 Conclusion

In this chapter, we have presented two efficient stream selection approaches for heterogeneous networks in order to reduce the complexity of the exhaustive search and, still, achieve a performance closed to the one of the exhaustive search. The proposed algorithms deal with the interference among the macro and pico cells; after each stream is selected, we perform orthogonal projections in order to handle the interference to and from the selected stream. Furthermore, the algorithms satisfy the constraint that at least one stream must be allocated to each user, which is not required by the existing stream selection approaches.

For the partially connected interference networks, the proposed algorithm called ISNSSS constructs a set of stream sequences by initializing each of them with the streams of the pico users. Then the best stream sequence that gives the highest sum rate is selected from the set.

For the fully connected interference networks, the proposed algorithm called ASNSSS selects the best stream sequence in terms of sum rate from a predetermined set of sequences that is constructed from an analysis of the behavior of the exhaustive search algorithm. It

is observed that initializing the stream sequences using the streams of pico users generally leads to better stream sequences since it is more likely for pico users to have a higher SNR value than the macro user.

The performance of the ISNSSS and the ASNSSS algorithms have been evaluated for different scenarios with different number of pico cells by varying the positions of pico BSs at the cell edge zone of the macro cell. The performance results indicate that the proposed algorithms outperform the existing stream selection approaches and iterative IA solutions by getting closer to the upper bound set by the exhaustive search while achieving significantly lower complexities. Moreover, as the number of pico cells increases, it has been observed that the performance gap between the ASNSSS and the exhaustive search decreases with an increased complexity which is still significantly lower than the one of the exhaustive search.

Part VI

part 6

Chapter 5

Interference alignment with imperfect CSI

5.1 Introduction

The algorithms proposed in the previous chapters assume that the CSI is perfectly known at the transmitters in a centralized topology. Thus, the interference can be perfectly aligned by designing the precoders and the postcoders. Since this assumption is not realistic for practical systems, feedback schemes have been commonly implemented in cellular networks (Love et al. [2008]).

In the feedback mechanism, receivers estimate the channel coefficients by using training sequences. After the channel estimation, receivers feedback the quantized CSI to the transmitters with a certain number of bits using codebooks known at both the transmitters and the receivers. Thus, precoders and postcoders can be calculated to align the interference. The quality of the obtained CSI by the limited feedback affects the performance of the IA. It has been shown that increasing the size of the codebook decreases the distortion caused by the limited feedback, and increases the feedback overhead in the network. Therefore, the number of bits for CSI should be optimized depending on the channel conditions (Özbek and Le Ruyet [2014b]).

Equal bit allocation in which the number of feedback-bits for each channel is fixed is not efficient for the heterogeneous networks due to different pathloss and shadowing effects.To increase the system throughput with the quantized channel, different feedback bit allocation schemes have been studied for the interference alignment in K pair MIMO systems. In order to minimize the effect of the distortion, an adaptive feedback bit allocation scheme that adaptively selects the number of feedback bits to the links of each transmitter-receiver pair have been designed in the studies of Cho et al. [2012]) and (Chen and Yuen [2014].

In the context of the heterogeneous networks, optimizing the bit allocation can increase the performance of the feedback schemes for IA technique by considering the distinctive features of the heterogeneous networks, such as unequal number of transmit antennas and transmit power levels (Niu et al. [2014]), (Rihan et al. [2015]).

In this chapter, we consider a limited feedback scheme for the proposed stream selection based IA algorithms. To decrease the intra-stream interference in the quantized CSI case, a restricted version of the ASNSSS algorithm is presented as restricted ASNSSS (RASNSSS) algorithm which does not select additional streams after the construction of the stream sequences. However, there are still multiple pico streams in the constructed stream sequences and it yields a performance degradation due to the quantization in the case of a reasonable number of limited feedback bits. To avoid the intra-stream interference and to decrease the feedback overhead, K-stream selection (KSS) algorithm is proposed where only the best streams of each user is selected. Instead of allocating equal number of feedback bits to each channel (Aycan et al. [2015]), an adaptive bit allocation scheme is presented to maximize the average sum-rate by optimizing the number of bits to quantize the CDI of each user. The adaptive bit allocation is presented for ISNSSS (Aycan Beyazit et al. [2016b]), RASNSSS (Aycan Beyazit et al. [2016c]) and KSS (Aycan Beyazit et al. [2016d]) algorithms. The performance is evaluated for both the partial and the fully connected interference network scenarios.

We first introduce the system model in Section 5.2 including the limited feedback model. Next, the stream selection based IA algorithms for the heterogeneous networks which are RASNSSS and KSS, are proposed for the imperfect CSI in Section 5.3 and Section 5.4, respectively. Different adaptive feedback bit allocation schemes are presented for the RASNSSS, KSS and ISNSSS algorithms in order to increase the sum rate of the network for a fixed feedback load per user in Section 5.5. Next, we evaluate the performance of the proposed algorithms in Section 5.6. Finally, we conclude the chapter in Section 5.7.

5.2 System Model

In this chapter, a K-pair heterogeneous network is considered as defined in Chapter 4. The transmission and the channel quantization model for the limited feedback scheme are given in the following sections.

5.2.1 Transmission Model

We modify Eq. (3.1) for the case of imperfect CSI and define the transmitted signal as follows.

$$\mathbf{x}_k = \sqrt{P_k}\tilde{\mathbf{T}}_k \mathbf{s}_k \tag{5.1}$$

where $\tilde{\mathbf{T}}_k$ is the unitary precoding matrix of the k^{th} transmitter with dimension $N_{T_k} \times q_k$ and it is obtained by the proposed algorithms under the quantized channel, $\tilde{\mathbf{H}}_{kj}$, between the j^{th} transmitter and the k^{th} receiver with dimension $N_{R_k} \times N_{T_j}$.

Each user decodes the received signals by multiplying them with the postcoding matrices, $\tilde{\mathbf{D}}_k$, of dimension $N_{R_k} \times q_k$ and they are obtained by the proposed algorithms under the quantized channel. Thus, the decoded data symbols are given as $\hat{\mathbf{y}}_k = \tilde{\mathbf{D}}_k^H \mathbf{y}_k$.

The evaluated data rate for the i^{th} stream of the k^{th} user can be expressed as follows.

$$\tilde{\mathrm{R}}_{ki} = \log_2(1 + \tilde{\gamma}_{ki}) \tag{5.2}$$

where $\tilde{\gamma}_{ki}$ is the evaluated SINR for the i^{th} stream of the k^{th} user and it is given by

$$\tilde{\gamma}_{ki} = \frac{(P_k/q_k)\,\alpha_{kk}^2 \left(\tilde{\mathbf{d}}_k^i\right)^H \tilde{\mathbf{H}}_{kk} \tilde{\mathbf{t}}_k^i \left(\tilde{\mathbf{t}}_k^i\right)^H \tilde{\mathbf{H}}_{kk}^H \tilde{\mathbf{d}}_k^i}{\left(\tilde{\mathbf{d}}_k^i\right)^H \tilde{\mathbf{B}}_{ki} \tilde{\mathbf{d}}_k^i} \qquad \forall k = 1, ..., K, \quad \forall i = 1, ..., q_k \tag{5.3}$$

where $\tilde{\mathbf{t}}_k^i$ is the i^{th} column vector of matrix $\tilde{\mathbf{T}}_k$ with the size of $N_{T_k} \times 1$ and $\tilde{\mathbf{d}}_k^i$ is the i^{th} column vector of matrix $\tilde{\mathbf{D}}_k$ with the size of $N_{R_k} \times 1$. Since the perfect CSI is not available at the transmitters, $\tilde{\mathbf{H}}_{kj}$ is used in the algorithms. The interference plus noise covariance matrix of the k^{th} receiver, $\tilde{\mathbf{B}}_k$, is defined as

$$\tilde{\mathbf{B}}_k = \sum_{\substack{l=1,\\ l\neq i}}^{q_k} \frac{P_k}{q_k} \alpha_{kk}^2 \tilde{\mathbf{H}}_{kk} \tilde{\mathbf{t}}_k^l \tilde{\mathbf{t}}_k^{lH} \tilde{\mathbf{H}}_{kk}^H + \sum_{\substack{j=1\\ j\neq k}}^{K} \sum_{q=1}^{q_j} \frac{P_j}{q_j} \alpha_{kj}^2 \tilde{\mathbf{H}}_{kj} \tilde{\mathbf{t}}_j^q \tilde{\mathbf{t}}_j^{qH} \tilde{\mathbf{H}}_{kj}^H + \sigma^2 \mathbf{I}_{N_{R_k}} \qquad k = 1, ..., K, \quad i = 1, ..., q_k \tag{5.4}$$

The evaluated sum rate is calculated as follows.

$$\tilde{\mathrm{SR}} = \sum_{k=1}^{K} \sum_{i=1}^{q_k} \tilde{\mathrm{R}}_{ki} \tag{5.5}$$

The achievable data rate for the i^{th} stream of the k^{th} user can be expressed as follows.

$$\tilde{\mathrm{R}}'_{ki} = \log_2(1 + \tilde{\gamma}'_{ki}) \tag{5.6}$$

where $\tilde{\gamma}'_k$ is the achievable SINR of the i^{th} stream of the k^{th} receiver and it is given by

$$\tilde{\gamma}'_{ki} = \frac{(P_k/q_k)\,\alpha_{kk}^2 \left(\tilde{\mathbf{d}}_k^i\right)^H \mathbf{H}_{kk} \tilde{\mathbf{t}}_k^i \left(\tilde{\mathbf{t}}_k^i\right)^H \mathbf{H}_{kk}^H \tilde{\mathbf{d}}_k^i}{\left(\tilde{\mathbf{d}}_k^i\right)^H \tilde{\mathbf{B}}'_{ki} \tilde{\mathbf{d}}_k^i} \qquad \forall k = 1, ..., K, \quad \forall i = 1, ..., q_k \tag{5.7}$$

The interference plus noise covariance matrix for stream i of the k^{th} receiver, $\tilde{\mathbf{B}}'_{ki}$, is defined as

$$\tilde{\mathbf{B}}'_{ki} = \sum_{\substack{l=1,\\ l\neq i}}^{q_k} \frac{P_k}{q_k} \alpha_{kk}^2 \mathbf{H}_{kk} \tilde{\mathbf{t}}_k^l \tilde{\mathbf{t}}_k^{lH} \mathbf{H}_{kk}^H + \sum_{\substack{j=1\\ j\neq k}}^{K} \sum_{q=1}^{q_j} \frac{P_j}{q_j} \alpha_{kj}^2 \mathbf{H}_{kj} \tilde{\mathbf{t}}_j^q \tilde{\mathbf{t}}_j^{qH} \mathbf{H}_{kj}^H + \sigma^2 \mathbf{I}_{N_{R_k}} \qquad \forall k = 1, ..., K, \quad \forall i = 1, ..., q_k \tag{5.8}$$

The achievable sum rate is calculated as follows.

$$\tilde{\mathrm{SR}}' = \sum_{k=1}^{K} \sum_{i=1}^{q_k} \tilde{\mathrm{R}}'_{ki} \tag{5.9}$$

In the stream selection algorithms, the sum rate is calculated using $\tilde{\mathrm{SR}}$, since only the quantized channel is available in the transmitters through the communication channels. On the other hand, the performances of the proposed algorithms are determined using $\tilde{\mathrm{SR}}'$. Therefore, the stream selection scheme aims to maximize the total sum rate of the network while guaranteeing to select at least one stream from each user as follows.

$$\left\{(\tilde{\mathbf{T}}_k^*, \tilde{\mathbf{D}}_k^*)\right\}_{k=1,\ldots,K} = \underset{\tilde{\mathbf{T}}_k, \tilde{\mathbf{D}}_k}{\operatorname{argmax}}\ \tilde{\mathrm{SR}} \tag{5.10a}$$

$$\text{s.t.} \quad q_k \geq 1 \quad k = 1, \ldots, K \tag{5.10b}$$

5.2.2 Limited Feedback Model

In this section, a limited feedback scheme is presented based on RVQ. The proposed IA algorithms require all the CSI to obtain all precoding and postcoding vectors. Therefore, a centralized feedback model is considered in which the macro BS collects all the CSIs from pico BSs through the error and delay free backhaul links. It is assumed that CQI is perfectly available at the BS and the receivers only feedback their CDI.

Each step of the feedback scheme that is illustrated in Figure 5.1 can be explained as follows.

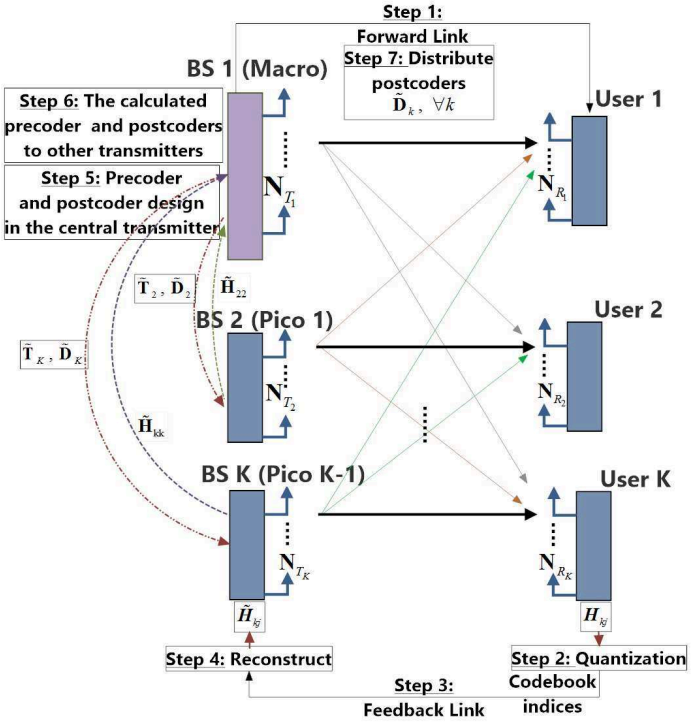

Figure 5.1: Centralized CSI Feedback Scheme (without an additional unit): Macro BS acts as the central unit

- **Step 1:** It is assumed that the CSI has been perfectly estimated at each receiver as $\mathbf{H}_{kj} = \bar{\mathbf{H}}_{kj} \times \|\mathbf{H}_{kj}\|_F$.
- **Step 2:** Each receiver quantizes the desired and the interference CDI. In order to quantize each CDI, codebooks are generated by using RVQ which contains $2^{B_{kj}}$ codewords. The codeword $\mathbf{c}_{kj}^{i*}$ is selected as the quantized CDI.
- **Step 3:** The indices of the selected codewords are fed back to the associated transmitters through feedback links.
- **Step 4:** Each pico BS receives the codebook indices and sends them to the macro BS through the backhaul links.
- **Step 5:** The macro BS reconstructs CSIs by using the codebooks known at both sides. After, the precoding and postcoding vectors are computed by implementing the proposed algorithm.
- **Step 6:** The macro BS distributes the precoding and the postcoding vectors to the pico BSs.
- **Step 7:** Each transmitter forwards the postcoders to the corresponding receivers using the forward link.

The Chordal distance metric is used in Step 2 to select the codeword $\mathbf{c}_{kj}^{i*}$. Since the codewords and normalized channel are lying in the non-Euclidean space of Grassmann manifolds, Chordal distance metric yields better performance than the Euclidean distance as shown in Figure 5.2. The comparison results are obtained using SNSSS algorithm with different number of $B_\delta = B_{kj}$, $\forall k, j$, bits for Scenario 2.1 given in Chapter 4.

5.3 Restricted Advanced Successive Null Space Stream Selection Algorithm

In this section, the restricted advanced successive null space stream selection (RASNSSS) algorithm is presented for the limited feedback scheme. As the number of the streams increases, the quantization error also increases for a given number of feedback bit. In other words, when the number of feedback bits is fixed, selecting less streams for each user can decrease the intra-stream interference in the limited feedback scheme. In the RASNSSS algorithm, after the stream sequences in the set Π_A are selected, there is no additional stream selection when compared to the ASNSSS algorithm. Therefore, RASNSSS algorithm given in Alg. 16 is the restricted version of the ASNSSS algorithm presented in Alg. 15 in Section 4.4.2. The RASNSSS algorithm applies Alg. 10 using $\tilde{\mathbf{H}}_{kj}$ $\forall k, j$ instead of $\mathbf{H}_{kj}$ $\forall k, j$.

The construction of stream sequence set, Π_A, is the same as the one given in Section 4.4.2.

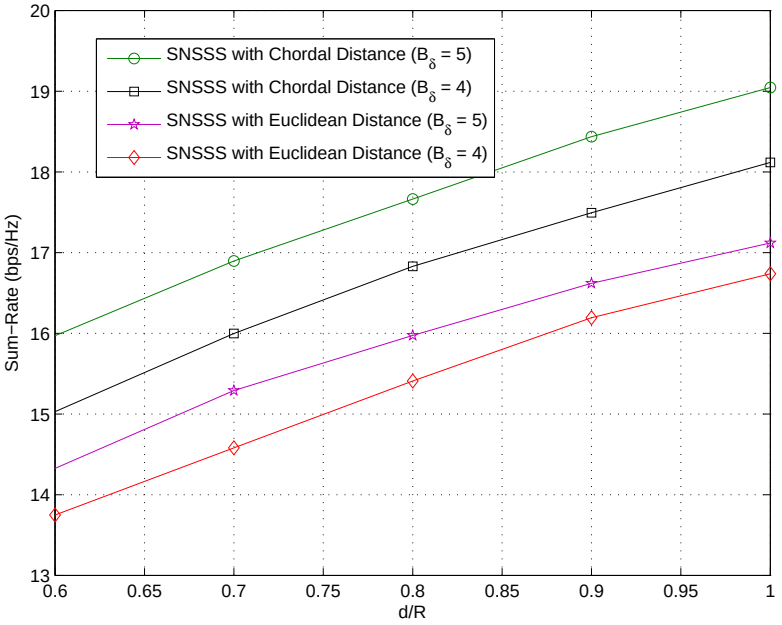

Figure 5.2: The comparison of two metrics for SNSSS with different B_δ values for Scenario 2.1.

Alg. 16 Restricted Advanced Successive Null Space Stream Selection

Input: α_{kj}, $\tilde{\mathbf{H}}_{kj}$ $\forall k, j$

Initialize the set Π_A

for each stream sequence $\pi \in \Pi_A$ **do**

Apply **Alg. 10**

end for

Select the best stream sequence according to Eq. (5.10)

$\pi_A^* = \underset{\pi \in \Pi_A}{\text{argmax}}\ \tilde{\text{SR}}_\pi$

$\tilde{\mathbf{T}}_k^* = (\tilde{\mathbf{T}}_k)_{\pi_A^*}$, $\tilde{\mathbf{D}}_k^* = (\tilde{\mathbf{D}}_k)_{\pi_A^*}$ for $k = 1, ..., K$

Output: $\tilde{\mathbf{T}}_k^*$, $\tilde{\mathbf{D}}_k^*$ $\forall k$

The Complexity of the RASNSSS Algorithm:

The number of calls to Alg. 9 at each stream selection step of the proposed algorithm can be formulated as follows:

$$\underbrace{\Big(\sum_{k'\in\Gamma} d_{k'}! \times \sum_{\substack{h'\in\Gamma \\ h'\neq k'}} (|\Gamma|-2)! \times \prod_{\substack{i\in\Gamma \\ i\neq k', i\neq h'}} d_i}_{\text{Total number of stream sequences}} \times \underbrace{(d_{k'} + (|\Gamma|-2)+2)}_{\substack{\text{Maximum number of} \\ \text{times Alg. 9 is called}}}\Big) \tag{5.11}$$

5.4 K-Stream Selection Algorithm

In this section, the K-stream selection (KSS) algorithm is described where a stream sequence is selected from a predetermined set of sequences of limited size. Each stream sequence is constructed with different combinations of the best streams of each user. So that all the stream sequences include one single stream per user to prevent the intra-stream interference. Each sequence is initialized with the streams of the pico users since the pico users are more likely to have higher SNR values on average.

To analyze the behavior of the stream selection process, the selection probabilities of the stream sequences in the exhaustive search with their average sum rate are given in Figure B.1 in Appendix B. It can be observed that the probability of selecting the first stream from the pico user is greater than selecting it from the macro user. In addition, the selection of pico streams as the initial streams is justified in Appendix A.

The construction of the stream sequences based on the regular structure is described as follows.

Each stream i can be expressed as $\pi_i = (k_i, l_i)$ where $k_i \in \{1,\ldots,K\}$, $l_i \in \{1,\ldots,q_{k_i}\}$ and $i \in \{1,\ldots,r\}$. The set of all permutations of length $j \in \{1,\ldots,r\}$ can be defined as follows.

$$\Phi_j = \Big\{\pi = (\pi_1\pi_2\ldots\pi_j) \,|\, \forall i,i' \in \{1,\ldots,j\},\ \pi_i \neq \pi_{i'} \text{ if } i \neq i'\Big\} \tag{5.12}$$

All stream sequences that include at least one stream from each BS-user pair are kept in set Π which can be defined as follows.

$$\begin{aligned}\Pi = \Big\{&\pi = (\pi_1\pi_2\ldots\pi_j) \,|\, \pi \in \Phi_j;\ j \geq K; \\ &\forall k, \exists m \in \{1,\ldots,j\} \text{ such that } k_m = k\Big\}\end{aligned} \tag{5.13}$$

The generated stream sequences are kept in the set Π_p and it is defined as follows.

$$\Pi_p = \Big\{\pi = (\pi_1\pi_2\ldots\pi_j) \,|\pi \in \Pi;\ j = K; l_1 = \ldots = l_j = 1;\ k_1 \in \Gamma\Big\} \tag{5.14}$$

Alg. 17 performs the KSS algorithm which applies Alg. 10 using $\tilde{\mathbf{H}}_{kj}\ \forall k,j$.

Alg. 17 KSS Algorithm

Input: α_{kj}, $\tilde{\mathbf{H}}_{kj}$ $\forall k, j$

Initialize the set Π_p as given in Eq.(5.14)

for each stream sequence $\pi \in \Pi_p$ **do**

Apply **Alg. 10**

end for

Select the precoding and postcoding matrices for the permutation that maximizes the sum-rate

$\pi_p^* = \underset{\pi \in \Pi_p}{\text{argmax}}\ \tilde{\text{SR}}_\pi$

$\tilde{\mathbf{T}}_k^* = (\tilde{\mathbf{T}}_k)_{\pi_p^*}$, $\tilde{\mathbf{D}}_k^* = (\tilde{\mathbf{D}}_k)_{\pi_p^*}$ for $k = 1, ..., K$

Output: $\tilde{\mathbf{T}}_k^*$, $\tilde{\mathbf{D}}_k^*$ $\forall k$

The Complexity of the KSS Algorithm:

The number of calls to Alg. 9 at each stream selection step of the proposed algorithm can be formulated as follows:

$$\Big(\underbrace{|\Pi_p|}_{\substack{\text{Total number of} \\ \text{stream sequences}}} \times \underbrace{K}_{\substack{\text{The number of} \\ \text{times Alg. 9 is called}}} \Big) \tag{5.15}$$

5.5 Adaptive Bit Allocation Scheme for Quantized CSI

In this section, an adaptive feedback bit allocation is presented. The main objective is to maximize the average sum rate by optimizing the number of bits to quantize the macro and pico CDIs for each user. Since optimizing the total number of bits for the whole system is too complex, an upper bound on the each user's data rate is obtained as defined in Eq. (5.2). In this way, the given total number of feedback bits for each user is adaptively and locally allocated to the channels.

The optimization problem of the bit allocation for the stream selection based IA algorithms can be formulated for the k^{th} user as follows.

$$\begin{aligned} &\max_{B_{kj}; j=1,...,K} \sum_{i=1}^{q_k} \mathbb{E}\left[\tilde{\text{R}}_{ki}\right] \\ &\text{s.t.} \sum_{j=1}^{K} B_{kj} \leq B_k \end{aligned} \tag{5.16}$$

where B_k is the total number of feedback bits for user k.

An approximate upper bound is derived for the solution of the bit allocation problem in Eq. (5.16). The upper bound for the total data rate of each user is the sum of the upper bounds of the rate of each stream. Therefore, an upper bound is obtained for each stream (Anand et al. [2013]). The problem is considered for the high SINR region where $\log_2(1+x) \approx \log_2(x)$ since the interference is mitigated by performing the stream selection based IA algorithms. Furthermore, the interfering and the desired channel terms are modeled as independently distributed random variables. Therefore, $\mathbb{E}\left[\tilde{\mathrm{R}}_{ki}\right]$ can be rewritten by using Eq. (5.6) as follows.

$$\mathbb{E}\left[\underbrace{\log_2\left((P_{kk}/q_k)\left(\tilde{\mathbf{d}}_k^i\right)^H \mathbf{H}_{kk}\tilde{\mathbf{t}}_k^i\tilde{\mathbf{t}}_k^{iH}\mathbf{H}_{kk}^H\tilde{\mathbf{d}}_k^i\right)}_{a}\right] - \underbrace{\mathbb{E}\left[\log_2\left(\underbrace{\sum_{\substack{l=1,\\ l\neq i}}^{q_k}(P_{kk}/q_k)\left(\tilde{\mathbf{d}}_k^l\right)^H \mathbf{H}_{kk}\tilde{\mathbf{t}}_k^l\tilde{\mathbf{t}}_k^{lH}\mathbf{H}_{kk}^H\tilde{\mathbf{d}}_k^l}_{b1} + \underbrace{\sum_{\substack{j=1\\ j\neq k}}^{K}\sum_{q=1}^{q_j}(P_{kj}/q_j)\left(\tilde{\mathbf{d}}_j^q\right)^H \mathbf{H}_{kj}\tilde{\mathbf{t}}_j^q\tilde{\mathbf{t}}_j^{qH}\mathbf{H}_{kj}^H\tilde{\mathbf{d}}_j^q}_{b2} + \sigma^2\mathbf{I}_{N_{R_k}}\right)\right]}_{b}} \tag{5.17}$$

where P_{kj} is the average received power at user k from BS j and it is calculated as $P_{kj} = P_j\alpha_{kj}^2$.

The channel matrix $\mathbf{H}_{kk}$ can be expressed as a function of the quantized channel matrix $\tilde{\mathbf{H}}_{kk}$ as given in Eq. (2.27). Accordingly, the first term of Eq. (5.17) can be rewritten as follows (Anand et al. [2013]).

$$a = \log_2\Big((P_{kk}/q_k)\left\|\mathbf{H}_{kk}\right\|_F^2\left|\left(\tilde{\mathbf{d}}_k^i\right)^H\left(\sqrt{1-e_{kk}}\tilde{\tilde{\mathbf{H}}}_{kk} + \sqrt{e_{kk}}\mathbf{Z}_{kk}\right)\tilde{\mathbf{t}}_k^i\right|^2\Big) \tag{5.18}$$

Assuming large number of feedback bits, the error magnitude, e_{kk}, is small, so that it can be neglected (Anand et al. [2013]). Consequently, Eq. (5.18) can be rewritten as follows.

$$a = \log_2\Big((P_{kk}/q_k)\left\|\mathbf{H}_{kk}\right\|_F^2\left((1-e_{kk})\left|\left(\tilde{\mathbf{d}}_k^i\right)^H\tilde{\tilde{\mathbf{H}}}_{kk}\tilde{\mathbf{t}}_k^i\right|^2\right)\Big) \tag{5.19}$$

Since $|x+y|^2 \leq (|x|+|y|)^2$, the third term of Eq. (5.17), $b2$, can be written as follows.

$$\begin{aligned} b2 \;\leq\; \sum_{\substack{j=1,\\ j\neq k}}^{K}\sum_{q=1}^{q_j}(P_{kj}/q_j)\left\|\mathbf{H}_{kj}\right\|_F^2\Bigg(&\underbrace{(1-e_{kj})\left|\left(\tilde{\mathbf{d}}_k^i\right)^H\tilde{\tilde{\mathbf{H}}}_{kj}\tilde{\mathbf{t}}_j^q\right|^2}_{v} + \\ &\left(e_{kj}\left|\left(\tilde{\mathbf{d}}_k^i\right)^H\mathbf{Z}_{kj}\tilde{\mathbf{t}}_j^q\right|^2\right) + \\ &\underbrace{2\sqrt{1-e_{kj}}\sqrt{e_{kj}}\left|\left(\tilde{\mathbf{d}}_k^i\right)^H\tilde{\tilde{\mathbf{H}}}_{kj}\tilde{\mathbf{t}}_j^q\right|\left|\left(\tilde{\mathbf{d}}_k^i\right)^H\mathbf{Z}_{kj}\tilde{\mathbf{t}}_j^q\right|}_{z}\Bigg) \end{aligned} \tag{5.20}$$

The term $\left|\left(\tilde{\mathbf{d}}_k\right)^H \tilde{\tilde{\mathbf{H}}}_{kj}\tilde{\mathbf{t}}_j\right|$ can be considered approximately zero due to the IA scheme. Therefore, the terms v and z vanish and Eq. (5.20) can be rewritten as follows.

$$b2 \leq \sum_{\substack{j=1\\ j\neq k}}^{K}\sum_{q=1}^{q_j}(P_{kj}/q_j)\left\|\mathbf{H}_{kj}\right\|_F^2\left(e_{kj}\left|\left(\tilde{\mathbf{d}}_k^i\right)^H\mathbf{Z}_{kj}\tilde{\mathbf{t}}_j^q\right|^2\right) \tag{5.21}$$

Similarly, $b1$ can be obtained as follows.

$$b1 \leq \sum_{\substack{l=1,\\ l\neq i}}^{q_k}(P_{kk}/q_k)\left\|\mathbf{H}_{kk}\right\|_F^2\left(e_{kk}\left|\left(\tilde{\mathbf{d}}_k^i\right)^H\mathbf{Z}_{kk}\tilde{\mathbf{t}}_k^l\right|^2\right) \tag{5.22}$$

Using Jensen's inequality, the upper bound for Eq. (5.17) can be obtained as follows.

$$\begin{aligned}
&\mathbb{E}[a]-\mathbb{E}[b]\leq\\
&\log_2\Big(\underbrace{\mathbb{E}\Big[(P_{kk}/q_k)\left\|\mathbf{H}_{kk}\right\|_F^2\left((1-e_{kk})\left|\left(\tilde{\mathbf{d}}_k^i\right)^H\tilde{\tilde{\mathbf{H}}}_{kk}\tilde{\mathbf{t}}_k^i\right|^2\right)\Big]}_{T1}\Big)-\\
&\log_2\Big(\underbrace{\sum_{\substack{l=1,\\ l\neq i}}^{q_k}\mathbb{E}\Big[(P_{kk}/q_k)\left\|\mathbf{H}_{kk}\right\|_F^2\left(e_{kk}\left|\left(\tilde{\mathbf{d}}_k^i\right)^H\mathbf{Z}_{kk}\tilde{\mathbf{t}}_k^l\right|^2\right)\Big]}_{T2}+\\
&\underbrace{\sum_{\substack{j=1\\ j\neq k}}^{K}\sum_{q=1}^{q_j}\mathbb{E}\Big[(P_{kj}/q_j)\left\|\mathbf{H}_{kj}\right\|_F^2\left(e_{kj}\left|\left(\tilde{\mathbf{d}}_k^i\right)^H\mathbf{Z}_{kj}\tilde{\mathbf{t}}_j^q\right|^2\right)\Big]}_{T3}\Big)
\end{aligned} \tag{5.23}$$

Since $\mathbb{E}\Big[\left\|\mathbf{H}_{kk}\right\|_F^2\Big]=N_{T_k}N_{R_k}$, the first term of Eq. (5.23), $T1$ can be expressed using the Eq. (2.28) as follows (Zhang and Andrews [2010]), (Özbek and Le Ruyet [2014a]).

$$\begin{aligned}
T1 &\approx (P_{kk}/q_k)\,2^{B_{kk}}\beta(2^{B_{kk}},\frac{N_{T_k}N_{R_k}}{N_{T_k}N_{R_k}-1})\\
&\leq (P_{kk}/q_k)\left(1-2^{-\frac{B_{kk}}{N_{T_k}N_{R_k}-1}}\right)
\end{aligned} \tag{5.24}$$

The second and the third term of Eq. (5.23), $T2$ and $T3$, can be expressed as follows (Ravindran and Jindal [2008]), (Jindal [2006]).

$$\begin{aligned}
T2+T3 &\approx \frac{P_{kk}(q_k-1)}{q_k}2^{B_{kk}}\beta(2^{B_{kk}},\frac{N_{T_k}N_{R_k}}{N_{T_k}N_{R_k}-1})+\sum_{\substack{j=1\\ j\neq k}}^{K}P_{kj}2^{B_{kj}}\beta(2^{B_{kj}},\frac{N_{T_j}N_{R_k}}{N_{T_j}N_{R_k}-1})\\
&\leq \frac{P_{kk}(q_k-1)}{q_k}2^{-\frac{B_{kk}}{N_{T_k}N_{R_k}-1}}+\sum_{\substack{j=1\\ j\neq k}}^{K}P_{kj}2^{-\frac{B_{kj}}{N_{T_j}N_{R_k}-1}}
\end{aligned} \tag{5.25}$$

.

Using Eq. (5.24) and Eq. (5.25) in Eq. (5.17), the optimization problem can be expressed for any stream of the k^{th} user as follows.

$$\begin{aligned}
&\max_{B_{kj};j=1,\ldots,K} \Bigg[\log_2 \left((P_{kk}/q_k) \left(1 - 2^{-\frac{B_{kk}}{N_{T_k} N_{R_k} - 1}} \right) \right) - \\
&\log_2 \left(\frac{P_{kk}(q_k - 1)}{q_k} 2^{-\frac{B_{kk}}{N_{T_k} N_{R_k} - 1}} + \sum_{\substack{j=1 \\ j \neq k}}^{K} P_{kj} 2^{-\frac{B_{kj}}{N_{T_j} N_{R_k} - 1}} \right) \Bigg] \\
&\text{s.t.} \sum_{j=1}^{K} B_{kj} \leq B_k
\end{aligned} \tag{5.26}$$

The solutions for the problem expressed in Eq. (5.26) are obtained by using a Matlab based software for convex optimization (Grant and Boyd [2014]). After obtaining the B_{kj} values which are real numbers, a round operation is applied to get integer values.

In order to perform the IA algorithms, each transmitter should know the complete quantized CSI of the network or obtain the precoding and the postcoding vectors (Anand et al. [2013]). Since it is achieved by the given feedback topology in Section 5.2.2, the optimization problem defined in Eq. (5.26) is also suitable for any IA algorithms such as Max-SINR or min-Leak.

On the other hand, depending on the stream selection approach, the solution to the optimization problem defined in Eq. (5.26) can be varied. The solutions of the adaptive bit allocation for the RASNSSS, KSS and ISNSSS algorithms are given in the following.

5.5.1 Adaptive Bit Allocation for RASNSSS Algorithm

RASNSSS algorithm proposed for the limited feedback scheme just selects the streams from the constructed stream sequences kept in set Π_A and do not continue to select streams as in the ASNSSS algorithm given as Alg. 15. In the constructed stream sequence, there is only one selected stream for the macro user; however, multiple streams can be selected for a pico user.

Since the number of selected streams is not known in advance for a pico user, the optimization problem is defined for the case where all the streams of all the pico users are selected.

Accordingly, the optimization problem for a pico user k where $k \in \Gamma$ can be expressed

as follows.

$$\max_{B_{kj};j=1,\ldots,K} \left[\log_2 \left((P_{kk}/q_k) \left(1 - 2^{-\frac{B_{kk}}{N_{T_k} N_{R_k} - 1}} \right) \right) - \log_2 \left(\frac{P_{kk}(q_k - 1)}{q_k} 2^{-\frac{B_{kk}}{N_{T_k} N_{R_k} - 1}} + \sum_{\substack{j=2 \\ j \neq k}}^{K} P_{kj} 2^{-\frac{B_{kj}}{N_{T_j} N_{R_k} - 1}} + P_{k1} 2^{-\frac{B_{k1}}{N_{T_1} N_{R_k} - 1}} \right) \right] \quad \text{s.t.} \sum_{j=1}^{K} B_{kj} \leq B_k \tag{5.27}$$

On the other hand, the optimization problem for a macro user where $k = 1$ can be expressed as follows.

$$\max_{B_{1j};j=1,\ldots,K} \left[\log_2 \left(P_{11} \left(1 - 2^{-\frac{B_{11}}{N_{T_1} N_{R_1} - 1}} \right) \right) - \sum_{j=2}^{K} P_{1j} 2^{-\frac{B_{1j}}{N_{T_j} N_{R_1} - 1}} \right] \quad \text{s.t.} \sum_{j=1}^{K} B_{1j} \leq B_1 \tag{5.28}$$

5.5.2 Adaptive Bit Allocation for the KSS Algorithm

The KSS algorithm constructs stream sequences by different stream combinations of the best streams of each user and each sequence is initialized by the streams of the pico users.

Since the intra-stream interference has a severe impact on the performance of the IA in the limited feedback schemes, each constructed stream sequence includes only one stream for each user. In this way, for a given number of feedback bits, transmission with single stream per each user reduces the quantization error compared to the transmission with multiple streams.

Avoiding the intra-stream interference for the limited feedback scheme, the optimization problem for the KSS algorithm can be expressed as follows.

$$\max_{B_{kj};j=1,\ldots,K} \left[\log_2 \left(P_{kk} \left(1 - 2^{-\frac{B_{kk}}{N_{T_k} N_{R_k} - 1}} \right) \right) - \log_2 \Big(\sum_{\substack{j=1, \\ j \neq k}}^{K} P_{kj} 2^{-\frac{B_{kj}}{N_{T_j} N_{R_k} - 1}} \Big) \right]; \quad \forall k \quad \text{s.t.} \sum_{j=1}^{K} B_{kj} \leq B_k \tag{5.29}$$

5.5.3 Adaptive Bit Allocation for the ISNSSS Algorithm

The ISNSSS algorithm given in Alg. 14 in the previous chapter is described assuming perfect CSI at the transmitters. In this chapter, the ISNSSS algorithm is evaluated for

the partially connected interference networks with the imperfect CSI. Therefore, Alg. 14 is performed using $\tilde{\mathbf{H}}_{kj}\ \forall k, j$ instead of $\mathbf{H}_{kj}\ \forall k, j$ and, thus, the precoding and the postcoding matrices are calculated using the quantized CSI.

Since the number of the selected streams is not known in advance for each user, the optimization problem is defined for the case where all the streams of all the users are selected. Therefore, the problem expressed in Eq. (5.26) is considered.

A similar case applies to the existing stream selection based IA algorithms, such as, ESNSSS and SNSSS (Amara et al. [2012b]).

5.6 Performance Results

The performances of the stream selection based IA algorithms with the quantized CSI are evaluated in Scenario 1.2 which is illustrated in Figure 4.5, Scenario 2.1 and Scenario 2.2 which are illustrated in Figure 4.9. For these scenarios, we consider that there are 2 transmit antennas for each pico cell and 4 transmit antennas for the macro cell. Each cell has one user that is randomly placed inside its coverage area. Each user has 2 receive antennas.

The locations of the pico BSs are varied with respect to macro BS. More precisely, pico BSs are initially placed relatively close to the macro BS and they are shifted together with the pico users from the inner area to cell edge area of the macro BS located at $(0, 0)$.

Locations of the pico cells are identified using the ratio d/R where R is the macro cell radius and d is the distance between the macro BS and each pico BS. Since, in practice, pico cells are generally deployed closer to the cell edge areas of the macro cells, the ratio ranges from 0.6 to 1.

Simulations are carried out using the system parameters listed in Table 4.1.

As in the previous chapter, both the fully and the partially interference networks are considered for the performance evaluations. For partially connected networks, the ISNSSS and the KSS algorithms are evaluated for the Scenario 1.2 and the RASNSSS and the KSS algorithms are evaluated for the Scenario 2.1 and the Scenario 2.2. For all the scenarios, different bit allocation schemes (BAS) are performed for the different total number of feedback bits $B_T = \sum_{k=1}^{K} B_k$, such as $B_T = 45$, $B_T = 63$, $B_T = 90$ and $B_T = 120$. The values of B_1, B_2 and B_3 for $B_T = 45$ is given as follows.

- BAS-1: $B_1 = 7$, $B_2 = B_3 = 19$
- BAS-2: $B_1 = B_2 = B_3 = 15$

The values of B_1, B_2 and B_3 for $B_T = 63$ is given as follows.

- BAS-3: $B_1 = 9$, $B_2 = B_3 = 27$
- BAS-4: $B_1 = B_2 = B_3 = 21$

The values of B_1, B_2 and B_3 for $B_T = 90$ is given as follows.

- BAS-5: $B_1 = 10$, $B_2 = B_3 = 40$
- BAS-6: $B_1 = B_2 = B_3 = 30$

The values of B_1, B_2 and B_3 for $B_T = 120$ is given as follows.

- BAS-7: $B_1 = 10$, $B_2 = B_3 = 55$
- BAS-8: $B_1 = B_2 = B_3 = 40$

In the considered scenarios, there are 9 channels including the desired channels and the interfering channels. Therefore, the number of allocated bits to each channel is 5 with $B_T = 45$, 7 with $B_T = 63$ and 10 with $B_T = 90$ in the equal bit allocation scheme (EBA).

For the KSS algorithm, the considered stream sequences are illustrated in Figure 5.3. The selected stream sequences are initialized by the pico streams, such as the best stream of Pico 1 user is $P1\_1$ and the best stream of Pico 2 user is $P2\_1$. $M1\_1$ is the best macro stream.

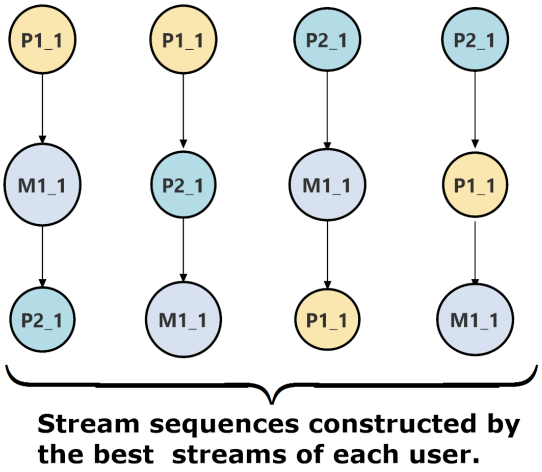

Figure 5.3: Stream sequences constructed by the KSS algorithm.

5.6.1 Scenario for Partially Connected Interference Networks

Scenario 1.2: d/R is changing for 2 Pico Cells

For partially connected interference networks, we evaluate the KSS and the ISNSSS algorithms for Scenario 1.2 as illustrated in Figure 4.5. Pico cells are deployed far away from each other, so that the pico cell users only receive interference from the macro BS.

The results are presented in two stages: First, the results for reasonable number of bits for the practical implementations of the limited feedback, $B_T = 45$ and $B_T = 63$, are presented. Later, the results for the number of limited feedback bits for theoretical analysis, $B_T = 90$ and $B_T = 120$, are given.

The performance comparisons of the KSS and the ISNSSS algorithms for $B_T = 45$ and $B_T = 63$ are given for different bit allocation schemes in Figure 5.4. The proposed adaptive feedback bit allocation scheme outperforms the EBA scheme using both the KSS and the ISNSSS algorithms. In addition, it can be observed that the performances of the ISNSSS and the KSS algorithms increase when more bits are allocated to the pico users.

The allocated bit numbers to each channel can be seen in detail in Table 5.1 for BAS-3 scheme with $B_T = 63$. For the KSS algorithm, the most of the bits are allocated to the interference channels between the macro BS and the pico users. Since, the interference generated from macro BS to pico users is very strong, more bits are required to have better information on the interference channels in the limited feedback case. For the ISNSSS algorithm, desired channels of pico have more bits than the other channels to decrease the intra-stream interference between the pico streams, since multiple streams are selected for the pico users.

Table 5.1: Scenario 1.2: Average Number of Allocated Bits for $B_T = 63$ at $d/R = 0.8$ for the KSS and the ISNSSS algorithms.

	$B_1 = 9$	$B_2 = 27$	$B_3 = 27$
KSS	$\boldsymbol{B_{11} = 4.7}$	$\boldsymbol{B_{21} = 21.8}$	$\boldsymbol{B_{31} = 21.8}$
	$B_{12} = 2.0$	$B_{22} = 5.2$	$B_{32} = 0$
	$B_{13} = 2.3$	$B_{23} = 0$	$B_{33} = 5.2$
ISNSSS	$\boldsymbol{B_{11} = 8.6}$	$B_{21} = 9.3$	$B_{31} = 9.3$
	$B_{12} = 0.2$	$\boldsymbol{B_{22} = 17.7}$	$B_{32} = 0$
	$B_{13} = 0.2$	$B_{23} = 0$	$\boldsymbol{B_{33} = 17.7}$

The comparisons between the KSS, the ISNSSS and the existing algorithms are shown in Figure 5.5 for BAS-3 scheme with $B_T = 63$. The KSS algorithm outperforms the ISNSSS and the SNSSS (Amara et al. [2012b]) algorithms since only one stream is selected for each user, so that the intra-stream interference is avoided. On the other hand, the KSS algorithm also outperforms the existing iterative max-SINR and min-Leak algorithms (Gomadam et al. [2011]), even they are performed with a single stream. It has been shown that the max-SINR and min-Leak algorithms are very sensitive to the imperfect CSI as demonstrated in the studies of Xie et al. [2013] and Razavi and Ratnarajah [2014].

The performance degradations between the evaluated and the achievable sum-rate shown in Figure 5.6 are approximately 3bps/Hz, 8.5bps/Hz and 7bps/Hz, in the KSS, max-SINR and min-Leak algorithms, respectively, at $d/R = 1$. Therefore, it can be observed that the KSS algorithm is more robust to channel uncertainties when compared to the iterative algorithms.

In addition, in Figure 5.7, we have compared the evaluated and the achievable sum-rate as a function of the number of iteration when the pico cells are located at $d/R = 0.8$ for the max-SINR algorithm. It can be seen that the increase in the evaluated sum-rate is approximately 4bps/Hz while the increase in the achievable sum-rate is only 2bps/Hz.

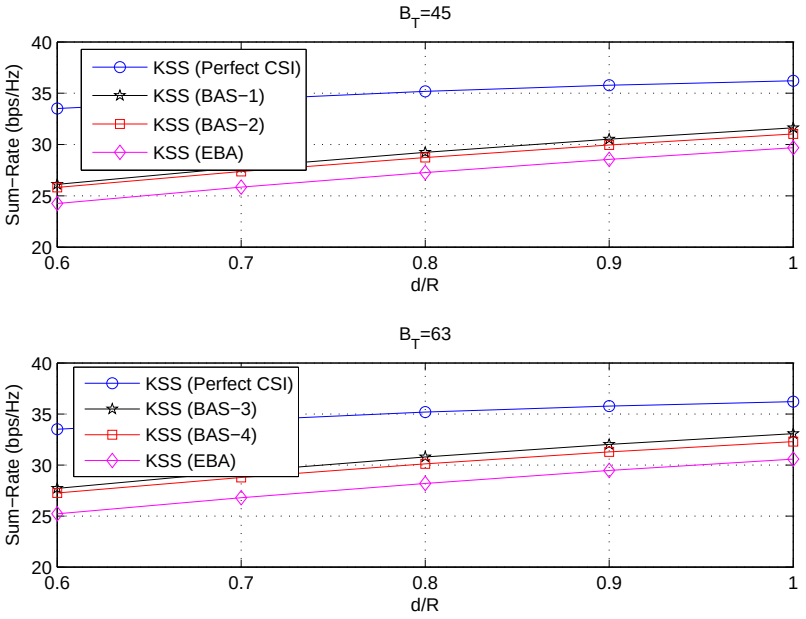

(a) Comparisons for KSS algorithm.

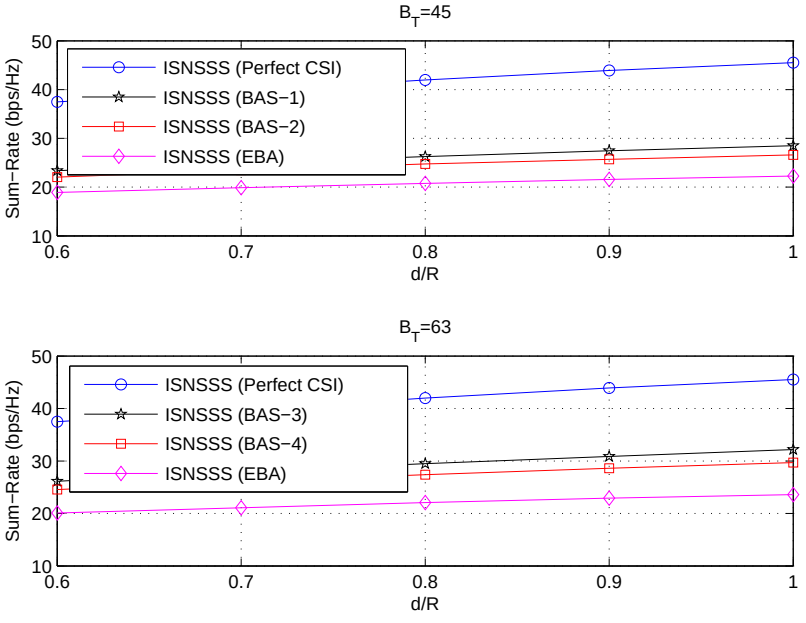

(b) Comparisons for the ISNSSS algorithm.

Figure 5.4: Scenario 1.2: Different adaptive bit allocation schemes with $B_T = 45$ and $B_T = 63$ for the KSS and the ISNSSS algorithms.

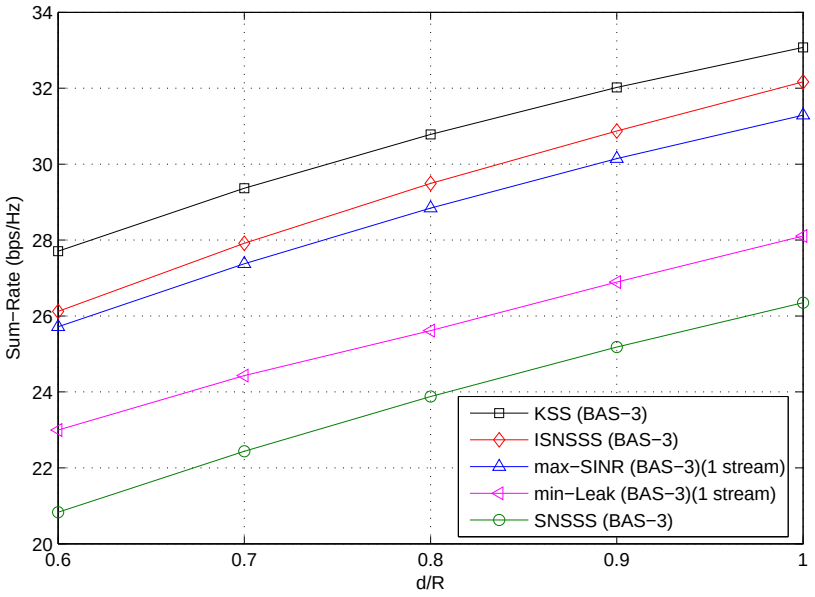

Figure 5.5: Scenario 1.2: Comparison of different algorithms for adaptive bit allocation for BAS-3 scheme with $B_T = 63$.

The performance comparisons for $B_T = 90$ and $B_T = 120$ are given in Figure 5.8. It can be observed that the increase in the performance of the ISNSSS algorithm is greater than the KSS algorithm for higher number of feedback bits.

Detailed comparisons of the algorithms for $B_T = 120$ can be seen in Figure 5.9. The ISNSSS algorithm outperforms the KSS algorithm and the other existing algorithms. Since the intra-stream interference is reduced with the decreasing quantization error, selecting multiple streams increases the performance. However, the feedback overhead increases as the number of the bits increases.

For $B_T = 120$, the detailed bit allocation to each channel is given in Table 5.2. It can be seen that the number of allocated bits for the interference channels between the macro BS and the pico users is greater when compared to the case $B_T = 63$. In addition, the pico desired channels can also have enough feedback bits to decrease the intra-stream interference between for the pico users. Accordingly, the ISNSSS algorithm achieves higher performance than the KSS algorithm.

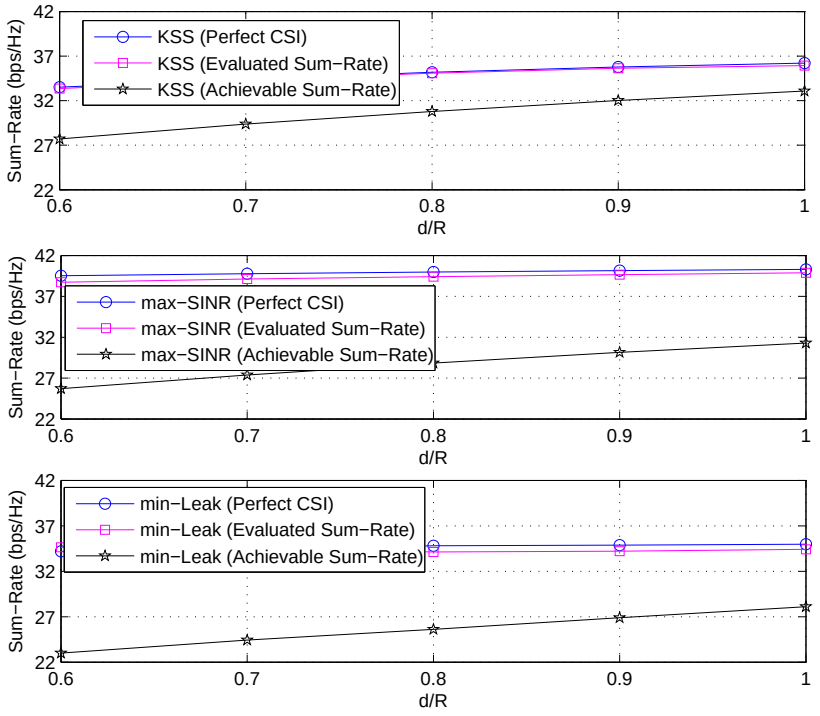

Figure 5.6: Scenario 1.2: Comparison of the achievable and the evaluated sum-rate for KSS, max-SINR and min-Leak algorithms for $B_T = 63$ and BAS-3 scheme.

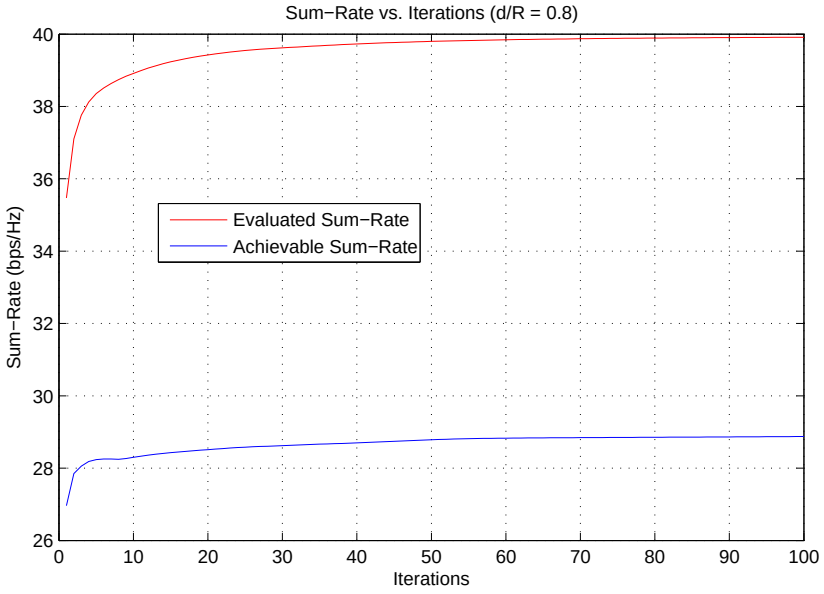

Figure 5.7: Scenario 1.2: Comparison of achievable and evaluated sum-rates vs. iterations at $d/R = 0.8$ for max-SINR algorithm

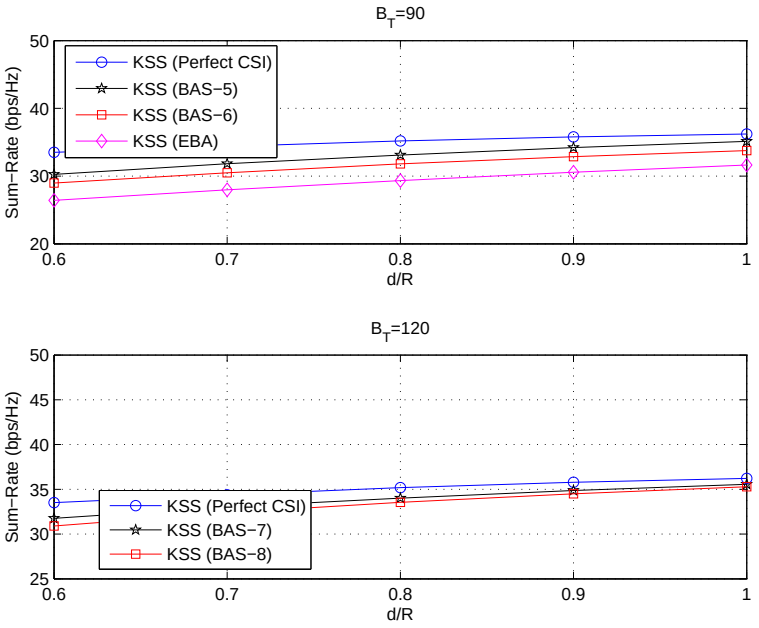

(a) Comparisons for the KSS algorithm.

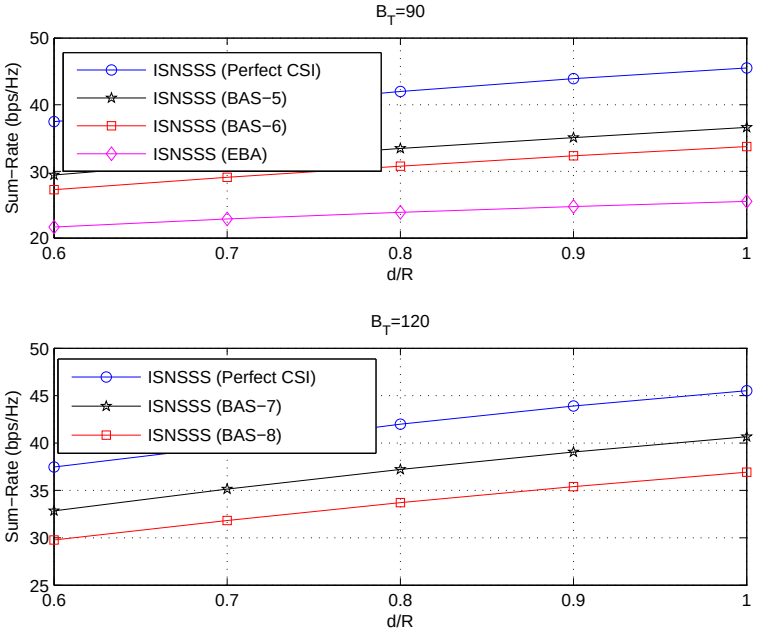

(b) Comparisons for the ISNSSS algorithm.

Figure 5.8: Scenario 1.2: Different adaptive bit allocation schemes with $B_T = 90$ and $B_T = 120$ for the KSS and the ISNSSS algorithms.

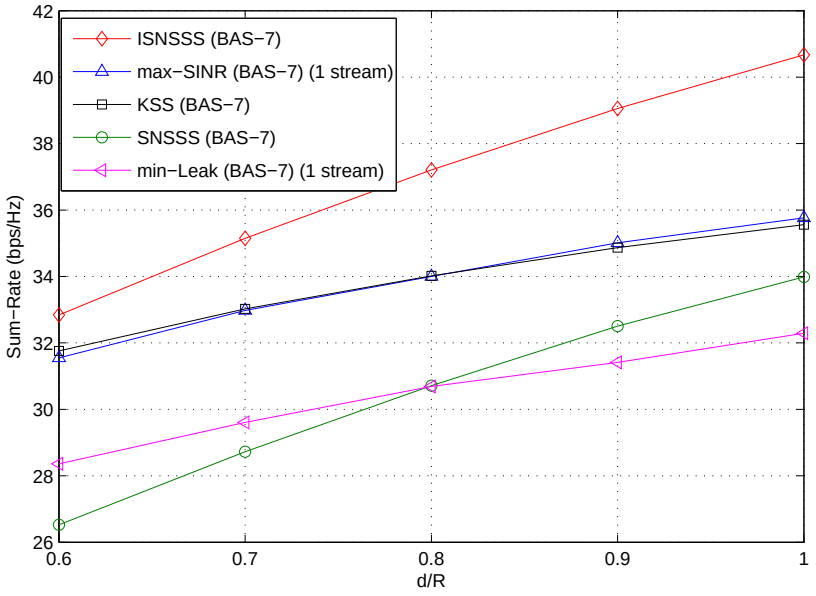

Figure 5.9: Scenario 1.2: Comparison of different algorithms for adaptive bit allocation for BAS-7 scheme with $B_T = 120$.

Table 5.2: Scenario 1.2: Average Number of Allocated Bits for $B_T = 120$ at $d/R = 0.8$ for the KSS and the ISNSSS algorithms.

	$B_1 = 10$	$B_2 = 55$	$B_3 = 55$
KSS	$\boldsymbol{B_{11} = 4.8}$	$\boldsymbol{B_{21} = 49.4}$	$\boldsymbol{B_{31} = 49.4}$
	$B_{12} = 2.5$	$B_{22} = 5.2$	$B_{32} = 0.4$
	$B_{13} = 2.7$	$B_{23} = 0.4$	$B_{33} = 5.2$
ISNSSS	$\boldsymbol{B_{11} = 9.5}$	$\boldsymbol{B_{21} = 26.5}$	$\boldsymbol{B_{31} = 26.5}$
	$B_{12} = 0.2$	$\boldsymbol{B_{22} = 28.2}$	$B_{32} = 0.3$
	$B_{13} = 0.3$	$B_{23} = 0.3$	$\boldsymbol{B_{33} = 28.2}$

5.6.2 Scenarios for Fully Connected Interference Networks

Scenario 2.1: d/R is changing while L is fixed

In Scenario 2.1, pico cells are shifted towards the cell edge of the macro cell by changing the ratio d/R. The distance between the pico cells is constant and is $L = 150$m. Once again, the results are presented in two parts: For $B_T = 45$ and $B_T = 63$, and for $B_T = 90$ and $B_T = 120$.

The performance comparisons of the KSS and the RASNSSS algorithms with $B_T = 45$ and $B_T = 63$ are given for different bit allocation schemes in Figure 5.10. The proposed adaptive feedback bit allocation outperforms the EBA scheme for both the KSS and the RASNSSS algorithms. In addition, it can be observed that the BAS-3 scheme performs better than the BAS-4 scheme. In other words, allocating more bits for the pico users improves the performance of the algorithms. The reason is that the interference generated from the macro BS to the pico users is very strong. Therefore, as the number of the feedback bits increases for the pico users, the quantization error can be decreased.

Table 5.3 shows the average numbers of bits allocated to each channel in detail for the KSS and the RASNSSS algorithms. For the KSS algorithm, since the interference generated from macro BS to pico users is very dominant, it is observed that the interference channels between the pico users and the macro BS allocates higher number of bits, B_{21} and B_{31}. On the other hand, for the RASNSSS algorithm, it is observed that the pico desired channels require higher number of bits, because a pico cell has more than one stream in the RASNSSS algorithm. In addition, the interference channels between the pico users and the macro BS have more bits than the other interference channels.

Table 5.3: Scenario 2.1: Average Number of Allocated Bits for $B_T = 63$ at $d/R = 0.8$ for the KSS and the RASNSSS Algorithms

	$B_1 = 9$	$B_2 = 27$	$B_3 = 27$
KSS	$\boldsymbol{B_{11} = 4.8}$	$\boldsymbol{B_{21} = 18.8}$	$\boldsymbol{B_{31} = 18.7}$
	$B_{12} = 2.1$	$B_{22} = 5.5$	$B_{32} = 2.8$
	$B_{13} = 2.1$	$B_{23} = 2.7$	$B_{33} = 5.5$
RASNSSS	$\boldsymbol{B_{11} = 4.8}$	$B_{21} = 9.1$	$B_{31} = 9.1$
	$B_{12} = 2.1$	$\boldsymbol{B_{22} = 16.5}$	$B_{32} = 1.1$
	$B_{13} = 2.1$	$B_{23} = 1.4$	$\boldsymbol{B_{33} = 16.8}$

Moreover, the proposed bit allocation is performed for the existing stream selection based IA algorithms, such as ESNSSS, SNSSS (Amara et al. [2012b]) and the iterative IA algorithms, such as max-SINR and min-Leak (Gomadam et al. [2011]) algorithms for the single stream case. The performance comparisons are shown in Figure 5.11 for BAS-3 scheme with $B_T = 63$. It can be observed that the KSS algorithm achieves higher performance than the max-SINR and the min-Leak algorithms. The reason is that the KSS algorithm is less sensitive to the channel uncertainties than the max-SINR and the

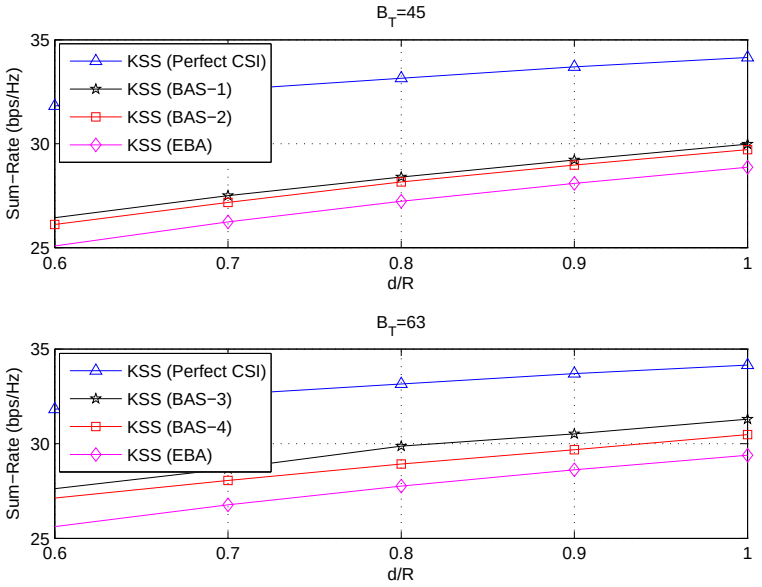

(a) Comparisons for the KSS algorithm.

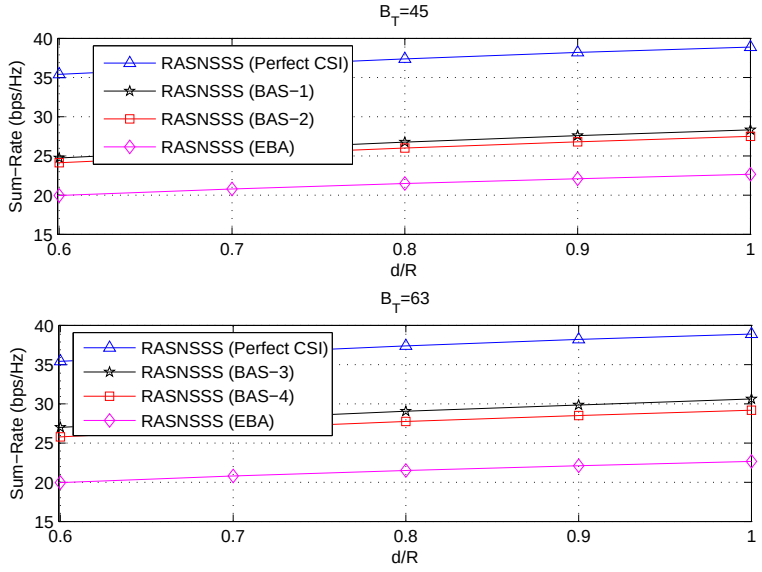

(b) Comparisons for the RASNSSS algorithm.

Figure 5.10: Scenario 2.1: Different adaptive bit allocation schemes with $B_T = 45$ and $B_T = 63$ for the KSS and the RASNSSS algorithms.

min-Leak algorithms as shown in Figure 5.12. The performance degradations between the evaluated and the achievable sum-rate for the KSS, the max-SINR and the min-Leak algorithms are observed as approximately 3bps/Hz, 8bps/Hz and 7bps/Hz, respectively, at $d/R = 1$.

In addition, in Figure 5.13, we have compared the evaluated and the achievable sum-

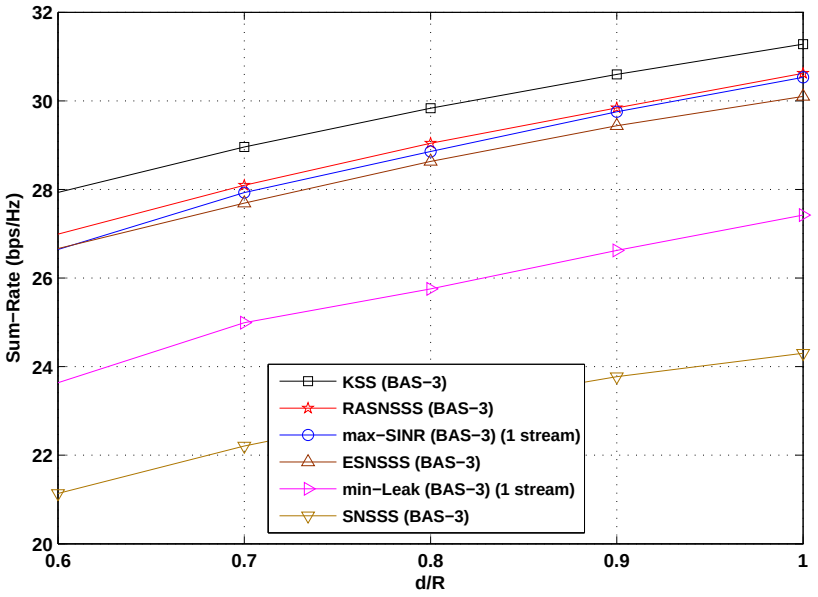

Figure 5.11: Scenario 2.1: Comparison of different algorithms for adaptive bit allocation for BAS-3 scheme with $B_T = 63$.

rate as a function of the number of iteration when the pico cells are located at $d/R = 0.8$ for the max-SINR algorithm. It can be seen that while the increase in the evaluated sum-rate is approximately 4bps/Hz, the increase in the achievable sum-rate is only 1.5bps/Hz.

When the total number of feedback bits is increased to $B_T = 90$ or $B_T = 120$ for both the KSS and the RASNSSS algorithms, similar behavior with $B_T = 45$ and $B_T = 63$ is observed as shown in Figure 5.14. As the number of allocated bits increases for the pico users, the average sum rate also increases.

In addition, the average numbers of allocated bits for $B_T = 90$ are given in Table 5.4 for the KSS and the RASNSSS algorithms considering the BAS-5 scheme. For the KSS algorithm, allocating more bits for B_{21} and B_{31} is important to handle the interference generated from the macro BS to the pico users. For the RASNSSS algorithm, it is seen that B_{22} and B_{33} have more bits for the pico desired channels to decrease the intra-stream interference.

The performance comparisons of the proposed and the existing algorithms are given in Figure 5.15 for the BAS-7 scheme with $B_T = 120$ since the BAS-7 scheme allocated more bits to pico users when compared to the BAS-6 scheme. In this case, the RASNSSS algorithm outperforms the KSS algorithm since the number of allocated bits is enough to resolve both the desired and the interference channels.

The detailed bit allocation to each channel is given in Table 5.5 for the BAS-7 scheme with $B_T = 120$. It can be seen that the number of allocated bits for the interference channels between the macro BS and the pico users increases when compared to the case $B_T = 90$.

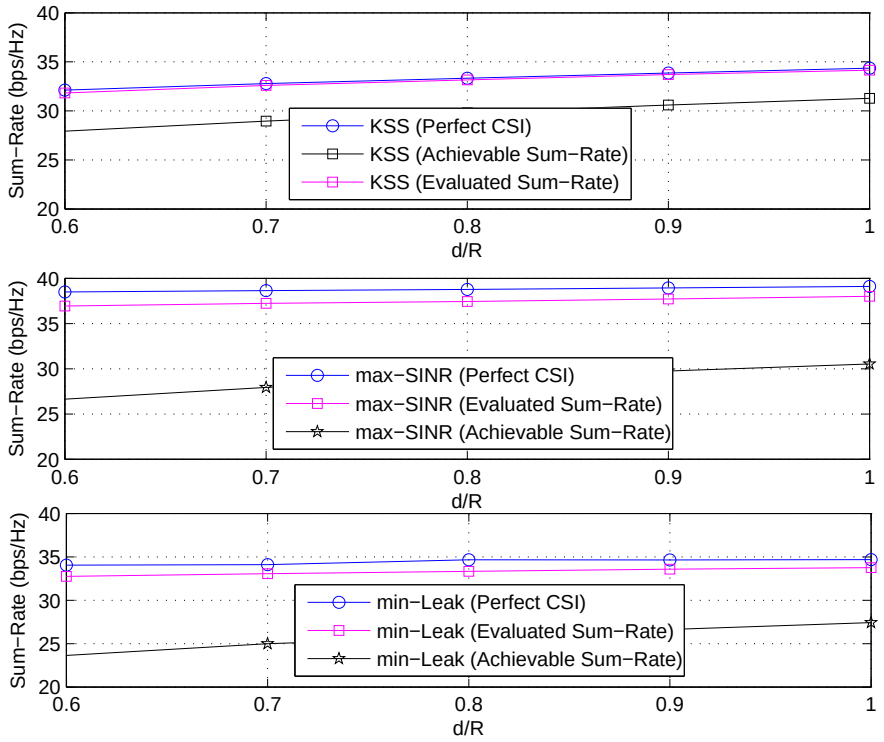

Figure 5.12: Scenario 2.1: Comparison of the achievable and the evaluated sum-rate for the KSS, max-SINR and min-Leak algorithms for $B_T = 63$ and BAS-3 scheme.

Table 5.4: Scenario 2.1: Average Number of Allocated Bits for $B_T = 90$ at $d/R = 0.8$ for the KSS and the RASNSSS Algorithms

	$B_1 = 10$	$B_2 = 40$	$B_3 = 40$
KSS	$\boldsymbol{B_{11} = 4.9}$	$\boldsymbol{B_{21} = 30.1}$	$\boldsymbol{B_{31} = 29.8}$
	$B_{12} = 2.5$	$B_{22} = 5.6$	$B_{32} = 4.4$
	$B_{13} = 2.6$	$B_{23} = 4.3$	$B_{33} = 5.8$
RASNSSS	$\boldsymbol{B_{11} = 4.9}$	$\boldsymbol{B_{21} = 16.2}$	$\boldsymbol{B_{31} = 16.2}$
	$B_{12} = 2.5$	$\boldsymbol{B_{22} = 21.4}$	$B_{32} = 2.4$
	$B_{13} = 2.6$	$B_{23} = 2.4$	$\boldsymbol{B_{33} = 21.4}$

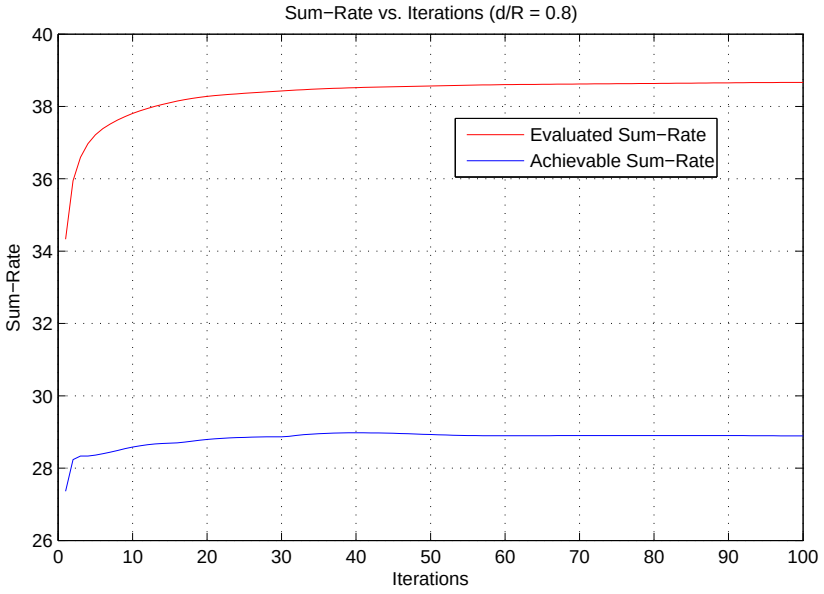

Figure 5.13: Scenario 2.1: Comparison of achievable and evaluated sum-rates vs. iterations at $d/R = 0.8$ for max-SINR algorithm

In addition, the pico desired channels can also have enough feedback bits to decrease the intra-stream interference for the pico users. Accordingly, the RASNSSS algorithm achieves higher performance than the KSS algorithm as the stream sequences constructed in the RASNSSS algorithm have higher probability of occurrence while performing the exhaustive search.

Table 5.5: Scenario 2.1: Average Number of Allocated Bits for $B_T = 120$ at $d/R = 0.8$ for the KSS and the RASNSSS Algorithms

	$B_1 = 10$	$B_2 = 55$	$B_3 = 55$
KSS	$\boldsymbol{B_{11} = 4.8}$	$\boldsymbol{B_{21} = 41.5}$	$\boldsymbol{B_{31} = 40.6}$
	$B_{12} = 2.5$	$B_{22} = 5.9$	$B_{32} = 8.5$
	$B_{13} = 2.7$	$B_{23} = 7.6$	$B_{33} = 5.9$
RASNSSS	$\boldsymbol{B_{11} = 4.8}$	$\boldsymbol{B_{21} = 23.7}$	$\boldsymbol{B_{31} = 23.6}$
	$B_{12} = 2.5$	$\boldsymbol{B_{22} = 27.3}$	$B_{32} = 4.1$
	$B_{13} = 2.7$	$B_{23} = 4.0$	$\boldsymbol{B_{33} = 27.3}$

Complexity Comparison of the Considered Algorithms:

We compare the complexities of the stream selection algorithms in terms of the number

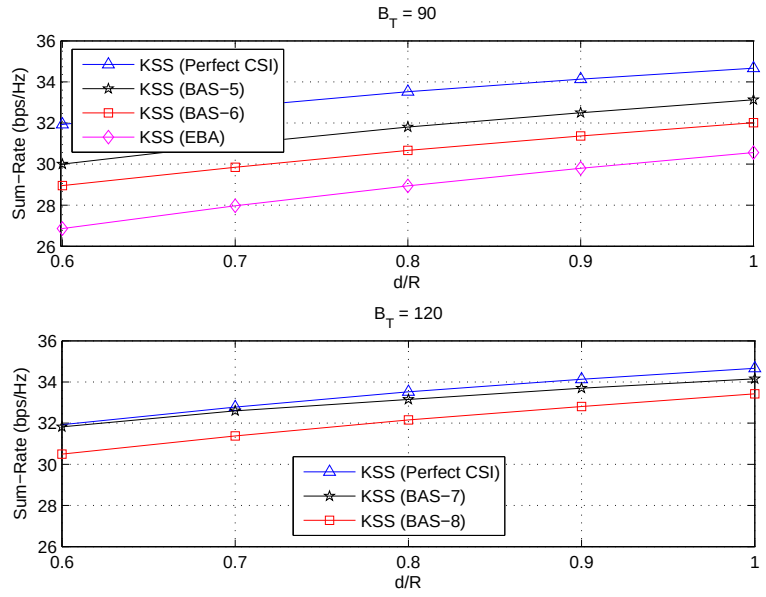

(a) Comparisons for the KSS algorithm.

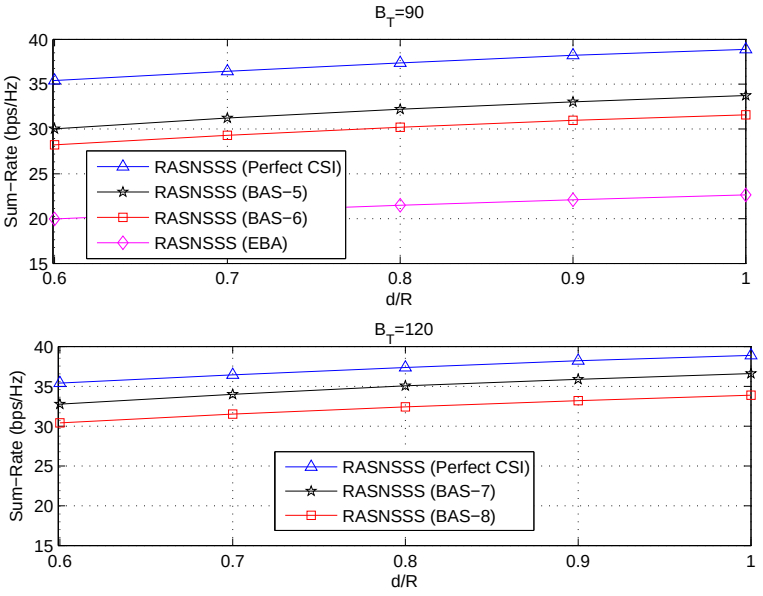

(b) Comparisons for the RASNSSS algorithm.

Figure 5.14: Scenario 2.1: Different adaptive bit allocation schemes with $B_T = 90$ and $B_T = 120$ for the KSS and the RASNSSS algorithms.

of calls to Alg. 9 and they are given in Table 5.6 for Scenario 2.1, since the total number of streams is the same in scenarios with the same network configurations. It can be observed that Alg. 9 is called by the KSS algorithm at most 12 times which is much fewer than invocations performed by the exhaustive search and also the other algorithms except for

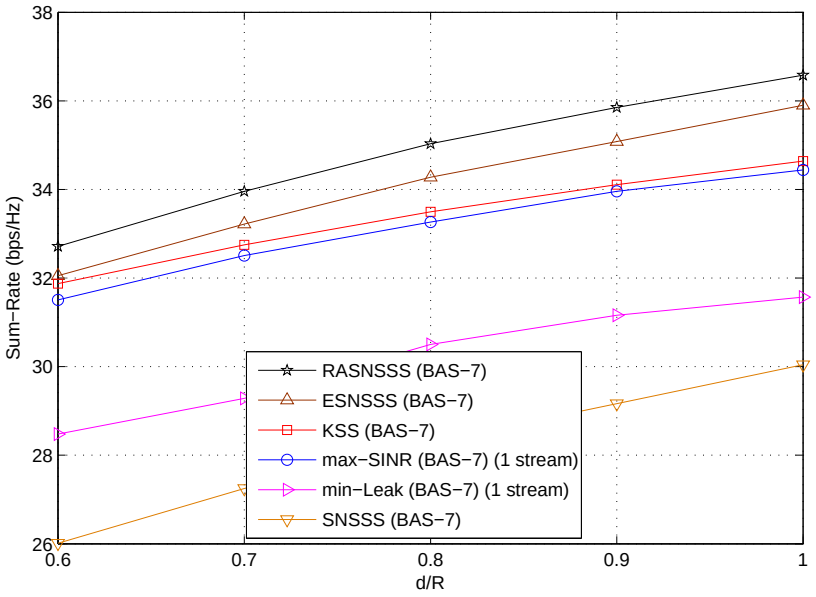

Figure 5.15: Scenario 2.1: Comparison of different algorithms for adaptive bit allocation for BAS-7 scheme with $B_T = 120$.

the SNSSS algorithm. However, the SNSSS algorithm has the poorest performance. It should be noted that these results represent upper bounds for the given algorithms, since the stream selection algorithms can select different stream sequences with different lengths.

Table 5.6: Complexity Comparisons of the Stream Selection Based IA Algorithms for 2 Pico Case in Scenario 2.1.

Exhaustive Search	**KSS**	**RASNSSS**	**ISNSSS**	**ESNSSS**	**SNSSS**
9720	12	16	24	36	6

On the other hand, the structures of the proposed stream selection based IA and the iterative algorithms are completely different. The proposed algorithms are successive algorithms while max-SINR and min-Leak algorithms are iterative algorithms. Therefore, the comparison of the complexities of these algorithms is not straightforward. The required number of the iterations increases in the high SNR regions for the iterative algorithms while the number of calls Alg. 9 does not change with different SNR values in the proposed stream selection based IA algorithms.

In fact, the given threshold and the maximum number of iterations affect the complexities of the iterative algorithms. The given threshold is the sum-rate difference between the previous iteration and the last iteration for the max-SINR and the min-Leak algorithms. As the threshold decreases, the complexity of the algorithms increases. If the threshold

cannot be achieved, then the algorithms are performed until the given maximum number of iterations is reached. We choose the threshold as 0.01 and the maximum number of the iterations as 3000 for Scenario 1.2 and Scenario 2.1. The average number of iterations is 107.20 for the max-SINR algorithm and 371.54 for the min-Leak algorithm.

5.7 Conclusion

In this chapter, we have studied imperfect CSI case for the RASNSSS and the ISNSSS algorithms presented in the previous chapter. In addition, we have proposed the KSS algorithm for the limited feedback schemes in the heterogeneous networks with an adaptive bit allocation to reduce the quantization error. Since the intra-stream interference has a severe impact on the performance of the IA with the limited feedback schemes, the KSS algorithm is proposed where we select only one stream for each user.

The precoders and postcoders have been obtained by the proposed algorithms under the quantized CDI. The presented adaptive bit allocation scheme has been performed for the heterogeneous networks. The number of bits of each user is optimized for the CDI feedback to maximize the average sum rate of the network.

The performance of the proposed algorithms, RASNSSS, KSS and ISNSSS, have been evaluated by varying the positions of pico BSs. Simulation results demonstrate that the KSS algorithm achieves higher performance gain when compared to the RASNSSS, ISNSSS and the existing stream selection based IA algorithms with the limited feedback scheme for a given number of feedback bits. Since the KSS algorithm selects only one stream for each user, quantization error can be reduced when compared to the other algorithms that can potentially select more streams for each user. On the other hand, the KSS algorithm is also compared with the max-SINR and min-Leak algorithms. It has been observed that the KSS algorithm achieves higher performance, although only one stream is considered for the max-SINR and min-Leak algorithms and it has been shown that the KSS algorithm is more robust to the channel uncertainties.

Furthermore, the presented adaptive bit allocation schemes improve the performances of the algorithms compared to the equal bit allocation. It has been observed that most of the bits should be allocated to the interference channels between the macro BS and pico users for the KSS algorithm, since the generated interference by the macro BS to the pico users is dominant. For the RASNSSS and the ISNSSS algorithms, on the other hand, since more streams can be selected for each user, the number of bits allocated to the desired channels also increases to reduce the intra-stream interference.

When the total number of bits increases, the RASNSSS and the ISNSSS algorithm achieve better performance than the KSS algorithm since the number of allocated bits is enough to decrease intra-stream interference for both the desired channels and the interference channels. In this case, the feedback overhead will also increase. Therefore, we propose the KSS algorithm for the practical implementations of the limited feedback scheme.

Conclusion

5.8 Summary

In this thesis, we have developed different stream selection based IA algorithms for the heterogeneous networks considering both perfect and imperfect CSI.

In Chapter 3, a general system model has been given assuming the perfect CSI is available at the transmitter side. The presented IA algorithms in this chapter have been evaluated in the homogeneous networks where the number of transmit and receive antennas are equal and the transmit power is the same for all the transmitters by assuming all users have the same distances from their serving BSs. The existing IA algorithms including iterative and stream selection based interference alignment algorithms, are explained and their performances are compared. In the iterative algorithms, the precoding and the postcoding matrices are designed in order to minimize the total interference experienced by all the receivers, or to maximize the SINR at each receiver. In the stream selection based algorithms, on the other hand, the precoding and the postcoding matrices are obtained by selecting the best stream sequences that maximizes the sum rate depending on the stream selection scheme. SNSSS algorithm constructs a single stream sequence by selecting the strongest streams, while ESNSSS constructs multiple stream sequences initialized with different streams and selects the best sequence. It has been observed that the performances of the mentioned IA approaches are almost identical in a homogeneous network model. In addition, the performance of the stream selection based IA algorithms increase when the search space of the stream sequences increases. Furthermore, the stream selection based IA algorithms construct stream sequences with a different number of streams depending on the selection criteria while iterative IA algorithms always select a fixed number of streams. However, this feature of the stream selection based IA approaches can not always guarantee for the users to receive a stream due to the channel conditions.

Allocating at least one stream to each user has been studied in Chapter 4 for heterogeneous networks assuming perfect CSI availability at the transmitters. Depending on the pico cell deployments, two different cases have been considered as partially connected and fully connected heterogeneous networks. ISNSSS algorithm has been presented for the partially connected interference network where the pico users do not receive interference from other pico BSs. Therefore, IA procedure is only performed to mitigate the interference generated to pico users from the macro BS and the interference generated to the macro user from the pico BSs. In order to construct better stream sequences, ISNSSS starts selecting streams from the pico users, because pico users have a higher SNR value than the macro user in general. On the other hand, ASNSSS algorithm has been proposed for fully connected interference networks where each pico cell generates interference to all other pico users. The sequences with the highest probability of occurrence while performing the exhaustive search are included in a predetermined set. It has been shown that the sequences in this predetermined set have a regular structure which requires selecting the initial streams from the pico users. Performance results show that both ISNSSS and ASNSSS algorithms achieve good performances when compared to the iterative IA algorithms. When compared to the existing stream selection based IA algorithms, the proposed algorithms can allocate more streams on average to the pico users while ensuring better service and increasing the sum rate. In addition, the ASNSSS and ISNSSS algorithms significantly reduce the complexity of the exhaustive search and achieve a closer performance

of the exhaustive search.

In the context of IA, the knowledge of CSI plays a very crucial role in designing precoding and postcoding matrices to achieve the perfect alignment. Since assuming the availability of the perfect CSI at the transmitter is not realistic for practical systems, a limited feedback scheme for the ISNSSS and the ASNSSS algorithms has been presented in Chapter 5. The ASNSSS algorithm has been modified as RASNSSS algorithm which is the restricted version of the ASNSSS algorithm by selecting less streams for each user to reduce the quantization error. In addition, a novel stream selection algorithm called KSS has been proposed. The KSS algorithm selects a single stream for each user to reduce the intra-stream interference with the imperfect CSI. Stream sequences are initialized with the pico streams and the selection continues with the best streams of the other users. In order to improve the performance of the algorithms in the limited feedback case, different adaptive feedback bit allocation schemes have been proposed for the algorithms. Performance results have shown that the adaptive bit allocation schemes improve the performances of the algorithms compared to the equal bit allocation. It has been observed that allocating more bits to the interference channels between the macro BS and pico users gives better results due to the dominant interference generated by the macro BS to the pico users. For a reasonable number of feedback bits, the KSS algorithm performs better than the existing stream selection and the iterative IA algorithms. On the other hand, when there is a sufficient number of bits to increase the CSI quality, the RASNSSS and the ISNSSS algorithms achieve better performance than the KSS algorithm. In other words, allocating more bits reduces the intra-stream interference; therefore, more streams can be selected for each user and as a result the average sum rate increases. However, the feedback load increases and the codebook design gets more complex with the increasing number of bits, which is not practical for the limited feedback schemes. Therefore, we propose the KSS algorithm for the practical implementations.

5.9 Perspectives

There are additional aspects that can be considered to further develop the approaches given in this thesis. These aspects can be identified as follows.

- Although most of the studies on IA have focused on interference channel, there are also IA studies to improve the user throughput in multi-user MIMO (MU-MIMO) cellular networks. Since the stream selection based IA algorithms have been investigated for single user MIMO systems so far, the extension to multi-user MIMO heterogeneous networks is a possible direction for future work. As a starting point, we can extend the scenarios that are described in this thesis by considering a heterogeneous network composed of one pico cell with one user and one macro cell with two users. In this case, the proposed algorithms are applicable with slight modifications. Further analysis can be carried out using exhaustive search to identify better criteria for constructing stream sequences.

- In case of multiple pico cells with multiple users, the number of transmit antennas will probably need to be increased to handle the interference in multi-user MIMO

heterogeneous networks, since, from the DoF perspective, as the number of the users increase, more antennas at the transmitters are required to perform the alignment properly. In other words, IA in the spatial domain is only achievable among a limited number of antennas. Therefore, user selection methods can be applied before the proposed stream selection based IA algorithms. There are different user scheduling algorithms based on different criteria, such as maximum SNR, minimum interference-to-noise ratio (INR), maximum SINR, Opportunistic IA (OIA), opportunistic maximum rate (OMR) (Maciel-Barboza et al. [2015]).

- Another possible extension for this thesis can be to consider dense deployment of small cells. In this case, clustering and user scheduling approaches can be jointly applied before the stream selection based IA algorithms. For instance, first, pico cells can be clustered depending on their interference level or their distance to each other and then the interference between the macro cell and the pico cells inside the clusters can be aligned. Next, the interference inside the cluster can be aligned by applying user scheduling algorithms. In such a scenario, a coordination between the pico cells is required (Chen et al. [2014]).

- On the other hand, fairness is important in terms of the QoS for the networks (Hong and Luo [2014]). Selecting multiple streams for each user in MU-MIMO systems is difficult to achieve in the areas with high user density. Therefore, achieving QoS targets becomes a challenging research problem, especially in the high SNR regime. There are studies that improve the worst user SINR by power control approaches (Liu et al. [2013], Yetis et al. [2014]). In this way, a fair transmission can be achieved with the cost of a reasonable sum-rate degradation. To this end, new stream selection criteria can be developed for MU-MIMO systems while ensuring fairness among the streams of each user.

- Acquiring accurate CSI is also an important problem to achieve perfect alignment. In this thesis, we have considered a limited feedback scheme in a centralized manner. In order to approximate the CSI more accurately, improving the codebook design to reduce the quantization error and the feedback overhead can further be investigated in future studies. In addition, it has been shown that achieving IA using the delayed CSI can be possible (Maddah-Ali and Tse [2012]), (Lee et al. [2014]). Therefore, the delayed CSI can be exploited to increase the performance of the proposed stream selection based IA algorithms under more realistic conditions.

Bibliography

3GPP. TR 36.814, further advancements for E-UTRA. 9, March 2010.

T. Akitaya and T. Saba. Hierarchical multi-stage interference alignment for downlink heterogeneous networks. In *Signal and Information Processing Association Annual Summit and Conference (APSIPA), 2013 Asia-Pacific*, pages 1–5, Oct 2013. doi: 10.1109/APSIPA.2013.6694381.

Salam Akoum, Marie Zwingelstein-Colin, Robert W. Heath, and Merouane Debbah. Cognitive cooperation for the downlink of frequency reuse small cells. *EURASIP Journal on Advances in Signal Processing*, 2011(1):1–11, 2010. ISSN 1687-6180. doi: 10.1155/2011/525271. URL `http://dx.doi.org/10.1155/2011/525271`.

M. Amara, D. Slock, and Yi Yuan-Wu. Near capacity linear closed form precoder design with recursive stream selection for MU-MIMO broadcast channels. In *Signal Processing Advances in Wireless Communications (SPAWC), 2011 IEEE 12th International Workshop on*, pages 336–340, June 2011. doi: 10.1109/SPAWC.2011.5990425.

M. Amara, M. Pischella, and D. Le Ruyet. Recursive stream selection for sum-rate maximization on the interference channel. In *2012 IEEE 13th International Workshop on Signal Processing Advances in Wireless Communications (SPAWC)*, pages 269–273, June 2012a. doi: 10.1109/SPAWC.2012.6292908.

M. Amara, M. Pischella, and D. Le Ruyet. Enhanced stream selection for sum-rate maximization on the interference channel. In *2012 International Symposium on Wireless Communication Systems (ISWCS)*, pages 151–155, August 2012b. doi: 10.1109/ISWCS.2012.6328348.

K. Anand, E. Gunawan, and Y.L. Guan. Beamformer design for the MIMO interference channels under limited channel feedback. *IEEE Transactions on Communications*, 61 (8):3246–3258, August 2013. ISSN 0090-6778.

E. Aycan, B. Ozbek, and D. Le Ruyet. Hierarchical successive stream selection for heterogeneous network interference. In *Wireless Communications and Networking Conference (WCNC), 2014 IEEE*, pages 1143–1148, Istanbul, Turkey, April 2014.

E. Aycan, B. Ozbek, and D. Le Ruyet. Improved Successive Stream Selection with Quantized Channel in Heterogeneous Networks . In *The Twelfth International Symposium on Wireless Communication Systems ISWCS 2015*, pages 1–5, Brussells, Belgium, August 2015.

E. Aycan Beyazit, B. Ozbek, and D. Le Ruyet. Interference alignment with improved stream selection in heterogeneous networks. In *Signal Processing and Communications Applications Conference (SIU), 2015 23th*, pages 1054–1057, May 2015. doi: 10.1109/SIU.2015.7130014.

E. Aycan Beyazit, B. Özbek, and D. Le Ruyet. On stream selection for interference alignment in heterogeneous networks. *EURASIP Journal on Wireless Communications and Networking*, 2016(1):1–18, 2016a. ISSN 1687-1499. doi: 10.1186/s13638-016-0575-7. URL `http://dx.doi.org/10.1186/s13638-016-0575-7`.

E. Aycan Beyazit, B. Ozbek, and D. Le Ruyet. Adaptive limited feedback scheme for stream selection based interference alignment in heterogeneous networks. In *Signal Processing and Communications Applications Conference (SIU), 2016 24th*, page to be published, May 2016b.

E. Aycan Beyazit, B. Ozbek, and D. Le Ruyet. Adaptive limited feedback scheme for stream selection based interference alignment in heterogeneous networks. In *Sensor Array and Multichannel Signal Processing Workshop, (SAM) 2016 9th*, page accepted, July 2016c.

E. Aycan Beyazit, B. Ozbek, and D. Le Ruyet. On stream selection for interference alignment with limited feedback in heterogeneous networks. In *Transactions on Emerging Telecommunications Technologies*, 2016d. doi: 10.1002/ett.3074.

F. Bernardo, R. Agusti, J. Cordero, and C. Crespo. Self-optimization of spectrum assignment and transmission power in ofdma femtocells. In *Telecommunications (AICT), 2010 Sixth Advanced International Conference on*, pages 404–409, May 2010. doi: 10.1109/AICT.2010.14.

Shengrong Bu, F.R. Yu, and H. Yanikomeroglu. Interference-aware energy-efficient resource allocation for OFDMA-based heterogeneous networks with incomplete channel state information. *IEEE Transactions on Vehicular Technology*, 64(3):1036–1050, March 2015. ISSN 0018-9545. doi: 10.1109/TVT.2014.2325823.

V. R. Cadambe and S. A. Jafar. Interference alignment and degrees of freedom of the K-User interference channel. *IEEE Transactions on Information Theory*, 54(8):3425–3441, Aug 2008. ISSN 0018-9448. doi: 10.1109/TIT.2008.926344.

Gen Cao, Dacheng Yang, Ruihong An, Xuan Ye, Ruiming Zheng, and Xin Zhang. An interference coordination scheme for dense femtocell environment. In *Broadband Network and Multimedia Technology (IC-BNMT), 2010 3rd IEEE International Conference on*, pages 417–421, Oct 2010. doi: 10.1109/ICBNMT.2010.5705124.

Gen Cao, Dacheng Yang, Ruihong An, Xuan Ye, Ruiming Zheng, and Xin Zhang. An adaptive sub-band allocation scheme for dense femtocell environment. In *Wireless Communications and Networking Conference (WCNC), 2011 IEEE*, pages 102–107, March 2011. doi: 10.1109/WCNC.2011.5779114.

Xiaoming Chen and Chau Yuen. Performance analysis and optimization for interference alignment over MIMO interference channels with limited feedback. *IEEE Transactions*

on Signal Processing, 62(7):1785–1795, April 2014. ISSN 1053-587X. doi: 10.1109/TSP.2014.2304926.

Y. F. Chen, L. C. Wang, and W. H. Sheen. Joint user scheduling and interference alignment beamforming in heterogeneous wireless networks. In *2014 IEEE 25th Annual International Symposium on Personal, Indoor, and Mobile Radio Communication (PIMRC)*, pages 1083–1087, Sept 2014. doi: 10.1109/PIMRC.2014.7136328.

Sungyoon Cho, Kaibin Huang, Dong Ku Kim, V.K.N. Lau, Hyukjin Chae, Hanbyul Seo, and Byoung-Hoon Kim. Feedback-topology designs for interference alignment in MIMO interference channels. *IEEE Transactions on Signal Processing*, 60(12):6561–6575, Dec 2012. ISSN 1053-587X. doi: 10.1109/TSP.2012.2214214.

P. de Kerret and D. Gesbert. MIMO interference alignment algorithms with hierarchical csit. In *Wireless Communication Systems (ISWCS), 2012 International Symposium on*, pages 581–585, 2012. doi: 10.1109/ISWCS.2012.6328434.

P. de Kerret, J. Hoydis, and D. Gesbert. Rate loss analysis of transmitter cooperation with distributed csit. In *Signal Processing Advances in Wireless Communications (SPAWC), 2013 IEEE 14th Workshop on*, pages 190–194, June 2013a. doi: 10.1109/SPAWC.2013.6612038.

Paul de Kerret, Maxime Guillaud, and David Gesbert. Degrees of freedom of certain interference alignment schemes with distributed CSIT. *CoRR*, abs/1305.1490, 2013b.

Y. Fadlallah, A. Aissa-El-Bey, K. Amis, and R. Pyndiah. Interference alignment: Improved design via precoding vectors. In *Vehicular Technology Conference (VTC Spring), 2012 IEEE 75th*, pages 1–5, 2012. doi: 10.1109/VETECS.2012.6240141.

A. Ghosh, N. Mangalvedhe, R. Ratasuk, B. Mondal, M. Cudak, E. Visotsky, T.A. Thomas, J.G. Andrews, P. Xia, H.S. Jo, H.S. Dhillon, and T.D. Novlan. Heterogeneous cellular networks: From theory to practice. *Communications Magazine, IEEE*, 50(6):54–64, June 2012. ISSN 0163-6804. doi: 10.1109/MCOM.2012.6211486.

Andrea Goldsmith. *Wireless Communications*. Cambridge University Press, New York, NY, USA, 2005. ISBN 0521837162.

Gene H. Golub and Charles F. Van Loan. *Matrix Computations (3rd Ed.)*. Johns Hopkins University Press, Baltimore, MD, USA, 1996. ISBN 0-8018-5414-8.

K. Gomadam, V. R. Cadambe, and S. A. Jafar. A distributed numerical approach to interference alignment and applications to wireless interference networks. *IEEE Transactions on Information Theory*, 57(6):3309–3322, June 2011. ISSN 0018-9448. doi: 10.1109/TIT.2011.2142270.

Krishna Srikanth Gomadam, Viveck R. Cadambe, and Syed Ali Jafar. Approaching the capacity of wireless networks through distributed interference alignment. *CoRR*, abs/0803.3816, 2008a.

Krishna Srikanth Gomadam, Viveck R. Cadambe, and Syed Ali Jafar. Approaching the capacity of wireless networks through distributed interference alignment. In *GLOBECOM*, pages 4260–4265, 2008b.

Michael Grant and Stephen Boyd. CVX: Matlab software for disciplined convex programming, version 2.1, March 2014. URL `http://cvxr.com/cvx`.

B. Guler and A. Yener. Interference alignment for cooperative mimo femtocell networks. In *Global Telecommunications Conference (GLOBECOM 2011), 2011 IEEE*, pages 1–5, Dec 2011. doi: 10.1109/GLOCOM.2011.6134195.

B. Guler and A. Yener. Selective interference alignment for MIMO cognitive femtocell networks. *IEEE Journal on Selected Areas in Communications*, 32(3):439–450, March 2014. ISSN 0733-8716. doi: 10.1109/JSAC.2014.140306.

Tao Han, Guoqiang Mao, Qiang Li, Lijun Wang, and Jing Zhang. Interference minimization in 5g heterogeneous networks. *Mob. Netw. Appl.*, 20(6):756–762, December 2015. ISSN 1383-469X. doi: 10.1007/s11036-014-0564-1.

Mingyi Hong and Zhi-Quan Luo. Signal processing and optimal resource allocation for the interference channel. In *Academic Press Library in Signal Processing: Communications and Radar Signal Processing*, volume 2, pages 409 – 469. Elsevier, 2014. doi: http://dx.doi.org/10.1016/B978-0-12-396500-4.00008-9.

S. A. Jafar and S. Shamai. Degrees of freedom region of the MIMO X channel. *IEEE Transactions on Information Theory*, 54(1):151–170, Jan 2008. ISSN 0018-9448. doi: 10.1109/TIT.2007.911262.

Syed Ali Jafar. Interference alignment: A new look at signal dimensions in a communication network. *Foundations and Trends in Communications and Information Theory*, 7 (1):1–136, 2011. URL `http://dblp.uni-trier.de/db/journals/ftcit/ftcit7.html#Jafar11`.

N. Jindal. MIMO broadcast channels with finite-rate feedback. *IEEE Transactions on Information Theory*, 52(11):5045–5060, Nov 2006. ISSN 0018-9448. doi: 10.1109/TIT.2006.883550.

Hyunduk Jung and Jaiyong Lee. Downlink resource management for OFDMA femtocells using stochastic subchannel allocation. *IEEE*, pages 249 – 254, 2010. doi: 10.1109/APCC.2010.5679775.

Hyunduk Jung and Jaiyong Lee. Interference-aware downlink resource management for OFDMA femtocell networks. *TIIS*, 5(3):508–522, 2011. doi: http://dx.doi.org/10.3837/tiis.2011.03.003.

J. S. Kim, S. H. Moon, S. R. Lee, and I. Lee. A new channel quantization strategy for mimo interference alignment with limited feedback. *IEEE Transactions on Wireless Communications*, 11(1):358–366, Jan 2012. ISSN 1536-1276. doi: 10.1109/TWC.2011.111211.110810.

R.T. Krishnamachari and M.K. Varanasi. Interference alignment under limited feedback for MIMO interference channels. pages 619–623, June 2010. doi: 10.1109/ISIT.2010.5513544.

S. Landstrom, H. Murai, and A. Simonsson. Deployment aspects of lte pico nodes. In *Communications Workshops (ICC), 2011 IEEE International Conference on*, pages 1–5, June 2011. doi: 10.1109/iccw.2011.5963602.

H. C. Lee, D. C. Oh, and Y. H. Lee. Mitigation of inter-femtocell interference with adaptive fractional frequency reuse. In *Communications (ICC), 2010 IEEE International Conference on*, pages 1–5, May 2010. doi: 10.1109/ICC.2010.5502298.

Namyoon Lee, Ravi Tandon, and Robert W. Heath Jr. Distributed space-time interference alignment. *CoRR*, abs/1405.0032, 2014.

Alberto Leon-Garcia. *Probability, Statistics, and Random Processes for Electrical Engineering*. Pearson/Prentice Hall, Upper Saddle River, NJ, 2008. ISBN 9780131471221 0131471228.

N. Lertwiram, P. Popovski, and K. Sakaguchi. A study of trade-off between opportunistic resource allocation and interference alignment in femtocell scenarios. *Wireless Communications Letters, IEEE*, 1(4):356–359, August 2012. ISSN 2162-2337. doi: 10.1109/WCL.2012.051712.120268.

Guoqing Liu, Min Sheng, Xijun Wang, Wanguo Jiao, Ying Li, and Jiandong Li. Interference alignment for partially connected downlink MIMO heterogeneous networks. *IEEE Transactions on Communications*, 63(2):551–564, Feb 2015. ISSN 0090-6778. doi: 10.1109/TCOMM.2015.2388450.

Y. F. Liu, Y. H. Dai, and Z. Q. Luo. Max-min fairness linear transceiver design for a multi-user MIMO interference channel. *IEEE Transactions on Signal Processing*, 61(9):2413–2423, May 2013. ISSN 1053-587X. doi: 10.1109/TSP.2013.2245125.

D. Lopez-Perez, A. Valcarce, G. de la Roche, and Jie Zhang. OFDMA Femtocells: A roadmap on interference avoidance. *Communications Magazine, IEEE*, 47(9):41–48, Sept 2009. ISSN 0163-6804. doi: 10.1109/MCOM.2009.5277454.

D. Lopez-Perez, I. Guvenc, G. de la Roche, M. Kountouris, T.Q.S. Quek, and Jie Zhang. Enhanced intercell interference coordination challenges in heterogeneous networks. *Wireless Communications, IEEE*, 18(3):22–30, June 2011. ISSN 1536-1284. doi: 10.1109/MWC.2011.5876497.

D.J. Love, R.W. Heath, V.K.N. Lau, D. Gesbert, B.D. Rao, and M. Andrews. An overview of limited feedback in wireless communication systems. *Selected Areas in Communications, IEEE Journal on*, 26(8):1341–1365, Oct 2008. ISSN 0733-8716. doi: 10.1109/JSAC.2008.081002.

Hao Lv, Tingting Liu, Xueying Hou, and Chenyang Yang. Adaptive interference alignment for femtocell networks. In *Signal Processing (ICSP), 2010 IEEE 10th International Conference on*, pages 1654–1657, Oct 2010. doi: 10.1109/ICOSP.2010.5656457.

F. M. Maciel-Barboza, J. Sánchez-García, F. R. Castillo-Soria, L. Soriano-Equigua, and V. H. Castillo-Topete. Practical user scheduling algorithms for the mimo interference channel. In *Information and Communication Technology Convergence (ICTC), 2015 International Conference on*, pages 275–279, Oct 2015. doi: 10.1109/ICTC.2015.7354547.

M. A. Maddah-Ali and D. Tse. Completely stale transmitter channel state information is still very useful. *IEEE Transactions on Information Theory*, 58(7):4418–4431, July 2012. ISSN 0018-9448. doi: 10.1109/TIT.2012.2193116.

Qin Niu, Zhimin Zeng, Tiankui Zhang, Qiubin Gao, and Shaohui Sun. Interference alignment and bit allocation in heterogeneous networks with limited feedback. In *Wireless Personal Multimedia Communications (WPMC), 2014 International Symposium on*, pages 514–519, Sept 2014. doi: 10.1109/WPMC.2014.7014872.

Nasr Obaid and Andreas Czylwik. The impact of deploying pico base stations on capacity and energy efficiency of heterogeneous cellular networks. In *Personal Indoor and Mobile Radio Communications (PIMRC), 2013 IEEE 24th International Symposium on*, pages 1904–1908, Sept 2013. doi: 10.1109/PIMRC.2013.6666454.

Kenta Okino, Taku Nakayama, Chiharu Yamazaki, Hirotaka Sato, and Yoshimasa Kusano. Pico cell range expansion with interference mitigation toward lte-advanced heterogeneous networks. 2011. doi: 10.1109/iccw.2011.5963603.

H. Osman, H. Zhu, and J. Wang. Downlink distributed antenna systems in indoor high building femtocell environments. In *21st Annual IEEE International Symposium on Personal, Indoor and Mobile Radio Communications*, pages 1016–1020, Sept 2010. doi: 10.1109/PIMRC.2010.5672090.

B. Özbek and D. Le Ruyet. Adaptive limited feedback links for cooperative multi-antenna multicell networks. *EURASIP Journal Wireless Commmunication and Networking*, 2014: 193, 2014a. doi: 10.1186/1687-1499-2014-193.

B. Özbek and D. Le Ruyet. *Feedback Strategies for Wireless Communication.* Springer Publishing Company, Incorporated, 2014b. ISBN 1461477409, 9781461477402.

Hyun-Seo Park, Ae-Soon Park, Jae-Yong Lee, and Byung-Chul Kim. Two-step handover for LTE HetNet mobility enhancements. In *ICT Convergence (ICTC), 2013 International Conference on*, pages 763–766, Oct 2013. doi: 10.1109/ICTC.2013.6675473.

Steven W. Peters and Robert W. Heath Jr. Interference alignment via alternating minimization. pages 2445–2448, 2009.

M. Rahman and H. Yanikomeroglu. Enhancing cell-edge performance: a downlink dynamic interference avoidance scheme with inter-cell coordination. *IEEE Transactions on Wireless Communications*, 9(4):1414–1425, April 2010. ISSN 1536-1276. doi: 10.1109/TWC.2010.04.090256.

M. Rahman, H. Yanikomeroglu, and W. Wong. Interference avoidance with dynamic inter-cell coordination for downlink lte system. In *Wireless Communications and Networking*

Conference, 2009. WCNC 2009. IEEE, pages 1–6, April 2009. doi: 10.1109/WCNC.2009.4917761.

Xiongbin Rao and V.K.N. Lau. Interference alignment with partial csi feedback in MIMO cellular networks. *IEEE Transactions on Signal Processing*, 62(8):2100–2110, April 2014. ISSN 1053-587X. doi: 10.1109/TSP.2014.2307283.

Xiongbin Rao, Liangzhong Ruan, and V.K.N. Lau. Limited feedback design for interference alignment on MIMO interference networks with heterogeneous path loss and spatial correlations. *IEEE Transactions on Signal Processing*, 61(10):2598–2607, May 2013. ISSN 1053-587X. doi: 10.1109/TSP.2013.2252168.

N. Ravindran and N. Jindal. Limited feedback-based block diagonalization for the MIMO broadcast channel. *Selected Areas in Communications, IEEE Journal on*, 26(8):1473–1482, Oct 2008. ISSN 0733-8716. doi: 10.1109/JSAC.2008.081013.

S. M. Razavi and T. Ratnarajah. Performance analysis of interference alignment under csi mismatch. *IEEE Transactions on Vehicular Technology*, 63(9):4740–4748, Nov 2014. ISSN 0018-9545. doi: 10.1109/TVT.2014.2316166.

M. Rihan, M. Elsabrouty, O. Muta, and H. Furukawa. Interference alignment with limited feedback for macrocell-femtocell heterogeneous networks. In *Vehicular Technology Conference (VTC Spring), 2015 IEEE 81st*, pages 1–5, May 2015. doi: 10.1109/VTCSpring.2015.7145883.

Kenneth H. Rosen. *Discrete Mathematics and Its Applications*. McGraw-Hill Higher Education, 5th edition, 2002. ISBN 0072424346.

Y.A. Sambo, M.Z. Shakir, K.A. Qaraqe, E. Serpedin, and M.A. Imran. Expanding cellular coverage via cell-edge deployment in heterogeneous networks: spectral efficiency and backhaul power consumption perspectives. *Communications Magazine, IEEE*, 52(6):140–149, June 2014. ISSN 0163-6804. doi: 10.1109/MCOM.2014.6829956.

Wiroonsak Santipach and M.L. Honig. Capacity of a multiple-antenna fading channel with a quantized precoding matrix. *IEEE Transactions on Information Theory*, 55(3):1218–1234, March 2009. ISSN 0018-9448. doi: 10.1109/TIT.2008.2011437.

D.A. Schmidt, Changxin Shi, R.A. Berry, M.L. Honig, and W. Utschick. Minimum mean squared error interference alignment. pages 1106–1110, 2009. ISSN 1058-6393. doi: 10.1109/ACSSC.2009.5470055.

J. Schreck, G. Wunder, and P. Jung. Robust iterative interference alignment for cellular networks with limited feedback. *IEEE Transactions on Wireless Communications*, 14(2):882–894, Feb 2015. ISSN 1536-1276. doi: 10.1109/TWC.2014.2361335.

Jan Schreck and Gerhard Wunder. Distributed interference alignment in cellular systems: Analysis and algorithms. In *Wireless Conference 2011 - Sustainable Wireless Technologies (European Wireless), 11th European*, pages 1–8, 2011.

R. Seno, T. Ohtsuki, W. Jiang, and Y. Takatori. Interference alignment in heterogeneous networks using pico cell clustering. In *Vehicular Technology Conference (VTC Fall), 2015 IEEE 82nd*, pages 1–5, Sept 2015. doi: 10.1109/VTCFall.2015.7390989.

Qingjiang Shi, M. Razaviyayn, Zhi-Quan Luo, and Chen He. An iteratively weighted mmse approach to distributed sum-utility maximization for a MIMO interfering broadcast channel. *IEEE Transactions on Signal Processing*, 59(9):4331–4340, 2011. ISSN 1053-587X. doi: 10.1109/TSP.2011.2147784.

Wonjae Shin, Wonjong Noh, Kyunghun Jang, and Hyun-Ho Choi. Hierarchical interference alignment for downlink heterogeneous networks. *IEEE Transactions on Wireless Communications*, 11(12):4549–4559, 2012. ISSN 1536-1276. doi: 10.1109/TWC.2012.101912.120421.

C. Suh, M. Ho, and D. Tse. Downlink interference alignment. In *Global Telecommunications Conference (GLOBECOM 2010), 2010 IEEE*, pages 1–5, Dec 2010. doi: 10.1109/GLOCOM.2010.5684033.

C. Sun and E. A. Jorswieck. Stream selection methods for non-regenerative mimo relay networks. In *Sensor Array and Multichannel Signal Processing Workshop, (SAM) 2016 9th*, page accepted, July 2016.

Liang Sun and M.R. McKay. Eigen-based transceivers for the MIMO broadcast channel with semi-orthogonal user selection. *IEEE Transactions on Signal Processing*, 58(10): 5246–5261, Oct 2010. ISSN 1053-587X. doi: 10.1109/TSP.2010.2053709.

Li Tan, Zhiyong Feng, Wei Li, Zhong Jing, and T.A. Gulliver. Graph coloring based spectrum allocation for femtocell downlink interference mitigation. In *Wireless Communications and Networking Conference (WCNC), 2011 IEEE*, pages 1248–1252, March 2011. doi: 10.1109/WCNC.2011.5779338.

Jie Tang and S. Lambotharan. Interference alignment techniques for MIMO multi-cell interfering broadcast channels. *IEEE Transactions on Communications*, 61(1):164–175, 2013. ISSN 0090-6778. doi: 10.1109/TCOMM.2012.100912.110644.

Peng Tian, Hui Tian, Liqi Gao, Jing Wang, Xiaoming She, and Lan Chen. Deployment analysis and optimization of macro-pico heterogeneous networks in lte-a system. In *Wireless Personal Multimedia Communications (WPMC), 2012 15th International Symposium on*, pages 246–250, Sept 2012.

M. Westreicher and M. Guillaud. Interference alignment over partially connected interference networks: Application to the cellular case. In *Wireless Communications and Networking Conference (WCNC), 2012 IEEE*, pages 647–651, 2012. doi: 10.1109/WCNC.2012.6214448.

C. Wilson and V. Veeravalli. A convergent version of the max sinr algorithm for the mimo interference channel. *IEEE Transactions on Wireless Communications*, 12(6):2952–2961, June 2013. ISSN 1536-1276. doi: 10.1109/TWC.2013.041913.121289.

Y. Yang X.Chu, D. López-Pérez and F. Gunnarsson. *Heterogeneous cellular networks: theory, simulation, and deployment*. Cambridge University Press, 2013. ISBN 978-1107023093.

B. Xie, Y. Li, H. Minn, and A. Nosratinia. Adaptive interference alignment with csi uncertainty. *IEEE Transactions on Communications*, 61(2):792–801, Feb 2013. ISSN 0090-6778. doi: 10.1109/TCOMM.2012.121112.110589.

Bin Yang, Guoqiang Mao, Xiaohu Ge, and Tao Han. A new cell association scheme in heterogeneous networks. In *Communications (ICC), 2015 IEEE International Conference on*, pages 5627–5632, June 2015. doi: 10.1109/ICC.2015.7249219.

C. M. Yetis, Y. Zeng, K. Anand, Y. L. Guan, and E. Gunawan. Balancing weighted substreams in MIMO interference channels. *IEEE Wireless Communications Letters*, 3 (5):513–516, Oct 2014. ISSN 2162-2337. doi: 10.1109/LWC.2014.2336247.

C.M. Yetis, Tiangao Gou, S.A. Jafar, and A.H. Kayran. On feasibility of interference alignment in MIMO interference networks. *IEEE Transactions on Signal Processing*, 58 (9):4771–4782, 2010. ISSN 1053-587X. doi: 10.1109/TSP.2010.2050480.

Taesang Yoo and A. Goldsmith. On the optimality of multiantenna broadcast scheduling using zero-forcing beamforming. *Selected Areas in Communications, IEEE Journal on*, 24(3):528–541, March 2006. ISSN 0733-8716. doi: 10.1109/JSAC.2005.862421.

Heli Zhang, Shanzhi Chen, Xi Li, Hong Ji, and Xiaojiang Du. Interference management for heterogeneous networks with spectral efficiency improvement. *Wireless Communications, IEEE*, 22(2):101–107, April 2015. ISSN 1536-1284. doi: 10.1109/MWC.2015.7096292.

Jun Zhang and J.G. Andrews. Adaptive spatial intercell interference cancellation in multicell wireless networks. *Selected Areas in Communications, IEEE Journal on*, 28(9): 1455–1468, Dec 2010. ISSN 0733-8716. doi: 10.1109/JSAC.2010.101207.

Yue Zhao, S.N. Diggavi, A. Goldsmith, and H.V. Poor. Convex optimization for precoder design in MIMO interference networks. In *Communication, Control, and Computing (Allerton), 2012 50th Annual Allerton Conference on*, pages 1213–1219, 2012. doi: 10.1109/Allerton.2012.6483356.

K.J. Zou, K.W. Yang, Mao Wang, Bingyin Ren, Jingsong Hu, Jingjing Zhang, Min Hua, and Xaohu You. Network synchronization for dense small cell networks. *Wireless Communications, IEEE*, 22(2):108–117, April 2015. ISSN 1536-1284. doi: 10.1109/MWC.2015.7096293.

Annexes

Appendix A

JUSTIFICATION FOR THE INITIALIZATION OF STREAM SEQUENCES WITH PICO-USER STREAMS

Although the collected data do not yield a complete criterion for step-by-step selection of each stream, it is possible and important to justify the selection of pico streams as the initial streams. The data show that stream paths leading to relatively higher sum rate values generally start with the streams of the user which has the greatest SNR value. Below, it is justified that with high probability, this user is a pico user.

Let $\rho_p = \frac{P_{r_p}}{P_n}$ and $\rho_m = \frac{P_{r_m}}{P_n}$ be the average SNR values of pico and macro users, respectively. Furthermore, let $P_{r_p} = P_k(dB) - P_{L_p}(dB)$ and $P_{r_m} = P_1(dB) - P_{L_m}(dB)$ be the received powers of the corresponding pico and macro users, respectively, where P_{L_p} and P_{L_m} are the path loss for pico and macro users, and $P_k,\ k \in \Gamma$ and P_1 are the transmitted powers of the corresponding pico and macro BSs, respectively. Also, P_n is the noise power.

In order to find the probability that the SNR of the pico user is greater than the SNR of the macro user, $P(\rho_p > \rho_m)$, the following inequality can be considered.

$$P(P_{t_p} - P_{L_p} > P_{t_m} - P_{L_m}) \tag{A.1}$$

Using the path loss equations given in Table 4.1 in Section 4.5, which are some of the most commonly employed path loss models in the heterogeneous network scenarios (Ghosh et al. [2012] 3GPP [2010]), Equation (A.1) can be expressed as follows.

$$P\Big((P_{t_p} - (140.7 + 36.7\log_{10}(r_p(km))) > P_{t_m} - (128.1 + 37.6\log_{10}(r_m(km))))(dB)\Big) =$$
$$P\Big(\log_{10}(r_p) < \frac{(P_{t_p} - P_{t_m})(dB) - 12.6 + 37.6\log_{10}(r_m)}{36.7}\Big) =$$
$$P\Big(\frac{r_p}{r_m} < 10^{(\frac{(P_{t_p} - P_{t_m})(dB) - 12.6}{36.7})}\Big)$$

where r_p is the distance between the pico user and the pico BS and r_m is the distance between the macro user and its BS. In addition, it is assumed that $37.6/36.7 \approx 1$. For heterogeneous networks, pico transmit power, $P_k,\ k \in \Gamma$, can range between 23dBm and 30dBm and typical macro transmit power, P_1, is 43dBm. Therefore, the probability of $P(\frac{r_p}{r_m} \leq Q)$ can vary between 0.12 to 0.2. In this study, Q is 0.1377 because $P_k,\ k \in \Gamma$ is 24dBm.

In order to calculate the probability that $P(\frac{r_p}{r_m} \leq Q)$, let X be the random variable to represent the distance between the pico BS and the pico user and Y be the random variable to represent the distance between the macro BS and the macro user. These random variables are independent and the cumulative distribution functions of X and Y are given as follows (Leon-Garcia [2008]).

$$P(X \leq x) = F_X(x) = \frac{x^2}{R_p^2}, \tag{A.2}$$
$$P(Y \leq y) = F_Y(y) = \frac{y^2}{R_m^2}$$

where R_p is the range of a pico BS and R_m is the range of a macro BS. Consequently, the probability density functions of X and Y are as follows.

$$f_X(x) = \frac{2x}{{R_p}^2}, \quad f_Y(y) = \frac{2y}{{R_m}^2} \tag{A.3}$$

To calculate the probability that $P(\frac{r_p}{r_m} \leq K)$, a new random variable $Z = X/Y$ can be used as follows (Leon-Garcia [2008]).

$$\begin{aligned} P(Z \leq z) = F_Z(z) = P(X/Y \leq z) &= P(X \geq zY, Y < 0) + P(X \leq zY, Y > 0) \\ &= \int_{-\infty}^{0} \left[\int_{yz}^{\infty} f_X(x) d_x \right] f_Y(y) d_y + \int_{0}^{\infty} \left[\int_{-\infty}^{yz} f_X(x) d_x \right] f_Y(y) d_y \end{aligned}$$

Since $x \in [0, R_p]$ and $y \in [0, R_m]$,

$$\begin{aligned} F_Z(z) &= \int_0^{R_m} \left[\int_0^{zy} f_X(x) d_x \right] f_Y(y) d_y \\ &= \int_0^{R_m} F_X(zy) \cdot f_Y(y) d_y \end{aligned} \tag{A.4}$$

where $F_X(x) = 1$ if $x > R_p$. For $z > R_p/R_m$,

$$F_Z(z) = \int_0^{R_p/z} \frac{y^2 z^2}{R_p^2} \frac{2y}{R_m^2} d_y + \int_{R_p/z}^{R_m} \frac{2y}{R_m^2} d_y = 1 - \frac{1}{2} \frac{R_p^2}{R_m^2} \frac{1}{z^2} \tag{A.5}$$

If $Z = Q = 0.1377$, $R_p = 0.1$km, $R_m = 1$km, then

$$\begin{aligned} P(X/Y < Q) = F_Z(Q) &= 1 - \frac{1}{2} \frac{0.1^2}{1^2} \frac{1}{0.1377^2} \\ &\approx 0.736 \end{aligned} \tag{A.6}$$

Thus, a pico user has a higher SNR value than a macro user with a probability of 73.6%. Note that these derivations are obtained for $K_p = 1$ where K_p is the number of pico users. For cases $K_p > 1$, then the probability of having higher SNR values for pico users becomes as follows.

$$1 - P(Z \geq Q)^{K_p} = 1 - (1 - P(Z < Q))^{K_p} \tag{A.7}$$

Therefore, pico users have higher SNR values than a macro user with a probability of 92.7% for $K_p = 2$ as in Scenario 2.1 and Scenario 2.2 and 98% for $K_p = 3$ as in Scenario 2.3 and Scenario 2.4.

For the given scenarios for partial and fully connected interference networks, the following Table A.1 supports the justification for the initialization of stream sequences with pico-user streams. It can be observed that the SNR values of the pico users are higher than the macro user.

Table A.1: SNR and SINR Values of Pico Users vs. Shift Number for Different Scenarios at $d/R = 0.8$

	Scenario 1.3		**Scenario 2.3**	
User Values (dB)	**SNR**	**SINR**	**SNR**	**SINR**
Macro User	36.09	35.84	35.40	27.32
Pico 1 User	39.32	14.78	39.32	3.46
Pico 2 User	38.97	14.12	38.97	14.90
Pico 3 User	39.59	14.93	39.59	15.32

Appendix B

EXHAUSTIVE SEARCH STATISTICAL ANALYSIS

In order to analyze the behavior of the stream selection algorithms depending on the position of the pico cell, the selection probabilities of each stream path and the average sum rate obtained after the possible selections are given in the stream sequence trees. In addition, the weighted sum-rates are computed by the production of the given probabilities. These results are obtained by the exhaustive search.

The proposed algorithm ISNSSS for the partially connected network achieves to construct stream sequences by examining certain metric values obtained from the exhaustive analysis. These metrics can be defined as follows.

- P is the selection probability of each stream sequences.
- SR is the average of the sum rates achieved by the sequence only when the sequence is selected.
- The multiplication of P and SR represents the sum rate contribution of the selected stream sequence.

Scenarios for Partially Connected Interference Networks:

P and $P \times$ SR are given in the stream trees, as in Figure B.1, Figure B.2 and Figure B.3 for Scenario 1.1, Scenario 1.2 and Scenario 1.3 studied in Chapter 4, respectively.

It can be seen that from the given stream trees for the three scenario considered for the partially connected networks, initializing the stream sequences with the streams from the pico user has higher probability than selecting the first streams from the macro user.

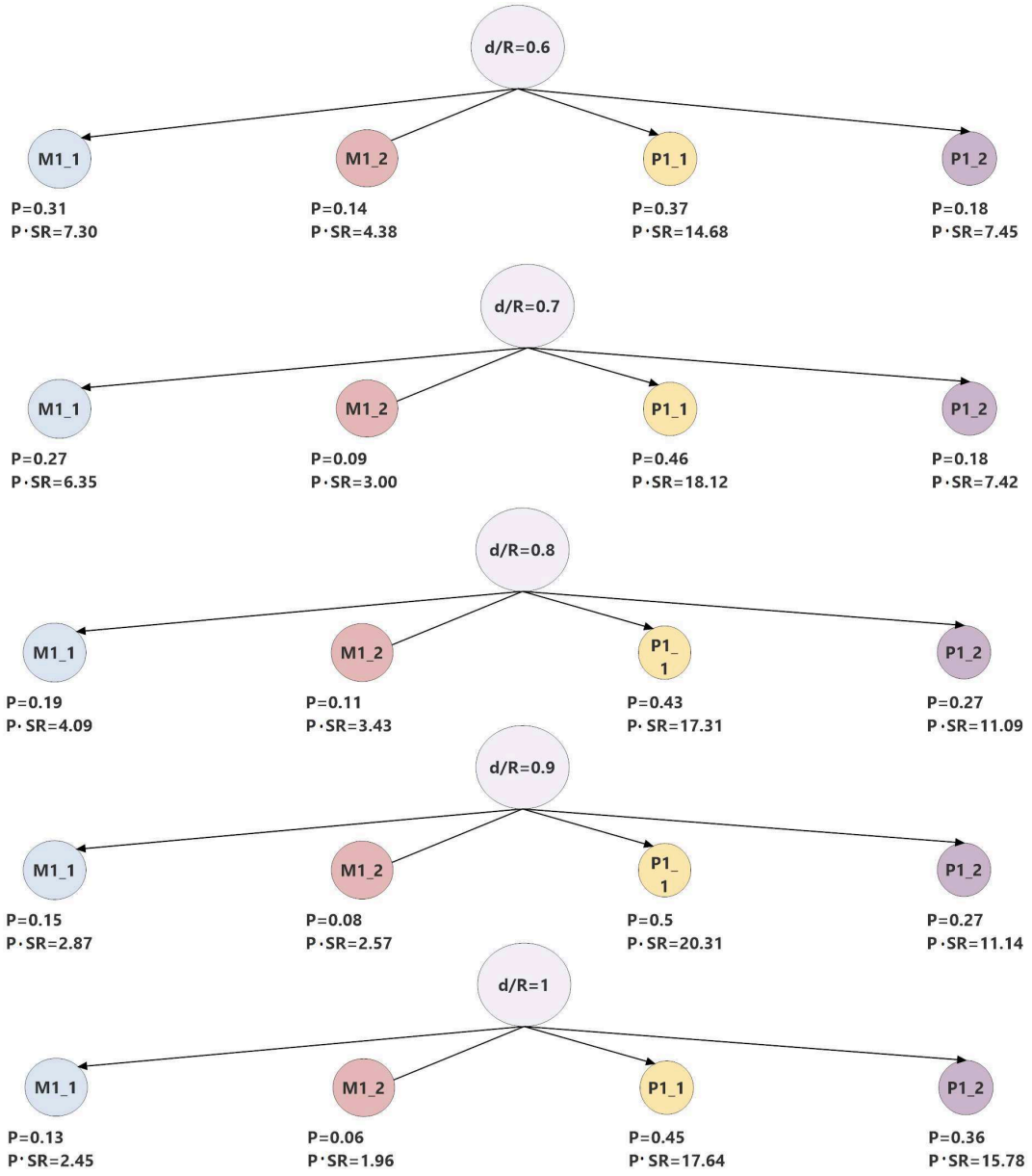

Figure B.1: Scenario 1.1: Tree Diagram for the total weighted sum rates of each branch

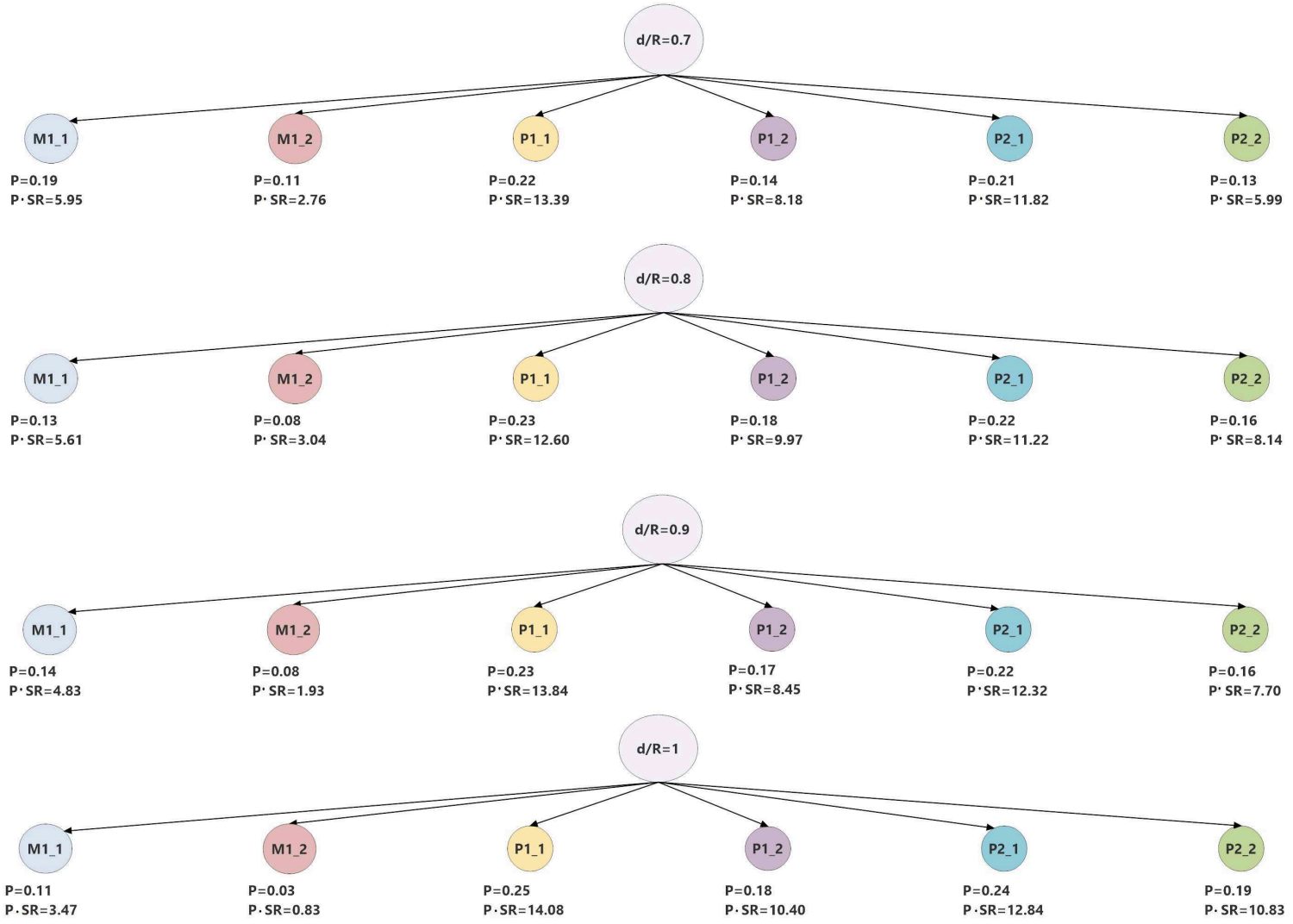

Figure B.2: Scenario 1.2: Tree Diagram with the total weighted sum rates of each branch

Scenarios for Fully Connected Interference Networks:

The construction of the stream sequence set by the ASNSSS algorithm is explained in Chapter 4. The selected stream sequences in the exhaustive search are analyzed by examining metrics P, SR and $P \times SR$.

The analysis in Scenario 2.1 show that different stream sequences with different lengths can be selected by the exhaustive search. The tree of the selected stream sequences starting from pico streams, such as $P1\_1$, $P1\_2$ which belong to pico 1 user and $P2\_1$, $P2\_2$ which belong to pico 2 user, can be seen in Figure B.4 for $d/R = 0.7$. The stream sequences constructed by the proposed ASNSSS algorithm are highlighted in the given tree. It can be also observed that the selected streams starting from macro streams, M_1 and M_2, have lower sum rate contributions. The predetermined set constructed by the proposed approach are highlighted in the tree. It can be seen that the weighted sum rate of the selected stream sequences ($P \times SR$) are higher than the other selected sequences in the exhaustive search. This observation can be used to achieve higher sum rate values while decreasing the size of the search tree. The tree given in Figure B.5 shows that it is possible to shrink the tree in Figure B.4 while still achieving high sum rate values.

The analysis for the Scenario 2.2 show that the weighted sum rate of the selected stream sequences ($P \times SR$) are higher than the other selected sequences in the exhaustive search and it can be illustrated in Figure B.6.

The stream sequences constructed by the ASNSSS algorithm for Scenario 2.3 and Scenario 2.4 can be seen in Figure B.7.

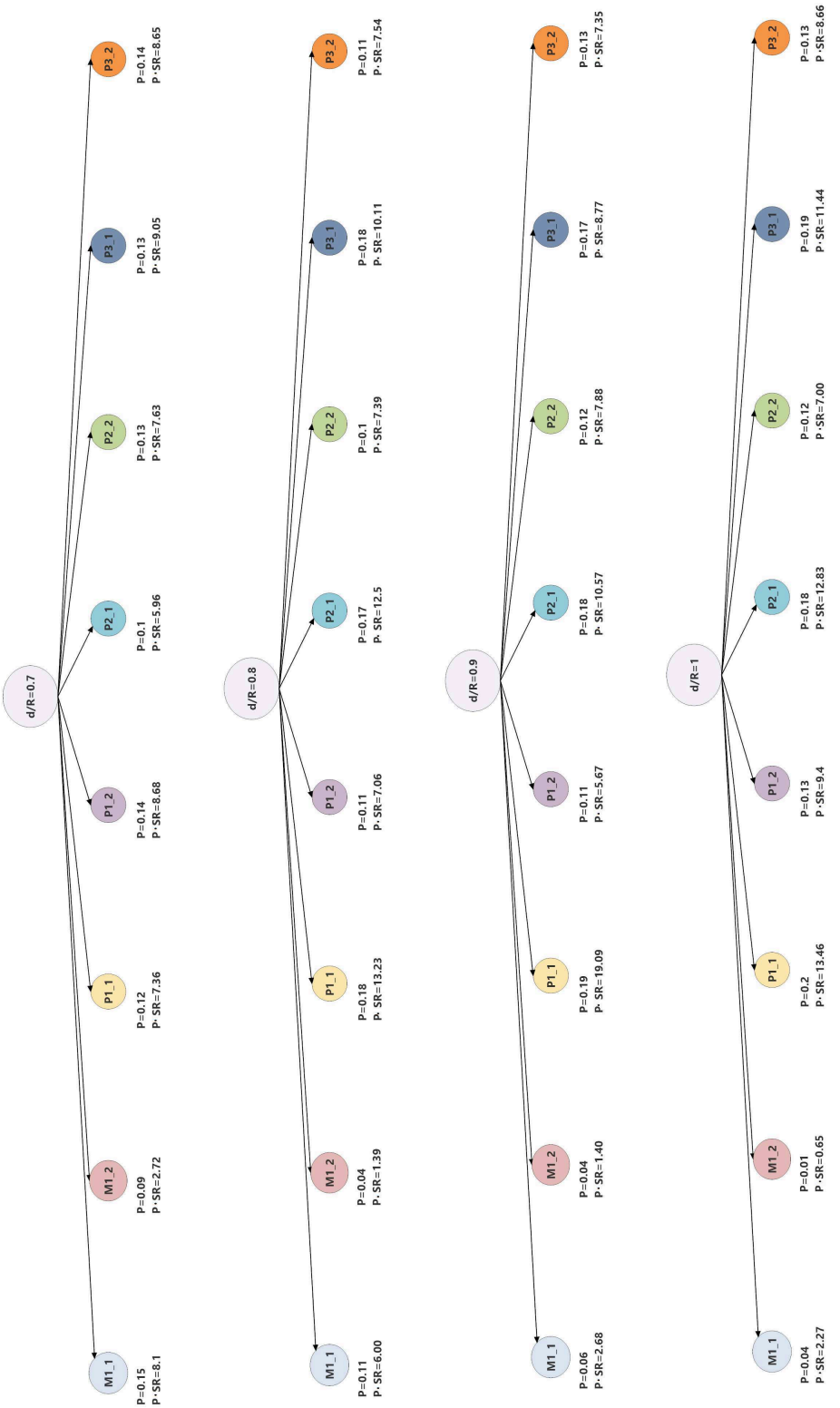

Figure B.3: Scenario 1.3: Tree Diagram with the total weighted sum rates of each branch

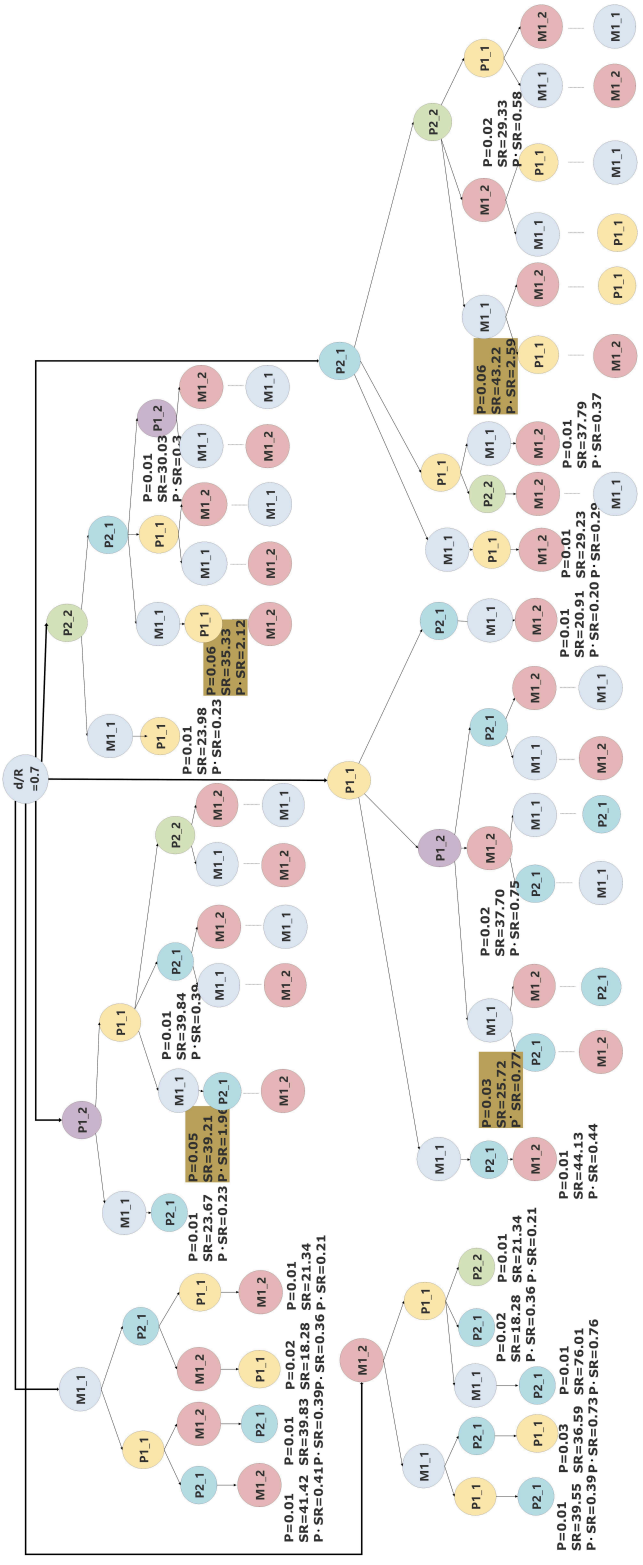

Figure B.4: Scenario 2.1: Exhaustive Analysis as Stream Tree

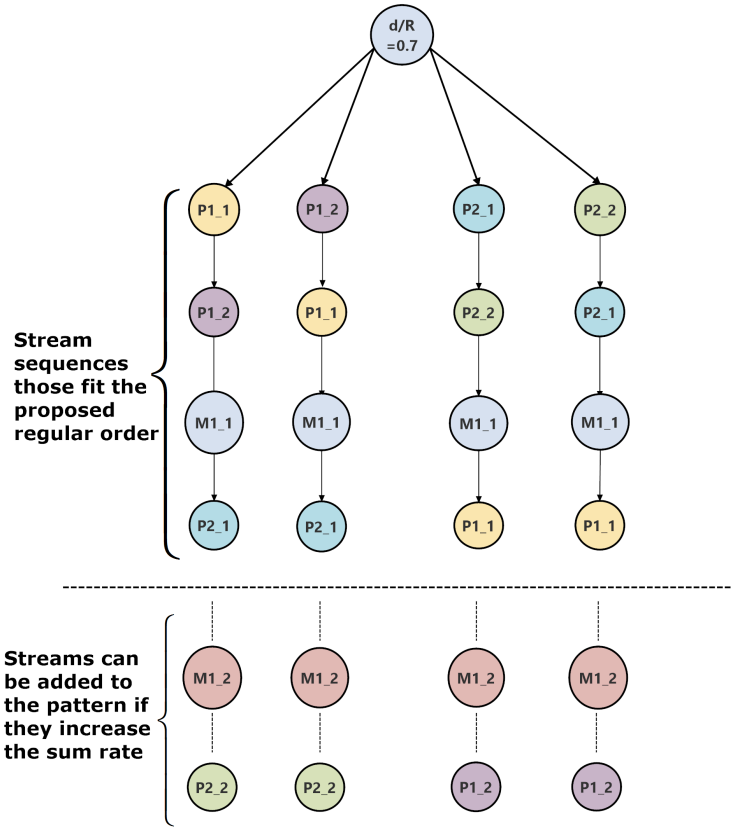

Figure B.5: Scenario 2.1: Stream sequences constructed by ASNSSS

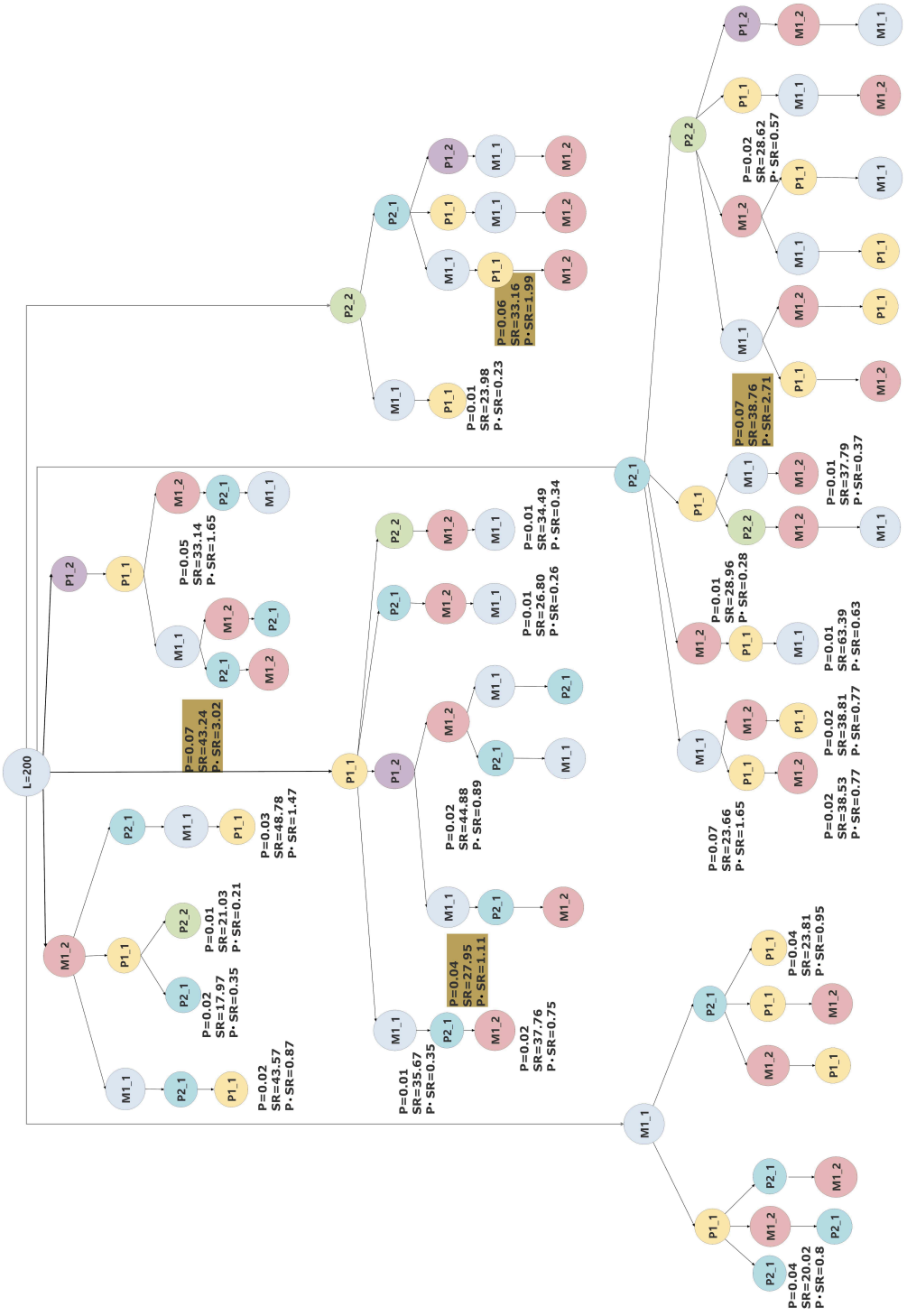

Figure B.6: Scenario 2.2: Exhaustive Analysis as Stream Tree

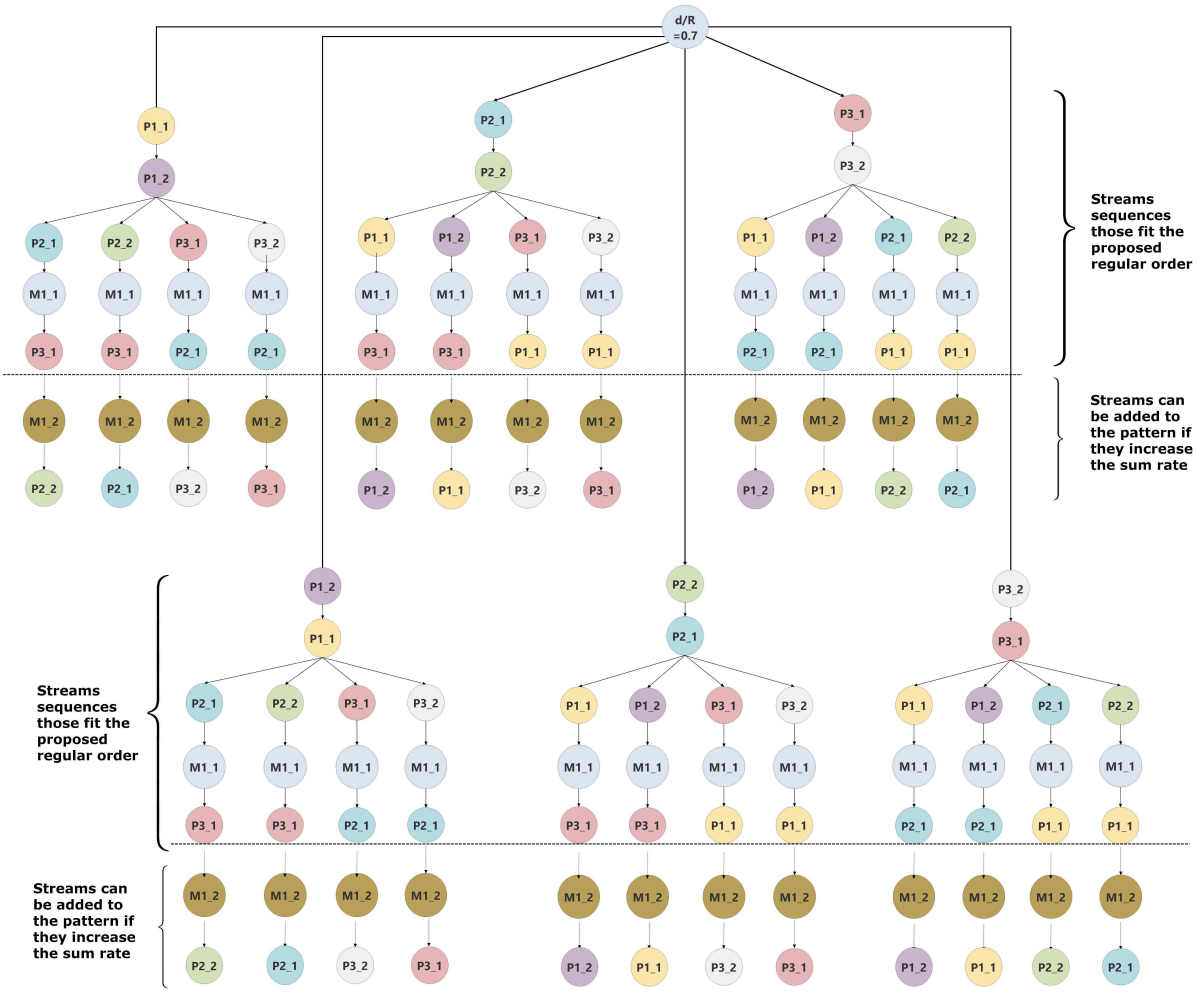

Figure B.7: Scenario 2.3: Sum-Rate vs d/R between 0.6 and 1

Acronyms

- $ASNSSS$: Advanced Successive Null Space Stream Selection
- BER : Bit Error Rate
- BS : Base Station
- CDI : Channel Direction Information
- CSI : Channel State Information
- $CSIT$: Channel State Information at the Transmitter
- CQI : Channel Quality Indicator
- CRE : Channel Range Expansion
- DoF : Degrees of Freedom
- $ESNSSS$: Enhanced Successive Null Space Stream Selection
- FDD : Frequency Division Duplex
- KSS : K-Stream Selection
- IA : Interference Alignment
- IC : Interference Channel
- $ISNSSS$: Improved Successive Null Space Stream Selection
- $\max - SINR$: Maximum Signal to Interference Noise Ratio
- $\min - Leak$: Minimum Interference Leakage
- $MIMO$: Multiple Input Multiple Output
- MSE : Mean Squared Error
- $RSSI$: Received Signal Strength Interference
- $SISO$:Single Input Single Output
- MSE : Mean Squared Error

- $SINR$: Signal to Interference Noise Ratio
- SNR : Signal to Noise Ratio
- $SNSSS$: Successive Null Space Stream Selection
- SR : Sum Rate
- SVD : Singular Value Decomposition
- RVQ : Random Vector Quantization
- TDD : Time Division Duplex
- VTC : Virtual Transmitting Channel
- VRC : Virtual Receiving Channel

Abbreviations

- N_{T_k}: The number of transmit antennas
- N_{R_k}: The number of receive antennas
- $\mathbf{n}_k$: Additive white Gaussian noise (AWGN) vector with dimension $N_{R_k} \times 1$
- $\mathbf{H}_{kj}$: Channel matrix between the j^{th} transmitter and the k^{th} receiver
- $\tilde{\mathbf{H}}_{kj}$: Quantized channel matrix between the j^{th} transmitter and the k^{th} receiver
- $\bar{\mathbf{H}}_{kj}$: CDI between the j^{th} transmitter and the k^{th} receiver
- $\tilde{\bar{\mathbf{H}}}_{kj}$: Quantized CDI between the j^{th} transmitter and the k^{th} receiver
- P_k: Transmit power of the k^{th} base station P_{kk}: Received power of the k^{th} user from the k^{th} base station
- $\mathbf{x}_k(t)$: Input signal transmitted by the k^{th} transmitter with dimension $N_{T_k} \times 1$
- q_k: Number of the selected streams of the k^{th} user
- d_k: Total number of the streams of the k^{th} user
- $\mathbf{s}_k$: Symbol vector with dimension of $q_k \times 1$
- $\mathbf{T}_k$: Precoding matrix of the k^{th} transmitter with dimension $N_{T_k} \times q_k$
- $\mathbf{t}_k^i$: i^{th} column vector of the precoding matrix $\mathbf{T}_k$ with dimension $N_{T_k} \times 1$
- $\mathbf{D}_k$: Postcoding matrix of transmitter k with dimension $N_{R_k} \times q_k$
- $\mathbf{d}_k^i$: i^{th} column vector of the precoding matrix $\mathbf{D}_k$ with dimension $N_{R_k} \times 1$
- γ_{ki}: SINR of the i^{th} stream of the k^{th} receiver
- $\mathbf{B}_{ki}$: Interference plus noise covariance matrix for the i^{th} stream of the k^{th} receiver
- B_{kj}: Number of quantization bits to quantize the channel between the j^{th} transmitter and the k^{th} receiver

Symbols

- Lower-case Letters: Scalars
- Bold Lower-case Letters: Vectors
- Bold Upper-case Letters: Matrices
- Capital Greek Letters (i.e. Φ): Sets
- $\emptyset$: Empty set
- rank($\mathbf{A}$): Rank of matrix $\mathbf{A}$
- $\mathbf{A}^T$: Transpose of matrix $\mathbf{A}$
- $\mathbf{A}^H$: Complex conjugate transpose of matrix $\mathbf{A}$
- det($\mathbf{A}$): Determinant of matrix $\mathbf{A}$
- $|\Phi|$: Cardinality of set Φ
- $\|\mathbf{a}\|$: Euclidean norm of vector $\mathbf{a}$
- $\|\mathbf{A}\|_F$: Frobenius norm of matrix $\mathbf{A}$
- $\mathbb{E}[\mathbf{A}]$: Expectation of random variable $\mathbf{A}$
- span($\mathbf{A}$): Space spanned by the column vectors of matrix $\mathbf{A}$
- vec($\mathbf{A}$) : Vectorization of a channel matrix $\mathbf{A} \in \mathbb{C}^{a \times b}$ as $\mathbf{a} \in \mathbb{C}^{ab \times 1}$

le cnam

Esra AYCAN BEYAZIT

INTERFERENCE ALIGNMENT TECHNIQUES FOR HETEROGENEOUS WIRELESS NETWORKS

le cnam

Résumé :
Dans cette thèse, nous étudions les algorithmes d'alignement d'interférence dans les réseaux hétérogènes basés sur la sélection des flux. Tout d'abord, nous considérons différents scénarios de déploiement des pico-cellules dans un contexte de connaissance parfaite des canaux de transmission au niveau des émetteurs. Deux algorithmes sont proposés respectivement pour les réseaux totalement et partiellement connectés. Afin d'assurer une équité entre les liens, les algorithmes garantissent qu'au moins un flux de chaque lien émetteur soit sélectionné. La séquence des flux est choisie parmi un ensemble qui contient les séquences les plus souvent sélectionnées en effectuant une recherche exhaustive. Ces algorithmes sont significativement moins complexes que la recherche exhaustive tout en ayant une performance proche de celle-ci. Après la sélection d'un flux, les interférences entre ce flux et les flux qui n'ont pas encore été sélectionnées sont alignées par projections orthogonales. Dans une deuxième partie de la thèse, l'impact de la connaissance partielle des canaux de transmission sur les algorithmes proposés est analysé. Il est montré que les interférences entre flux causent alors une forte dégradation des performances en raison des erreurs de quantification. Pour réduire cette dégradation, un nouvel algorithme est développé pour ce contexte. Finalement, des schémas d'allocation adaptative des bits pour les voies de retour sont proposés afin d'augmenter les performances des algorithmes précédents.

Mots clés :
les réseaux de communication hétérogenes; alignement d'interférences; sélection de flux, rétroaction limitée

Abstract :
In this thesis, we study the stream selection based interference alignment (IA) algorithms, which can provide large multiplexing gain, to deal with the interference in the heterogeneous networks. Firstly, different deployment scenarios for the pico cells are investigated assuming perfect channel state information (CSI) at the transmitters. Two different stream selection IA algorithms are proposed for fully and partially connected interference networks and selecting at least one stream is guaranteed for each user. A stream sequence is selected among a predetermined set of sequences that mostly contribute to the sum-rate while performing an exhaustive search. In the proposed algorithms, the complexity of the exhaustive search is significantly decreased while keeping the performance relatively close. After selecting a stream, the interference generated between the selected and the unselected streams is aligned by orthogonal projections. Then, the influence of the imperfect CSI on the proposed algorithms is analyzed and it is observed that the intra-stream interference causes a significant degradation in the performance due to the quantization error. Therefore, we propose an algorithm for the limited feedback scheme. Finally, adaptive bit allocation schemes are presented to maximize the overall capacity for all the proposed algorithms. The performance evaluations are carried out considering different scenarios with different number and placements of pico cells. It is shown that the proposed algorithm for the limited feedback is more robust to channel imperfections compared to the existing IA algorithms.

Keywords :
heterogeneous networks, interference alignment, stream selection, feedback schemes